The University of Manitoba

A Mass spectrometric Study of Some Beta-diketonate and Monothio-Beta-diketonate Complexes of Ni(II), Zn(II), Pd(II), Co(III) and Rh(III).

by

Gary A. Stern

A Thesis Submitted to
The Faculty of Graduate Studies and Research
In Partial Fulfillment
of the Requirements for the Degree
MASTER OF SCIENCE.

Chemistry Department
University of Manitoba
Winnipeg, Manitoba

ISBN 0-315-34043-6

A MASS SPECTROMETRIC STUDY OF SOME BETA-DIKETONATE AND MONOTHIO-BETA-DIKETONATE COMPLEXES OF NI(II), ZN(II), PD(II), CO(III) AND RH(III)

BY

GARY A. STERN

A thesis submitted to the Faculty of Graduate Studies of the University of Manitoba in partial fulfillment of the requirements of the degree of

MASTER OF SCIENCE

ACKNOWLEDGEMENTS

I wish to thank Dr. J.B. Westmore, my research supervisor for his advice, helpful suggestions and enlightening discussions throughout this project.

I also wish to thank Mark Reimer and Terry Lee for their help in the preparation of some of the compounds used in this study.

TO MY GRANDPARENTS

ABSTRACT

A mass spectral study has been carried out on the beta-diketonates and monothio-beta-diketonates of Ni(II), Zn(II), Pd(II), Co(III) and Rh(III). Fragmentation of the chelates is influenced by the odd- or even-electron character of the ion. Unit change of valency of the metal present in an ion effects the subsequent fragmentation by changing the ion's odd- or even-electron character. In the case of the fluorinated metal beta-diketonates and monothio-beta-diketonates a competition between pathways involving fluorine migration to the metal and reduction of the metal is evident. Which pathway predominates is dependent upon the ability of the metal to undergo reduction and the hardness of the metal as an acid. That fluorine migration to the metal is dependent upon the hardness of the metal as an acid is seen when a comparison is made between hexafluoro-acetylacetonates and trifluoro-acetylacetonates of the same metal. The additional CF_3 group in the former tends to harden the metal environment and thus an increase in fluorine migration is observed (increase in the relative intensity of the $[MetL-CF_2]^+$ ion). The replacement of an oxygen atom by sulfur in the ligand is seen to have the opposite effect in that the metal environment is softened by the presence of the sulfur atom. When comparing the trifluoro-

monothioacetylacetonates to the trifluoro-acetylacetonates of the same metal a small difference in fluorine migration to the metal is observed for the former.

A rough comparison of the volatilities of the compounds studied in this thesis was made by comparing the probe temperatures necessary to volatilize the compounds into the mass spectrometer. It was generally noted that substitution of fluorine atoms for hydrogen atoms in the ligand shell greatly increases the volatility of both the beta-diketonate and monothio-beta-diketonate complexes.

TABLE OF CONTENTS

LIST OF FIGURES

Figure page

LIST OF TABLES

Table page

Table

page

CHAPTER 1

INTRODUCTION

PART A: VOLATILITY AND THERMAL STABILITY

i) Introduction

Increasing interest in volatile chelating agents for separation of metals by distillation, gas chromatography, for ultratrace analysis of metals or metal mixtures, for vapor deposition, for use as solvent extraction reagents, and for use as reagents that react directly with metals or oxides to form chelates has prompted the synthesis and examination for many years of chelates formed from beta-diketones (1-13) and more recently, monothio-beta-diketones (14,15). Which factors influence volatility and thermal stability of these metal chelates will be summarized in this section.

Eisentraut and Sievers (1) reported that the thermogravimetric method can be an extremely powerful technique for comparing the relative volatilities of a group of metal beta-diketonates and mono-thio-beta-

*The following abbreviations have been used throughout this thesis:

H(acac): 2,4-pentanedione
H(tfa): 1,1,1-trifluoro-2,4-pentanedione
H(hfa): 1,1,1,5,5,5-hexafluoro-2,4-pentanedione
H(pta): 1,1,1-trimethyl-5,5,5-trifluoro-2,4-pentanedione
H(thd): 2,2,6,6-tetramethyl-3,5-heptanedione
H(dfhd): 1,1,1,2,2,3,3,7,7,7-decafluoro-4,6-heptanedione
H(fod): 1,1,1,2,2,3,3-heptafluoro-7,7-dimethyl-4,6-octanedione
H(bzac): 1-phenyl-1,3-butanedione
H(tpb): 4,4,4-trifluoro-1-phenyl-1,3-butanedione
H(Sacac): 2-mercaptopent-2-en-4-one
H(Stfacac): 1,1,1-trifluoro-2-mercaptopent-2-en-4-one
H(Shfacac): 1,1,1,5,5,5-hexafluoro-2-mercaptopent-2-en-4-one

diketonates. Through examination of thermograms, information regarding volatility changes upon substitution of various chemical substituents in the R_1, R_2 and R_3 positions of the ligand may be obtained. The technique can also be used to detect volatility differences in the chelates of the same ligand coordinated to different metals. Studies of vapor pressures and heats of vaporization or sublimation by either the isoteniscope or Knudsen effusion methods allow a more quantitative analysis of volatilities and thermal stabilities of these chelates to be done (2,3).

Information regarding the temperature required to vaporize a certain chelate with minimum decomposition and the ability to predict how changes such as variation of chemical substituents on the ligand or how different metals coordinated to the same ligand may effect volatility is of great interest in mass spectrometry. For example, when a sample is introduced to the ion source by direct insertion probe, the probe must not be heated too quickly or taken to temperatures above the point at which decomposition is a factor if true fragmentation and relative intensity data for the chelate are to be attained.

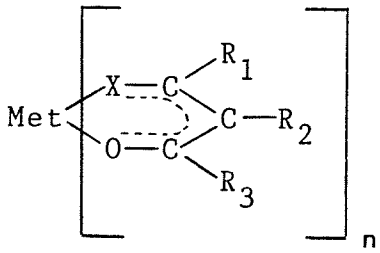

X = O or S
n = 2,3 or 4

ii) Beta-diketonate metal complexes

Substitution of fluorine atoms for hydrogen atoms in the ligand shell greatly increases the volatility of the beta-diketonate complexes (1,2,4,5). This increase may be attributed to a reduction in the Van der Waals forces, and possibly to a decrease in the intermolecular hydrogen bonding. Increase in volatility may also be due to the prevention of the close packing in the crystal lattice by the presence of the somewhat larger fluorine atoms which usually form a shell, with rather lower attractive tendencies, around the complex molecule as compared with an analogous non-fluorinated complex.

Thermograms of some Cr(III) beta-diketonate chelates show trends in volatility with substitution of the R_1 and R_2 groups as shown in figure 1 (1). The fluorine-substituted chelates show greater volatility than the non-fluorinated substituted species. Thermograms of the n-hydrocarbons undecane and tetracosane (curves A and H), are included for comparison. The completely fluorinated species, $Cr(hfa)_3$ is more volatile than the partially fluorinated species, $Cr(tfa)_3$. Furthermore, $Cr(dfhd)_3$ is more volatile than the less extensively fluorinated $Cr(fod)_3$ which in turn is more volatile than $Cr(thd)_3$. Thermograms of a series of Al(III) chelates of a variety of beta-diketone ligands are shown in figure 2 (1). It is once again important to notice the increased volatility of

Figure 1

Thermogravimetric curves of some volatile Cr(III) beta-diketonates

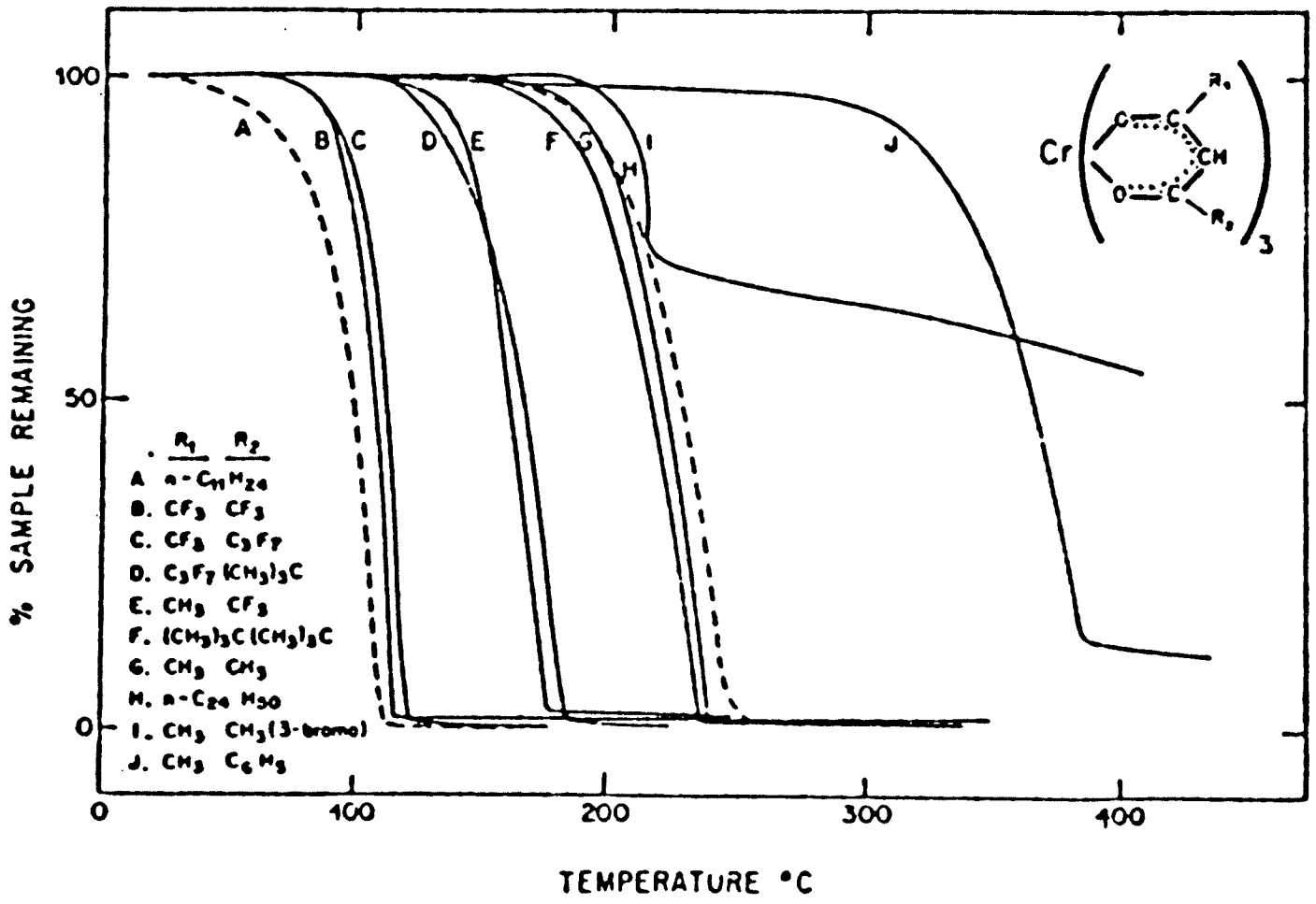
100
50
0
0
100
200
300
400
% SAMPLE REMAINING
TEMPERATURE °C
A
B
C
D
E
F
G
H
I
J
R1 R2
A n-C11H24
B. CF3 CF3
C. CF3 C3F7
D. C3F7 (CH3)3C
E. CH3 CF3
F. (CH3)3C (CH3)3C
G. CH3 CH3
H. n-C24 H50
I. CH3 CH3(3-bromo)
J. CH3 C6H5
Cr
CH
3

Figure 2

Thermogravimetric curves of some volatile Al(III) beta-diketonates

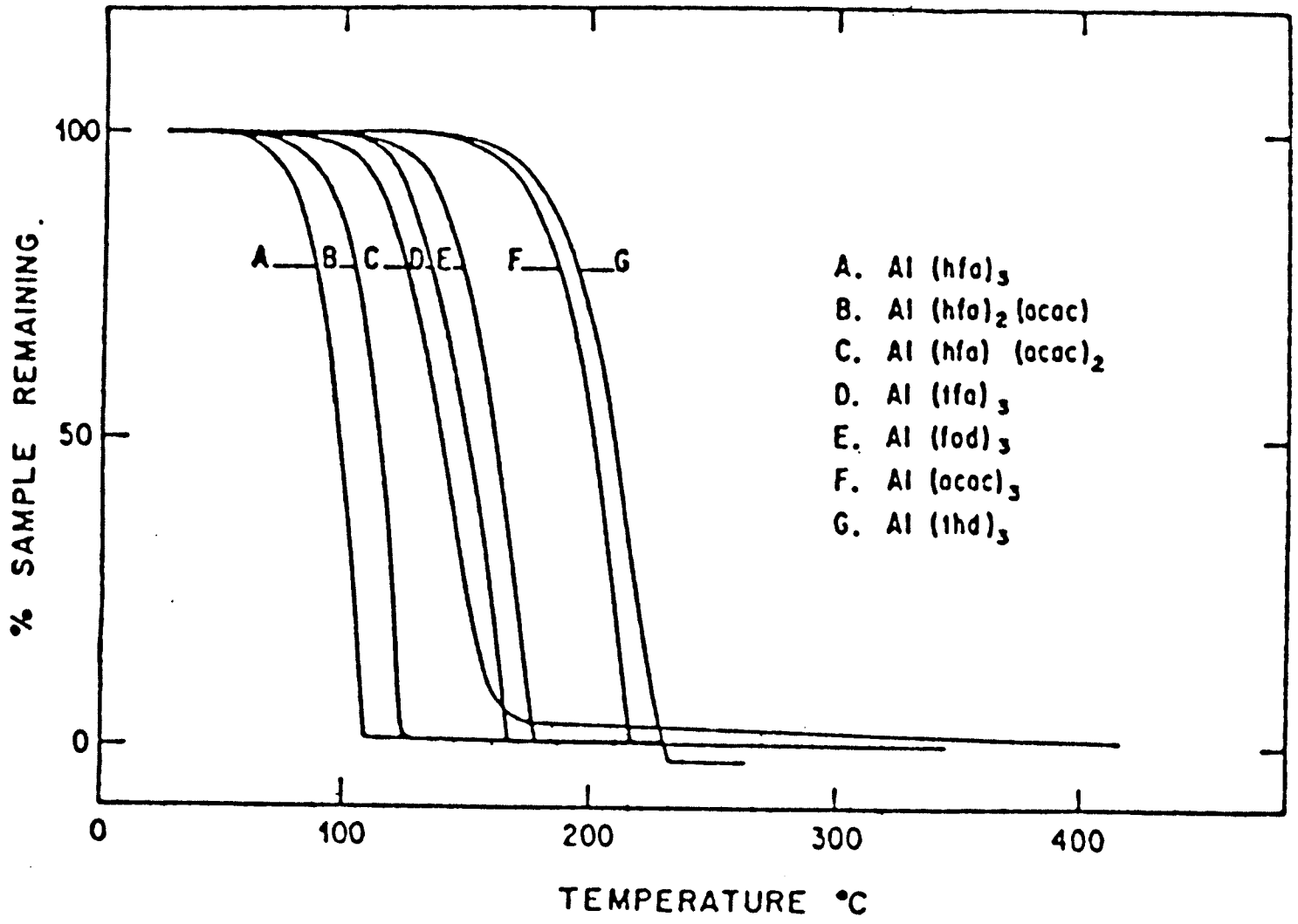
100
50
0
% SAMPLE REMAINING.
A
B
C
D
E
F
G
0
100
200
300
400
TEMPERATURE °C
A. Al (hfa)3
B. Al (hfa)2 (acac)
C. Al (hfa) (acac)2
D. Al (tfa)3
E. Al (fod)3
F. Al (acac)3
G. Al (thd)3

the Al(III) chelates with increasing fluorine substitution in the chelate ligand. The order of decreasing volatility is seen to be $Al(hfa)_3$ > $Al(hfa)_2(acac)$ > $Al(hfa)(acac)_2$ > $Al(tfa)_3$ > $Al(fod)_3$ > $Al(acac)_3$ > $Al(thd)_3$. Figure 3 shows the difference in volatilities in a group of Fe(III) and Rh(III) beta-diketones. In all cases shown, the Fe(III) chelates are more volatile than the corresponding Rh(III) chelates containing the same ligand. Once again, however, it is seen that the more highly fluorinated chelates are the more volatile ones.

Clausius-Clapeyron plots of vapor pressure as a function of temperature are shown in figure 4 (2). They depict the effect of fluorine content on the volatility of the metal complex. It can be seen from figure 4 that the volatility of these complexes is strongly dependent upon the ligand, with chelates of the more highly fluorinated ligands being more volatile in the order hfa >> tfa > fod >> acac. It can also be seen that the square planer fod complexes of Cu(II) and Pd(II) have vapor pressures greater than the tris fod complexes which are in turn more volatile than the tetrakis Hf(IV) complex. The $Cr(hfa)_3$, $Rh(hfa)_3$ and $Al(fod)_3$ chelates showed no thermal decomposition over the range of temperatures studied. The $Fe(fod)_3$ chelate showed slight decomposition above 175 °C and the $Pd(fod)_2$ and $Cu(fod)_2$ chelates showed decomposition above 160 °C. The $Hf(fod)_4$ compound

Figure 3

Thermogravimetric curves of some volatile Fe(III) and Rh(III) beta-diketonates

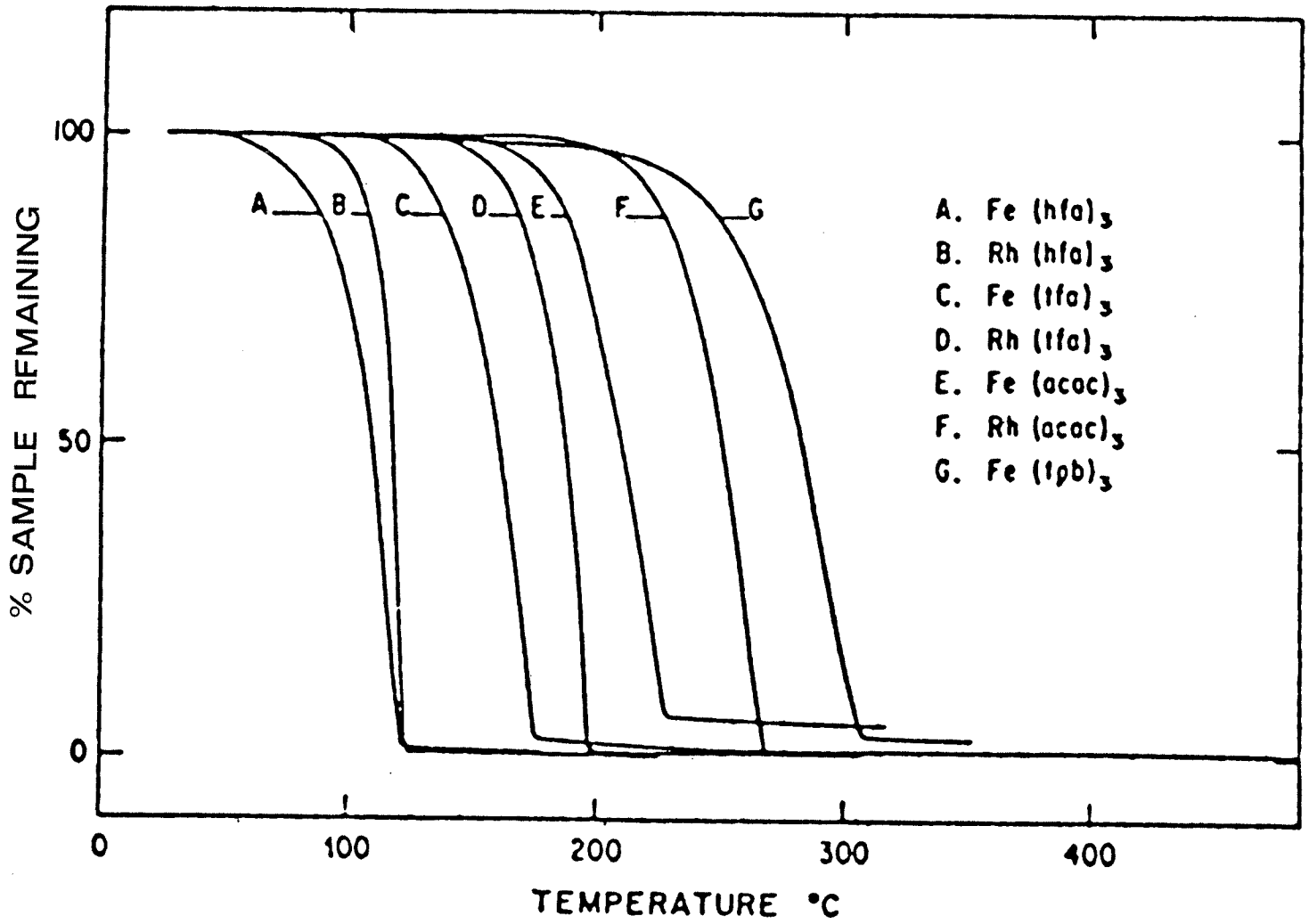
% SAMPLE RFMAINING
100
50
0
0
100
200
300
400
TEMPERATURE °C
A
B
C
D
E
F
G
A. Fe (hfa)3
B. Rh (hfa)3
C. Fe (tfa)3
D. Rh (tfa)3
E. Fe (acac)3
F. Rh (acac)3
G. Fe (tpb)3

Figure 4

Clausius-Clapeyron plots

for metal beta-diketonates.

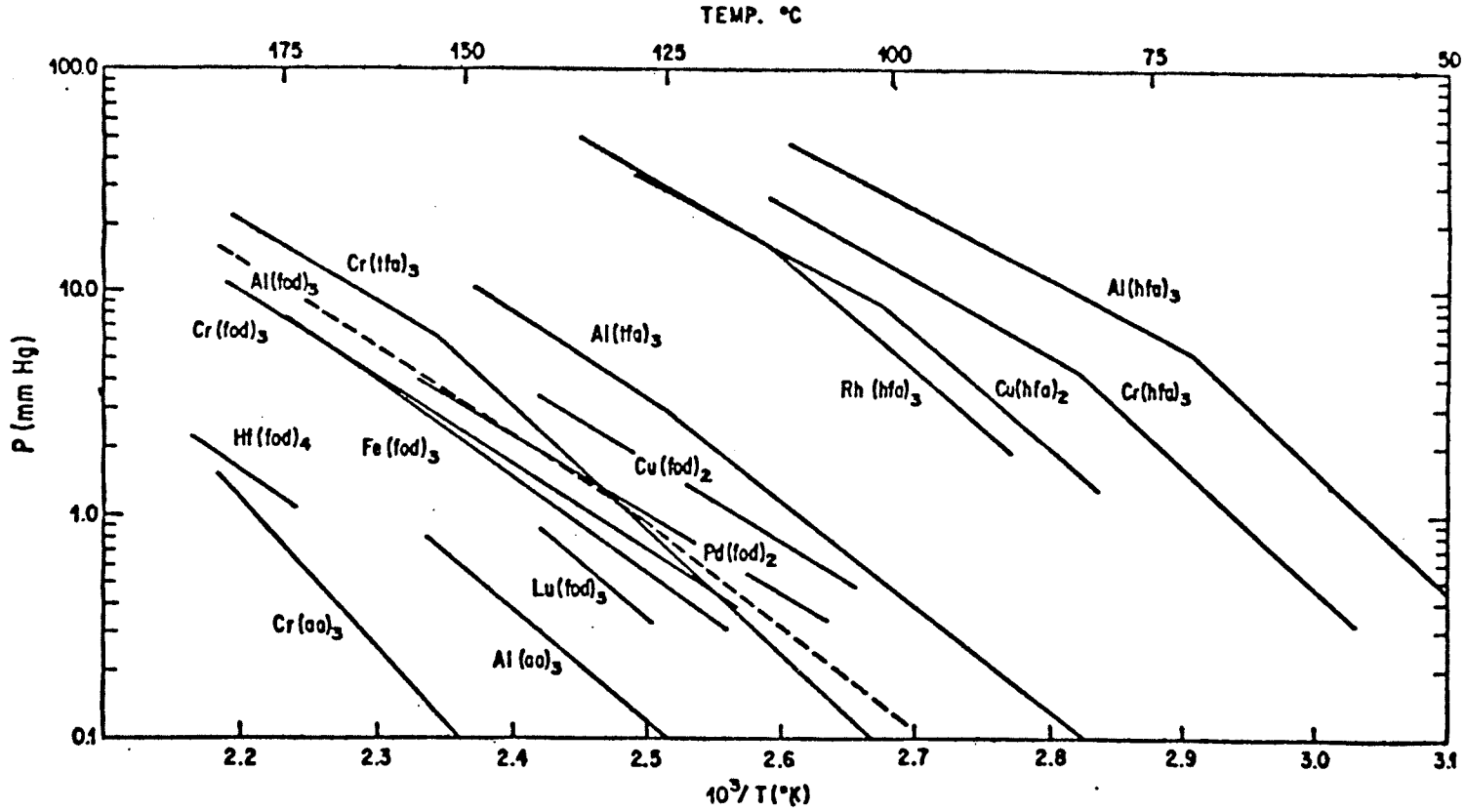
TEMP. °C
175
150
125
100
75
50
100.0
10.0
1.0
0.1
P (mm Hg)
Cr(tfa)3
Al(fod)3
Cr(fod)3
Al(tfa)3
Al(hfa)3
Rh(hfa)3
Cu(hfa)2
Cr(hfa)3
Hf(fod)4
Fe(fod)3
Cu(fod)2
Pd(fod)2
Lu(fod)3
Cr(aa)3
Al(aa)3
2.2
2.3
2.4
2.5
2.6
2.7
2.8
2.9
3.0
3.1
10³/ T(°K)

exhibited the lowest thermal stability, where slight decomposition was observed at the melting point, 174°C and decomposition became extensive above 190°C.

The prevalence of hydration in beta-diketonates seems to produce undesirable effects on thermal stability (6). Brown, Steinback and Wagner (7) suggested that the incorporation of sufficiently bulky ligands would reduce this possibility of hydration.

Sievers and coworkers (1,2,8,9,10) have made a detailed comparative study on the thermal stability of derivatives of rare earth chelates with different beta-diketones in an effort to clearly demonstrate the enhancement of volatility and stability of these complexes when both ligand size and extent of fluorination of the ligand are considered. The relative effects of fluorination and ligand size on the stability and volatility of various rare earth chelates are listed in table 1 (9). Chelates with the acac ligand are thermally unstable and are not volatile, while those of hfa do sublime, however, there is considerable decomposition. This is thought to be due to hydration. When larger ligands or ligands containing fluorine (eg., Hpta, Hfod, Hthd and Hdfhd) are used, the thermal stability becomes great enough to permit volatilization without decomposition of the chelate.

TABLE 1

Effects of Ligand Size and Degree of Fluorination of various Rare Earth Chelates $Ln(RCOCHCOR')_3 \cdot nH_2O$

Ligand	R	R'	n	Volatility Characteristics
acac	CH_3	CH_3	0,1,2,3	Negligibly volatile
tfa	CH_3	CF_3	2	Slightly volatile
hfa	CF_3	CF_3	2,3	Subl with considerable dec
pta	$C(CH_3)_3$	CF_3	?	Subl without dec (Sm-Lu)
fod	$C(CH_3)_3$	$n\text{-}C_3F_7$	0,1	Subl completely without dec
thd	$C(CH_3)_3$	$C(CH_3)_3$	0	Subl completely without dec
dfhd	CF_3	$n\text{-}C_3F_7$	2	Subl with only slight dec

It has been shown that rare earth metal chelates which contain ligands smaller than dfhd and fod might be hydrated and thus hydrolytically unstable at the temperature required for sublimation (6,9,11). For example, the TGA data shown in figure 5 (9) shows that the rare earth tris-dfhd chelates are quite volatile. Only the lighter rare earth chelates (La, Pr and Nd) decompose to any considerable extent. This small degree of decomposition for dfhd chelates contrasts greatly with the hfa chelates $Ln(hfa)_3 \cdot 2H_2O$, where decomposition is extensive even at the heavy end of the series as seen in figure 6 (9). The greater thermal stability of the dfhd chelates may be related to the fact that the dfhd chelates

Figure 5

Thermogravimetric curves for some rare earth dfhd chelates

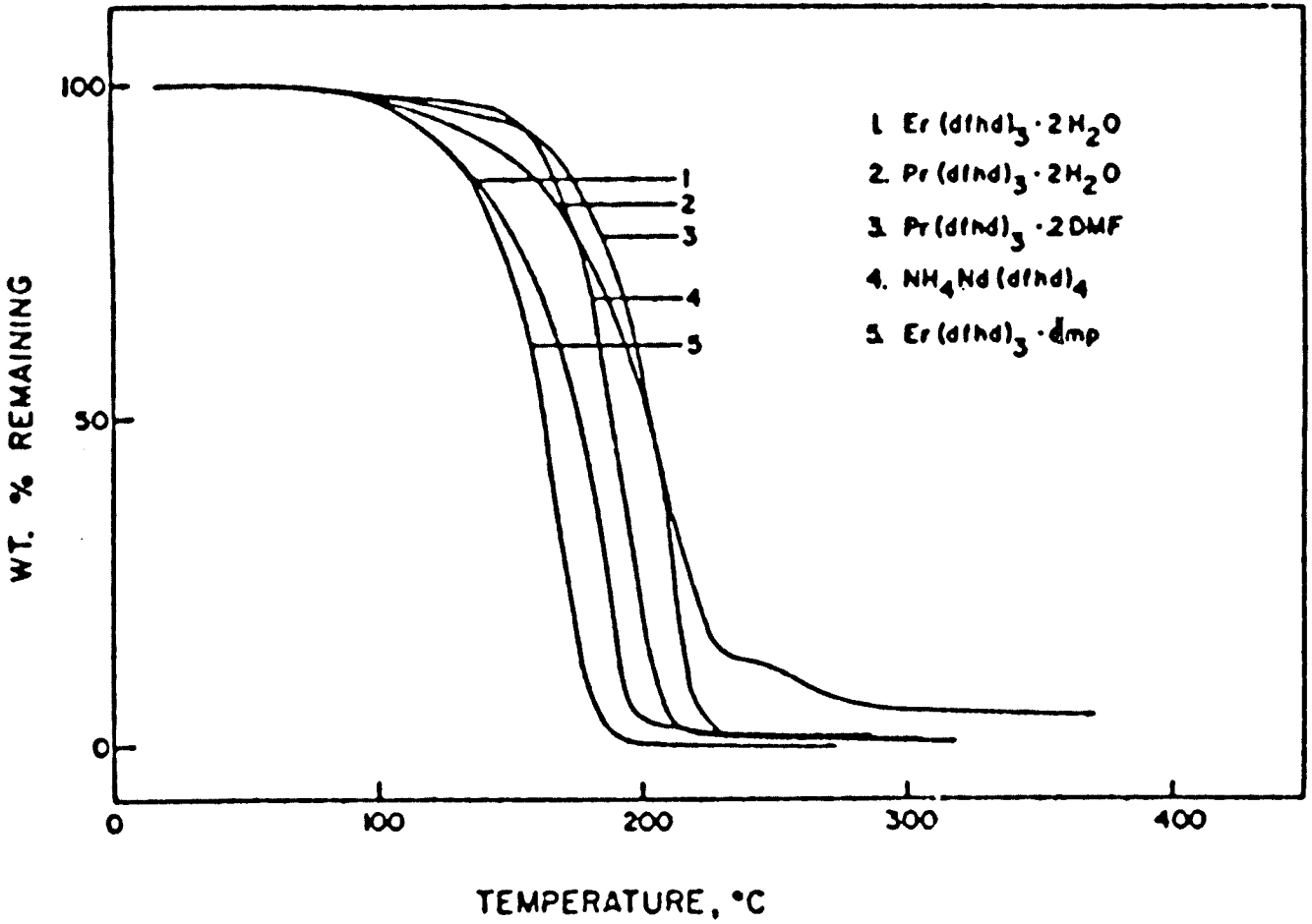
100
50
0
0
100
200
300
400
WT. % REMAINING
TEMPERATURE, °C
1
2
3
4
5
1. Er (dfhd)$_3$ · 2H$_2$O
2. Pr (dfhd)$_3$ · 2H$_2$O
3. Pr (dfhd)$_3$ · 2DMF
4. NH$_4$Nd (dfhd)$_4$
5. Er (dfhd)$_3$ · dmp

Figure 6

Thermogravimetric curves for some rare earth hfa chelates

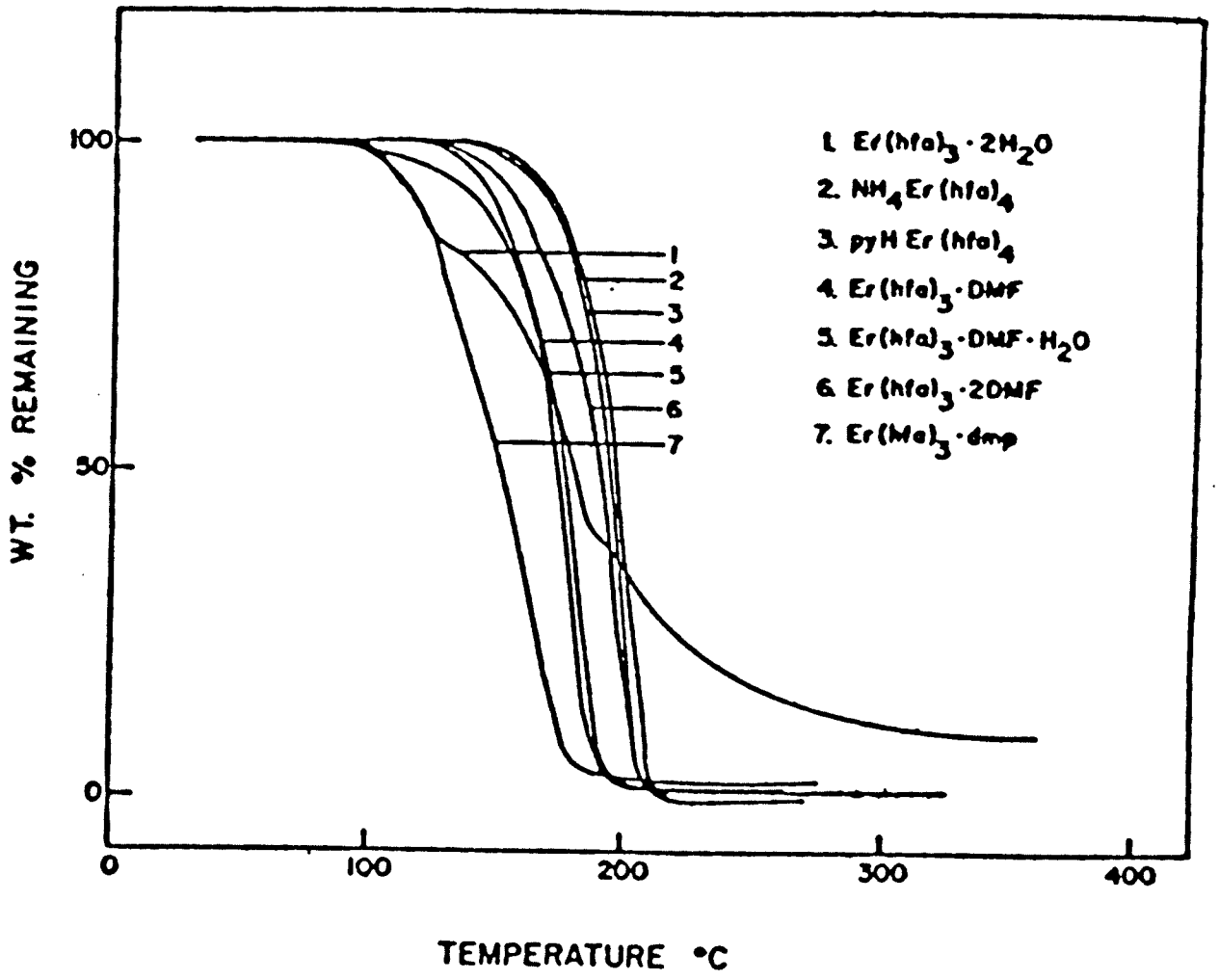
1. Er(hfa)3 · 2H2O
2. NH4Er(hfa)4
3. pyH Er(hfa)4
4. Er(hfa)3 · DMF
5. Er(hfa)3 · DMF · H2O
6. Er(hfa)3 · 2DMF
7. Er(Ma)3 · 6mp
WT. % REMAINING
100
50
0
0
100
200
300
400
TEMPERATURE °C

are fairly easily dehydrated at room temperature, whereas the hfa chelates slowly decompose to non-stoichiometric products. Empirically this indicates that reactions of the type in equations 1 and 2 occur more readily in the hfa chelates than the dfhd chelates.

$$Ln(L)_3 \cdot 2H_2O \longrightarrow Ln(L)_3 \cdot H_2O + H_2O \qquad 1$$

$$Ln(L)_3 \cdot H_2O \longrightarrow Ln(L)_2(OH) + HL \qquad 2$$

Sievers et al (9) also pointed out that water of hydration may not necessarily always have an adverse effect on thermal stability. In cases where water is not coordinated to the metal or where the metal-water bond is much weaker than the metal-ligand bonds, (eg., $Ln(dfhd)_3 \cdot 2H_2O$ and $Ln(fod)_3 \cdot H_2O$) hydrolysis causes negligible decomposition. In cases where an adduct is formed, such that water is completely removed from the coordination sphere, the thermal stability can be increased greatly. It can be seen from the TGA curves in figure 6 for example that the 1:1 and 2:1 dimethyl formamide (DMF) adducts of Er chelates (curves 4 and 6) and the $Pr(dfhd)_3 \cdot 2DMF$ chelate in figure 5 (curve 3) volatilize completely without decomposition.

An interesting trend in the volatilities of beta-diketonate complexes is the greater volatility of the rare earth metals with smaller atomic radii compared to those with larger atomic radii. This difference in volatilities

is demonstrated by the thermogravimetric curves of volatile metal chelates of thd shown in figure 7 (1). Each of the rare earth chelates shows a smooth curve that approaches 100% weight loss. The thermograms of tetrakis chelate $Zr(thd)_4$ and Na(thd) are also included in figure 7. It can be seen that the volatilities of these chelates are less than that of the thd rare earth chelates. It should be noted that even though the atomic weight of yttrium is only about half that of erbium, $Y(thd)_3$ exhibits a TGA curve which lies in almost the same position as does the TGA curve of $Er(thd)_3$. Therefore any mass effects on the volatilities can be ruled out. This volatility trend was also observed in the tris rare earth chelates of fod seen in figure 8 (6), as well as the Al(III), Ga(III), In(III) family (8) and the alkali metals (12). The ionic radii of the trivalent rare earth ions of coordination number 6 are given in table 2 below (1).

Table 2

Rare earth ion	Sc(III)	Y(III)	Lu(III)	Yb(III)	Tm(III)	Er(III)
Ionic radius Å	0.68	0.88	0.848	0.859	0.869	0.881

Rare earth ion	Ho(III)	Dy(III)	Tb(III)	Gd(III)	Eu(III)	Sm(III)
Ionic radius Å	0.894	0.908	0.923	0.938	0.950	0.964

Rare earth ions	Pm(III)	Nd(III)	Pr(III)	Ce(III)	La(III)
Ionic radius Å	0.979	0.995	1.013	1.034	1.061

Figure 7

Thermogravimetric curves for some rare earth thd chelates

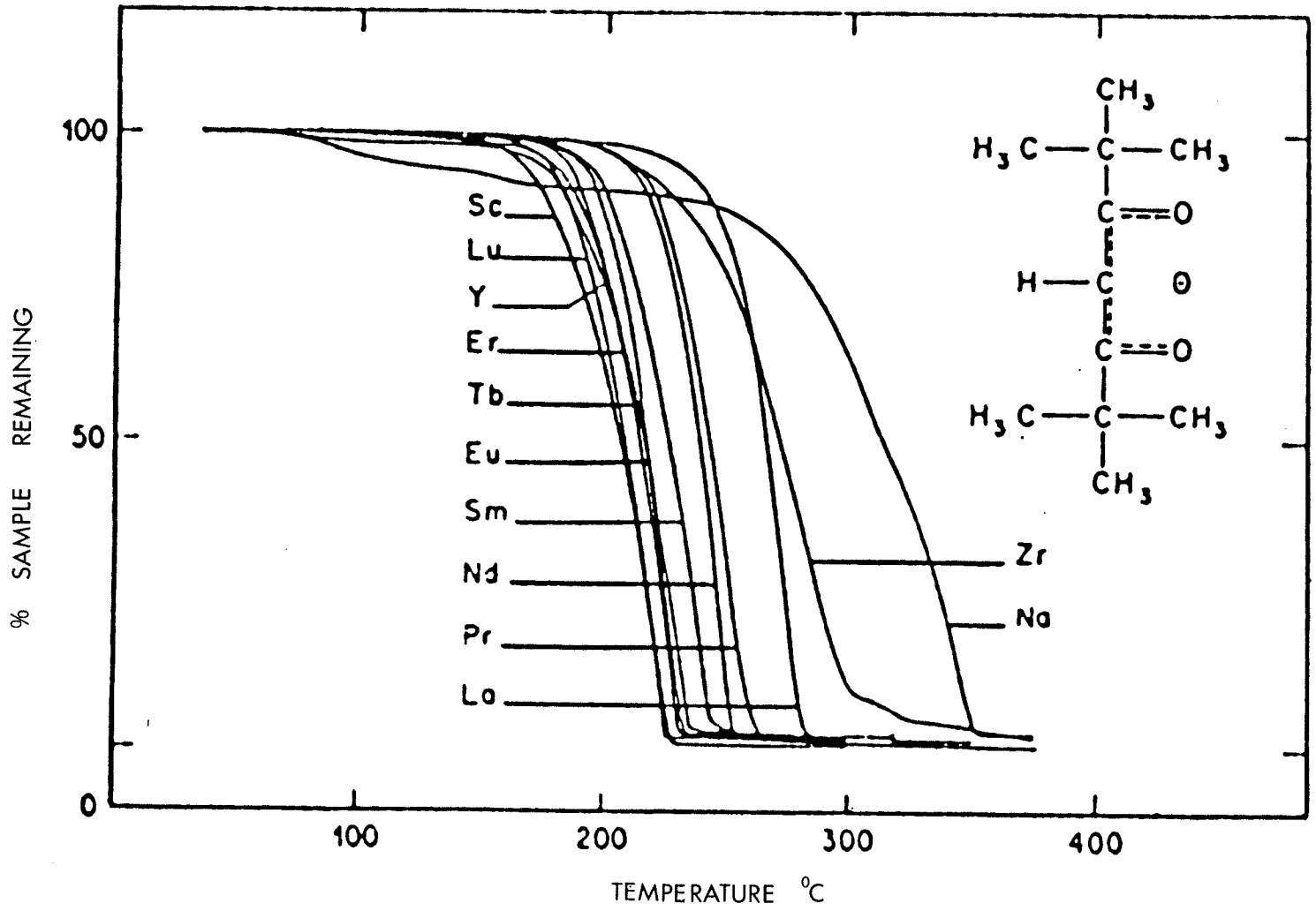
100
50
0
% SAMPLE REMAINING
100
200
300
400
TEMPERATURE °C
Sc
Lu
Y
Er
Tb
Eu
Sm
Nd
Pr
La
Zr
Na
CH3
H3C — C — CH3
C=O
H — C O
C=O
H3C — C — CH3
CH3

Figure 8

Thermogravimetric curves for some rare earth fod chelates

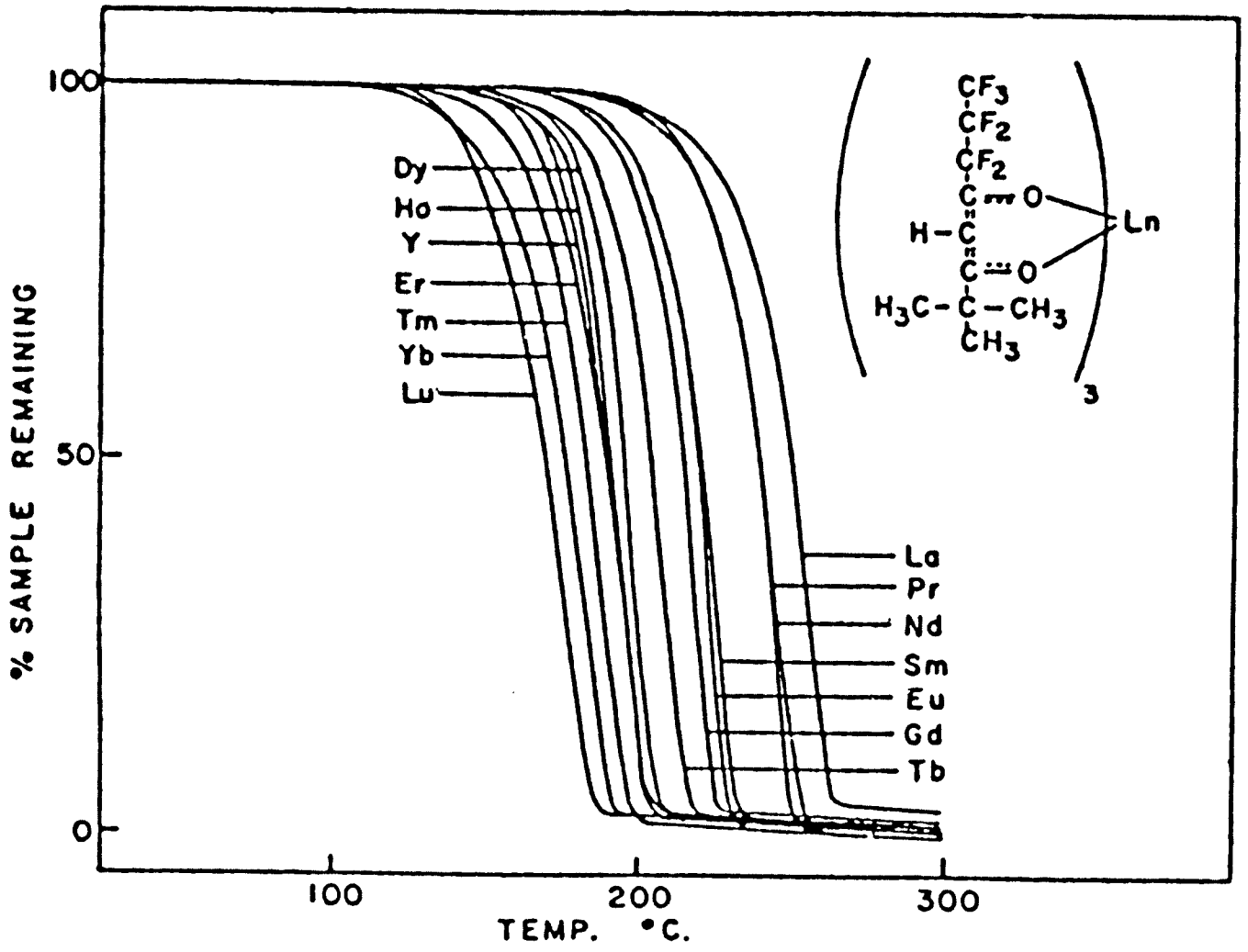
100
50
0
% SAMPLE REMAINING
100
200
300
TEMP. °C.
Dy
Ho
Y
Er
Tm
Yb
Lu
La
Pr
Nd
Sm
Eu
Gd
Tb
CF3
CF2
CF2
O
H
O
H3C
CH3
CH3
Ln
3

Several possible explanations have been offered to account for the correlation between the volatilities of the complex and the size of the metal ion (1,3,6,8,13). All beta-diketonate chelates, irrespective of the symmetry of the ligand, have small permanent local dipoles, and if it is assumed that the size of the of the chelate decreases with decreasing radius of the central metal ion, then these local dipoles might be expected to decrease in magnitude or to become effectively shielded as the size of the central metal ion decreases. Further, as the size of the molecule decreases one would also expect the polarizability to be reduced. All these factors would be expected to decrease the dipole-dipole (molecular or local) interactions, the dipole-induced dipole interactions and consequently to increase the volatility as the ionic radius becomes smaller. It has been observed that there is no appreciable effect on monomer-polymer equilibria with change in the radius of the central metal ion (6).

Sicre and coworkers (3) studied the vapor pressures of the lanthanide thd complexes as a function of temperature. The effect of decreasing ionic radius of the central metal ion on the volatility of the complexes is apparent in the Clausius-Clapeyron plot in figure 9. This confirms in a quantitative manner the observations made using thermogravimetric analysis. When vapor pressures of

Figure 9

Clausius-Clapeyron plots for some rare earth thd chelates

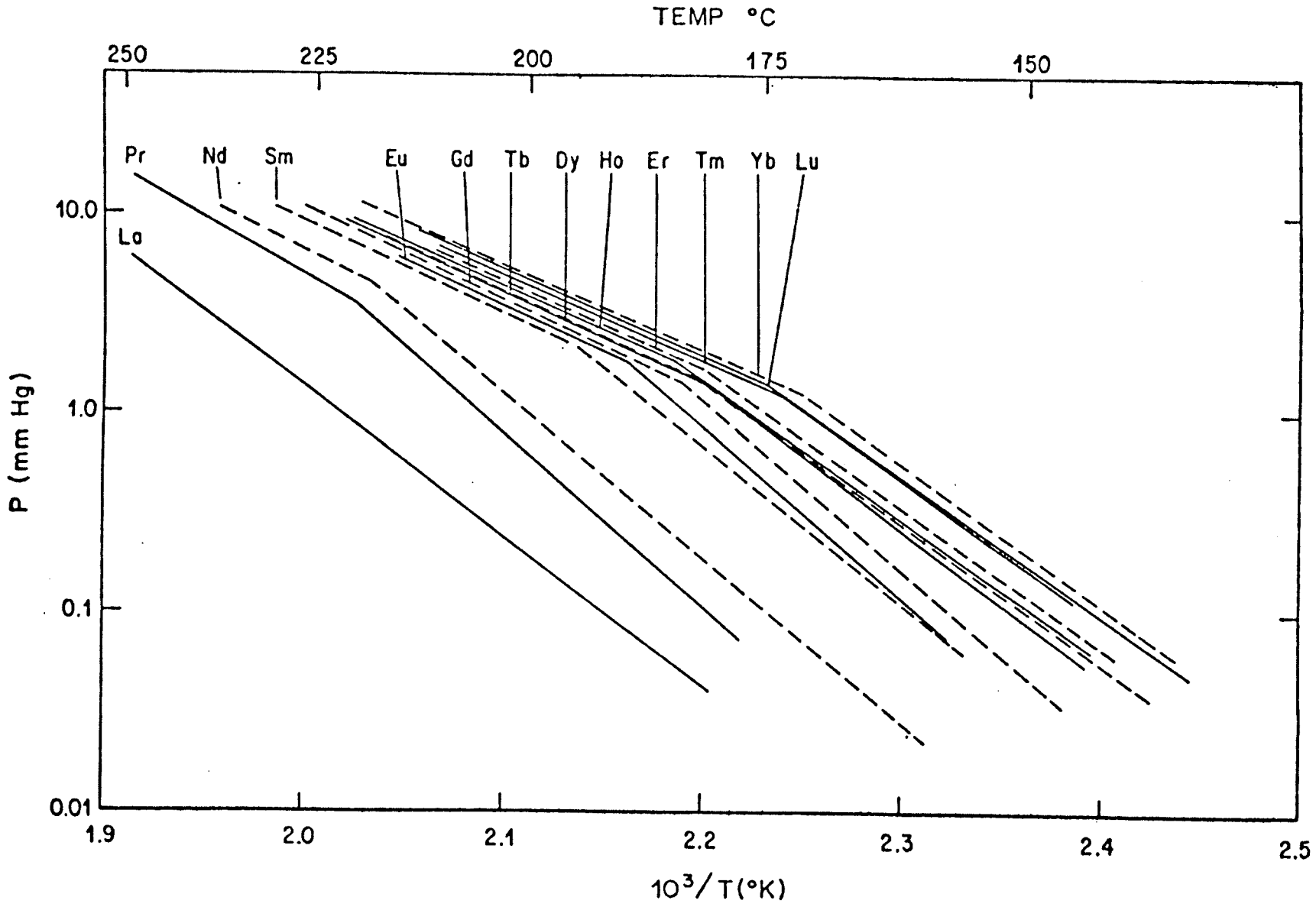
TEMP °C
250
225
200
175
150
Pr
Nd
Sm
Eu
Gd
Tb
Dy
Ho
Er
Tm
Yb
Lu
La
10.0
1.0
0.1
0.01
P (mm Hg)
1.9
2.0
2.1
2.2
2.3
2.4
2.5
10³/T(°K)

these complexes were compared to that of the saturated hydrocarbon, n-tetracosane, it was found that more than half of the complexes have higher vapor pressures than this compound. This was unexpected, particularly when it is recalled that the empirical formula of the lanthanide complexes is $Ln(C_{33}H_{57}O_6)$ as compared to $C_{24}H_{50}$ for n-tetracosane (ie., n-tetracosane has a much lower carbon number) and that bonding in the lanthanide complexes has always been thought to have large ionic contributions with the resulting dipoles rendering the compounds nonvolatile. Stereochemical factors must therefore play an important role in altering the physiochemical properties of the complexes. The bulky ligands may be invisioned as forming a hydrocarbon shell at the periphery which partially shields the six polar metal-oxygen bonds from interactions with neighboring molecules.

iii) Monothio-beta-diketonate metal complexes

In recent years considerable attention has been aimed at the study of monothio-beta-diketones and their metal chelates (14,15). Monothio-beta-diketonates readily form stable monomeric bis chelates with many metals that give hydrated or polymeric chelates with the analogous beta-diketones. Figure 10 (14) shows the thermograms of five monothio-beta-diketonate metal chelates. Of the five chelates only $Ni(Sacac)_2$ volatitilized completely, the

Figure 10

Thermogravimetric curves of five monothio-beta-diketonate complexes

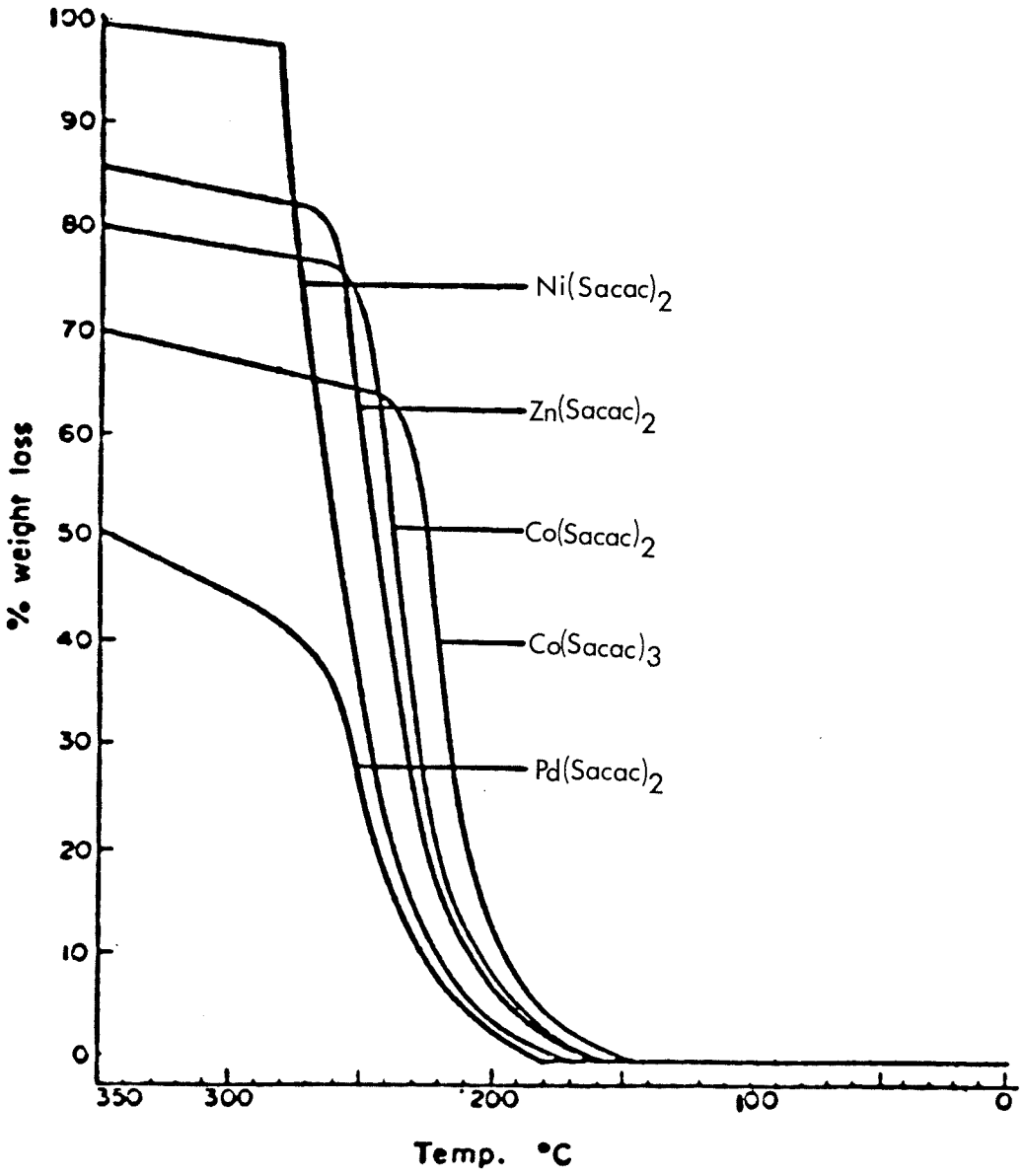
100
90
80
70
60
50
40
30
20
10
0
% weight loss
Ni(Sacac)2
Zn(Sacac)2
Co(Sacac)2
Co(Sacac)3
Pd(Sacac)2
350
300
200
100
0
Temp. °C

remaining chelates showed signs of decomposition in addition to sublimation. $Pd(Sacac)_2$ showed the most decomposition. Exothermic changes (decomposition) were evident at 190°C when examined by Differential Scanning Calorimetry (D.S.C.). However, the major weight loss was due to sublimation between 190 and 250°C. The D.S.C. examination of $Co(Sacac)_2$ and $Zn(Sacac)_2$ showed only small amounts of decomposition at 216 and 208°C respectively. Once again the major weight loss was due to sublimation. $Co(Sacac)_3$ showed 67% weight loss with decomposition occurring at 180°C. It is evident from the thermograms in figure 8 that the $Co(Sacac)_3$ chelate is the most volatile.

Figure 11 (15) shows the thermograms of Ni(II), Zn(II), Co(III), Pd(II) and Pt(II) chelates of monothiotrifluoroacetylacetone. $Zn(Stfcac)_2$, $Co(Stfacac)_3$ and $Ni(Stfacac)_2$ were completely volatilzed, while $Pd(Stfacac)_2$ showed 85% volatilization and $Pt(Stfacac)_2$ 65% volatilization. Examination by D.S.C. showed decomposition exotherms for $Pt(Stfacac)_2$ at 205°C and for $Pd(Stfacac)_2$ at 212°C. No decomposition of $Ni(Stfacac)_2$ was evident at 250°C, but decomposition exotherms were obtained at 195°C for $Zn(Stfacac)_2$ and at 208°C for $Co(Stfacac)_3$. $Zn(Stfacac)_2$ was the most volatile chelate of the five studied.

The following table, using data from figures 10 and 11, illustrates that as in the beta-diketonate

Figure 11

Thermogravimetric curves of five fluorinated bis-monothio-beta-diketonate complexes

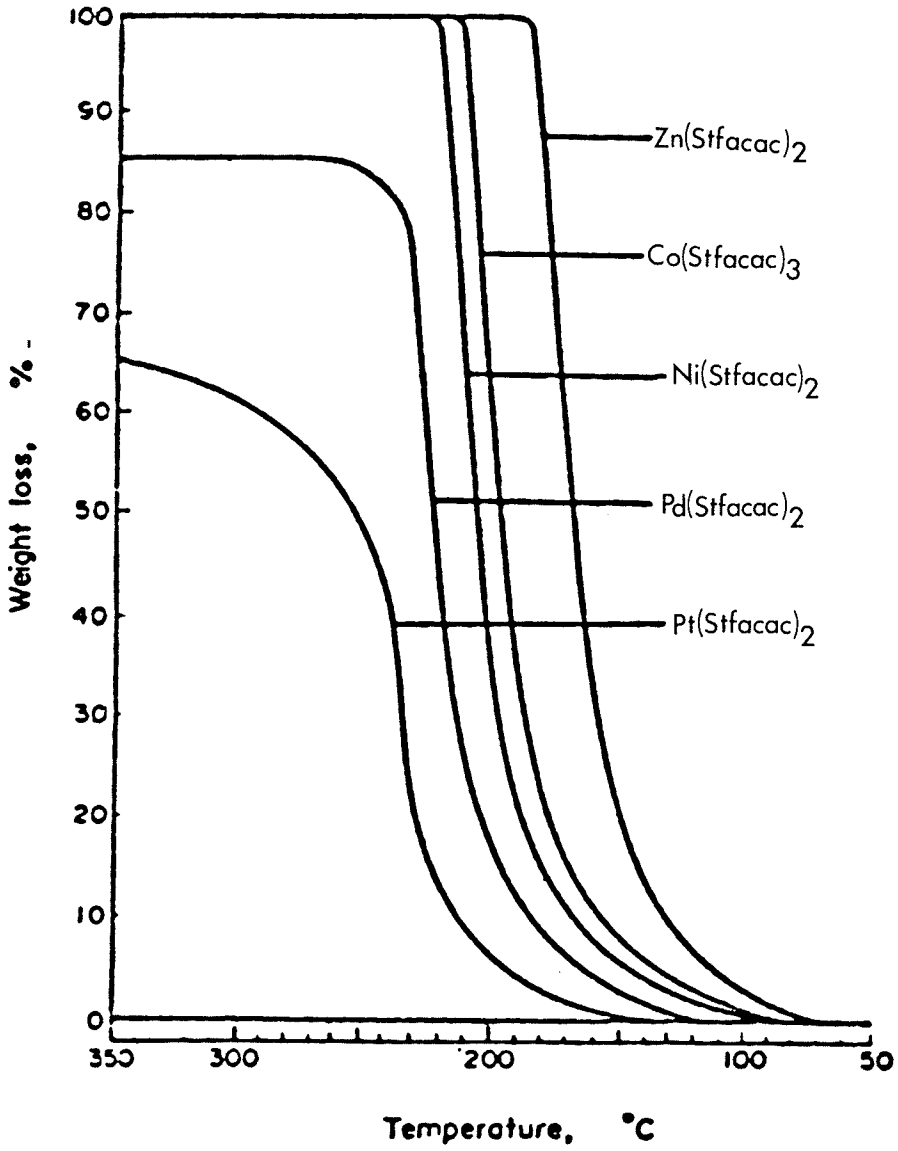
100
90
80
70
60
50
40
30
20
10
0
Weight loss, %
350
300
200
100
50
Temperature, °C
Zn(Stfacac)2
Co(Stfacac)3
Ni(Stfacac)2
Pd(Stfacac)2
Pt(Stfacac)2

complexes the fluorinated monothio-beta-diketonate complexes display greater volatility than the analogous nonfluorinated monothio-beta-diketonate complexes.

Table 3

Comparison between volatilities of monothio-beta-diketonate and trifluoromonothio-beta-diketonate metal complexes.

Metal	Ligand	Half Temp.°C*	Volatilization %	Decomposition Temp°C
Ni(II)	Sacac	262.8	100	-
Ni(II)	Stfacac	207.3	100	-
Co(III)	Sacac	226.7	70	180(s)
Co(III)	Stfacac	195.1	100	208(s)
Zn(II)	Sacac	246.5	85	208(s)
Zn(II)	Stfacac	165.9	100	195(s)
Pd(II)	Sacac	341.8	51	190(1)
Pd(II)	Stfacac	222.0	85	212(s)
Co(II)	Sacac	241.8	80	216(s)
Pt(II)	Stfacac	253.7	65	205(1)

s = slight decomposition 1 = large decomposition

*Half temperature is the temperature attained at 50% weight loss.

PART B: HARD AND SOFT ACIDS AND BASES

i) Introduction

Although monothio-beta-diketones are stronger acids than the analogous beta-diketones, stability data indicate that some metals form more stable complexes with the monothio than with the diketones (16). Beta-diketonate chelates of Ti(IV), Al(III) and Co(III) are more stable than their monothio analogues. For chelates of Ag(I), Hg(II) and Pt(II) the situation is reversed. Ligands and metal ions were classified as belonging to either type (a) or (b) according to their preferential bonding (16). Class (a) metal ions include those of alkali metals, alkaline earth metals and lighter transition metals in higher oxidation states such as Ti(IV), Cr(III), Fe(III), Co(III) and the hydrogen ion, H^+. Class (b) metal ions include those of heavier transition metals and those in lower oxidation states such as Cu(I), Ag(I), Hg(I), Pd(II) and Pt(II). Depending on their preferences toward either class (a) or class (b) metal ions, ligands also may be classified as either type (a) or (b). Stability of these complexes may be summarized as shown in table 4 (16).

Table 4

Tendency to complex with class (a) metal ions	Tendency to complex with class (b) metal ions
N >> P > As > Sb	N << P > As > Sb
O >> S > Se > Te	**O << S** < Se = Te
F > Cl > Br > I	F < Cl < Br < I

It can be seen from table 4 that a beta-diketone will have a greater tendency to coordinate with class (a) metal ions while monothio-beta-diketonate will have a greater tendency to coordinate with class (b) metal ions.

It has been suggested by Pearson (17), that the members of classes (a) and (b) be described using the terms "hard" and "soft" respectively. Therefore a hard acid is a type (a) metal ion and a hard base is a ligand such as ammonia or the fluoride ion. Conversely, a soft acid is a type (b) metal ion and a soft base is a ligand such as phosphine or the iodide ion. In hard and soft interactions the hard species, both acids and bases, tend to be small, slightly polarizable species and the soft acids and bases tend to be large and more polarizable. A simple rule of thumb sometimes called Pearsons's principle, helps in predicting qualitatively the relative stability of complexes formed between acids and bases. This rule states that: Hard acids prefer to bind to hard bases and soft acids prefer to bind to soft bases.

Tables 5 and 6 list some hard and soft acids and

bases (16). The borderline acids and bases indicated in these tables imply that the terms hard and soft are relative ones. There is no sharp dividing line between them. Even within a group of hard or soft, not all will have equivalent hardness or softness. Therefore, even though all alkali metal ions are hard, a cesium ion, for example which is larger and more polarizable than a lithium or scandium ion will be a softer acid. Similarly, although nitrogen is usually hard because of its small size, the presence of polarizable substituents will have the effect of softening the base. Pyridine, for example, is significantly softer than ammonia and should be considered as borderline.

Hardness and softness refer to special stability of hard-hard and soft-soft interactions and should be carefully distinquished from acid and base strength. For example, both the OH^- and F^- ions are hard bases; yet the hydroxide ion is a much stronger base than the fluoride ion. It is possible for a strong acid to displace a weaker acid or a strong base to displace a weaker base, even though this appears to contradict the principle of hard and soft acids and bases. For example, a sulfite ion which is a strong, soft base can displace a fluoride ion which is a weak, hard base from a hard acid, the proton, H^+ (Equation 3). Similarly, a very strong, hard base such as the hydroxide ion, can displace this strong, soft base

Table 5

Classification of hard and soft acids

Hard acids

H^+, Li^+, Na^+, K^+(Rb^+, Cs^+)

Be^{+2}, $Be(CH_3)_2$, Mg^{+2}, Ca^{+2}, Sr^{+2} (Ba^{+2})

Sc^{+3}, La^{+3}, Ce^{+4}, Gd^{+3}, Lu^{+3}, Th^{+4}, U^{+4}, $UO2^{+2}$, Pu^{+4}

Ti^{+4}, Zr^{+4}, Hf^{+4}, VO^{+2}, Cr^{+3}, Cr^{+6}, MoO^{+3}, WO^{+4}, Mn^{+2},

Mm^{+7}, Fe^{+3}, Co^{+3}

BF_3, BCl_3, $B(OR)_3$, Al^{+3}, $Al(CH_3)_3$, $AlCl_3$, AlH_3, Ga^{+3}, In^{+3}

CO_2, RCO^+, NC^+, Si^{+4}, Sn^{+4}, CH_3Sn^{+3}, $(CH_3)_2Sn^{+2}$

N^{+3}, RPO_2^+, $ROPO_2^+$, As^{+3}

SO_3, RSO_2^+, $ROSO_2^+$

Cl^{+3}, Cl^{+7}, I^{+5}, I^{+7}

HX(hydrogen-bonding molecules)

Borderline acids

Fe^{+2}, Co^{+2}, Ni^{+2}, Cu^{+2}, Zn^{+2}

Rh^{+3}, Ir^{+3}, Ru^{+3}, Os^{+2}

$B(CH_3)_3$, GaH_3

R_3C^+, $C_6H_5^+$, Sn^{+2}, Pb^{+2}

NO^+, Sb^{+3}, Bi^{+3}

SO_2

Table 5 continued

Soft acids
$Co(CN)_5^{-3}$, Pd^{+2}, Pt^{+2}, Pt^{+4}
Cu^+, Ag^+, Au^+, Cd^{+2}, Hg^+, Hg^{+2}, CH_3Hg^+
BH_3, $Ga(CH_3)_3$, $GaCl_3$, $GaBr_3$, GaI_3, Tl^+, $Tl(CH_3)_3$
CH_2, carbenes
Pi-acceptors: trinitrobenzene, chloroanil, quinones, tetracyanoethylene, etc
HO^+, RO^+, RS^+, RSe^+, Te^{+4}, RTe^+
Br_2, Br^+, I_2, I^+, ICN, etc
O, Cl, Br, I, N, RO , RO_2
M (metal atoms)and bulk metals

Table 6

Classification of hard and soft bases

Hard bases
NH_3, RNH_2, N_2H_4
H_2O, OH^-, O^{-2}, ROH, RO^-, R_2O
CH_3COO^-, CO_3^{-2}, NO_3^-, PO_4^{-3}, SO_4^{-2}, ClO_4^-
Borderline bases
$C_6H_5NH_2$, C_5H_5N, N_3^-, N_2
NO_2^-, SO_3^{-2}
Br^-
Soft bases
H^-
R^-, C_2H_4, C_6H_6, CN^-, RNC, CO
SCN^-, R_3P, $(RO)_3P$, R_3As
R_2S, RSH, RS^-, $S_2O_3^{-2}$
I^-

from the soft acid, the methylmercury cation (Equation 4).

$$\underset{}{SO_3^{2-}} + \underset{(H-H)}{HF} \longrightarrow \underset{(H-S)}{HSO_3^-} + F^- \qquad K_{eq} = 10^4 \qquad 3$$

$$OH^- + \underset{(S-S)}{CH_3HgSO_3^-} \longrightarrow \underset{(S-H)}{CH_3HgOH} + SO_3^{2-} \qquad K_{eq} = 10^7 \qquad 4$$

Therefore because of the strengths of these bases ($SO_3^{2-} > F^-$) and ($OH^- > SO_3^{2-}$) reactions 3 and 4 were forced to the right in spite of the hard and soft acid and base principle. If, however, a competitive situation existed in which both strength and hardness-softness must be considered, the hard-soft principle works (Equations 5 and 6).

$$\underset{(S-H)}{CH_3HgF} + \underset{(H-S)}{HSO_3^-} \longrightarrow \underset{(S-S)}{CH_3HgSO_3^-} + \underset{(H-H)}{HF} \qquad K_{eq} = 10^3 \qquad 5$$

$$\underset{(S-H)}{CH_3HgOH} + \underset{(H-S)}{HSO_3^-} \longrightarrow \underset{(S-S)}{CH_3HgSO_3^-} + \underset{(H-H)}{H_2O} \qquad K_{eq} > 10^7 \qquad 6$$

Thus when considering acid-base interactions one must consider both strength and hardness-softness. Table 7 lists the strengths of various bases toward the proton, H^+, and the methylmercury cation, CH_3Hg^+ (16).

Table 7

Basicity toward the proton and methylmercury cation

Base	Linking atom	pK_s (CH_3Hg^+)	pK_h (H^+)
F^-	F	1.50	2.85
Cl^-	Cl	5.25	-7.0
Br^-	Br	6.62	-9.0
I^-	I	8.60	-9.5
OH^-	O	9.37	15.7
HPO_4^-	O	5.03	6.79
S^{2-}	S	21.20	14.2
$HOC_2H_4S^-$	S	16.12	9.52
SCN^-	S	6.05	4
SO_3^{2-}	S	8.11	6.75
$S_2O_3^{2-}$	S	10.90	negative
NH_3	N	7.60	9.42
$NH_2C_6H_4SO_3^-$	N	2.60	3.06
$(C_6H_5)_2PC_6H_4SO_3^-$	P	9.15	0
$Et_2PC_2H_4OH$	P	14.6	8.1
Et_3P	P	15.0	8.8

$pK_s = \log[CH_3HgB]/[CH_3Hg^+][B]$ $\quad pK_h = \log[HB]/[H^+][B]$

Bases such as the sulfide ion (S^{2-}) and triethylphosphine (Et_3P) are very strong toward both the methylmercury ion and the proton but about a million times better toward the

methylmercury ion, therefore they are considered to be soft. The hydroxide ion (OH^-) is a strong base toward both acids, but in this case about a million times better toward the proton, therefore it is considered to be hard. The fluoride ion (F^-) is not a particularly good base toward either acid, but slightly better toward the proton as would be expected since it is a hard base.

ii) Theoretical basis of hardness and softness.

Pearson (18) pointed out an interesting irregularity between the rule of hard and soft acids and bases and Pauling's original method of defining electronegativity. According to the latter, the greatest bond energies would occur when bonds are formed between elements furthest apart in electronegativity, such as cesium and fluorine. Based on this principle one would therefore expect the following reaction to proceed as shown in equation 7.

$$CsI + LiF \longrightarrow LiI + CsF \qquad 7$$

Experimentally, however, it is found that the reaction actually proceeds in the reverse direction where the two harder species (Li^+, F^-) prefer each other and the two softer species (Cs^+, I^-) also seem to prefer each other (equation 8).

$$LiI + CsF \longrightarrow LiF + CsI \qquad \triangle H = \sim -63\ kJmol^{-1} \qquad 8$$

By considering the heats of atomization of the four compounds in equation 7: LiF = +573, CsF = +502, LiI = +347 and CsI = +335 ($kJmol^{-1}$) it can be seen that the hard-hard interaction (LiF) forms the strongest bond, while the soft-soft interaction is the least stable. It appears that the driving force for equation 8 is the hard-hard interaction and that this causes the reaction to proceed to the right in spite of the weak soft-soft interaction (rather than being hindered by it as might have been expected). A similar result is obtained as shown in equation 9 in which a more typical soft-soft species is involved.

$$\underset{(S-H)}{HgF_2} + \underset{(H-S)}{BeI_2} \longrightarrow \underset{(H-H)}{BeF_2} + \underset{(S-S)}{HgI_2} \qquad \Delta H = \sim -397\ kJmol^{-1} \qquad 9$$

The heats of atomization of the species are: BeF_2 = +1264, HgF_2 = +536, BeI_2 = +577 and HgI_2 = +293 ($kJmol^{-1}$). The driving force for this reaction is almost entirely the very high bond energies in BeF_2. The extremely high bond energy of the hard-hard interaction is thought to be due to the possibility that these two atoms can form a strong covalent bond as well as the possibility of forming a strong electrostatic attraction. As pointed out earlier, hard species (both acid and base) tend to be small,

slightly polarizable species and soft acids and bases tend to be larger and more polarizable. Small atoms form stronger covalent bonds because their orbitals have the largest overlap and large atoms form weaker covalent bonds due to a small amount of orbital overlap. The electrostatic energy of an ion pair is inversely proportional to the interatomic distance; thus, the smaller the ions involved the greater is the attraction between the acid and base. Attempts to calculate the relative importance of these two methods of bonding are only approximate, but they indicate that each contributes to an appreciable extent in LiF. Of the total energy of the LiF bond (573 $kJmol^{-1}$) approximately one fourth comes from covalent bonding, one half from an electrostatic attraction between the partial charges on the lithium and fluorine atoms (approximately 2/3 of an electrostatic charge) and about one fourth from the transfer of partial charge from the more electropositive lithium atom to the more electronegative fluorine atom (Pauling's ionic resonance energy) (19,20).

The availability of d-electrons for pi bonding has been suggested as possibly contributing to soft-soft interactions (21). Pi bonding occurs most readily in those metal ions that have low oxidation states and large numbers of d-electrons. Class (b) metal ions (soft acids) satisfy this criterion. Futhermore, the important pi

bonding ligands such as phosphines, and heavier halogens are all soft bases. The presence of d-orbitals on the ligand enhances the pi bonding. Therefore the second row elements N, O and F cannot partake in this type of interaction due to the lack of pi bonding orbitals. It should also be pointed out that London dispersion energies increase with increasing size and polarizability and might thus stabilize a bond between two large, polarizable soft atoms.

In review, one might say that the strong hard-hard interactions are due to the ability of the two atoms to form bonds which are both covalent and ionic, while the weak soft-soft interactions are attributed only to the pi bonding abilities of the acid and base and to some extent London dispersion energies. Thus when referring to a hard and soft acid-base reaction (equations 8 and 9) one might say that; Soft acids prefer to bond to soft bases only while hard acids are preferentially bonded to hard bases.

iii) HSAB theory applied to halogen transfer in mass spectrometry.

Miller et al.(22) have discussed the application of hard and soft acid base (HSAB) theory to the phenomenon of halogen transfer in 70eV electron impact mass spectra of organometallic compounds; in particular fluorine transfer from fluoroaromatic ligands such as C_6F_5. When the spectra

of the series $(C_6X_5)_2Hg$ (X = F, Cl and Br) were examined the observations in table 8 were made.

Table 8

Molecule	Rearrangement ions	% observed
$(C_6F_5)_2Hg$	HgF^+ or $C_6F_5HgF^+$	-
$(C_6Cl_5)_2Hg$	$HgCl^+$ or $C_6Cl_5HgCl^+$	-
$(C_6Br_5)_2Hg$	$C_6Br_5HgBr^+$	8.2
"	$HgBr_2^+$	1.2
"	$HgBr^+$	0.7

In comparison, spectra of C_6X_5 derivatives of groups IV and V elements (all reasonably hard acids with respect to the halide as the base) gave the following results. For $(C_6F_5)_4M$ (M = Si, Ge, Sn and Pb) MF^+ is maximized for M = Sn, MF_3^+ is maximized for M = Si, $(C_6F_5)_2MF^+$ is maximized for M = Sn, $C_6F_5MF_2^+$ is maximized for M = Sn and the MF_n neutral species are maximized for Si and Ge. Similarly, for $(C_6F_5)_3M$ (M = P, As and Sb) M^+, MF^+, MF_2^+ and $C_6F_5MF^+$ species are maximized for M = Sb while the MF_n neutral species are maximized for M = P or Sb (no statement was made with regard to how data pertaining to relative intensities of the neutral species were obtained).

If the halide is treated as the base and the central atom as the acid, these data make sense in terms of HSAB theory. Mercury, being particularly soft favours the

softer bromide ligand in preference to the harder fluoride or chloride ligands. The elements of groups IV and V, all being reasonably hard acids, favour the harder fluorine ligand. Similarly a series of C_6F_5Pt derivatives was studied, and for none of these was any Pt-F containing species observed. However, for the slightly softer chlorine from platinum systems containing aromatic chlorides, slight traces of Pt-Cl containing species were observed.

Even though the original work on HSAB theory in solution (23) suggested that solution factors might be critical, preventing any predictions concerning behavior in the gas phase, Miller et al, based on these previous data, suggested that these interactions may indeed persist even in the gas phase. Morris and Koob (24) later suggested that Miller's hypothesis might be tested by checking to see whether HSAB theory could correctly predict the importance of fluorine migration in mass spectra of fluorinated metal beta-diketonates, for it had been well established by observation of metastable transitions that these rearrangements occur as unimolecular gas-phase ion reactions (25). The complexes of the anions of Hhfa with Co(II), Fe(II), Fe(III), Cr(III), Al(III), Zn(II), Ni(II), Mn(II) and Cu(I) were examined in a mass spectrometer. Many exhibited peaks corresponding to rearrangement of a fluorine to metal, and

several demonstrated the loss of neutral metal fluorides via metastable transitions (table 9).

Table 9

Fluorine Migration to Metal for some $M(hfa)_n$ Chelates

Metal	Neutral frament MF_n	Precursor ion $MF_x(L\text{-}CF_3)^+$
Mn(II)	C	C
Al(III)	E	C
Cr(III)	C	C
Fe(III)	C	C
Fe(II)	C	C
Co(II)	C	C
Ni(II)	C	C
Zn(II)	D	C
Cu(I)	D	D

n = 2, 3. x = 1, 2. C = Reaction indicated by metastable transition. D = Product not observed. E = AlF_2L is eliminated as a neutral in formation of this product.

Rearrangement of fluorine to the metal to form either M-F containing ions or neutral species occurs as shown in figure 12, with the exception of the Cu(I) chelate.

Morris and Koob had found no conflict between the hypothesis of Miller et al and their data, even though

Figure 12

Generalized Scheme for Fluorine Rearrangement to Metal and loss of Neutral Metal Fluorides for $M^{III}(hfa)_3$

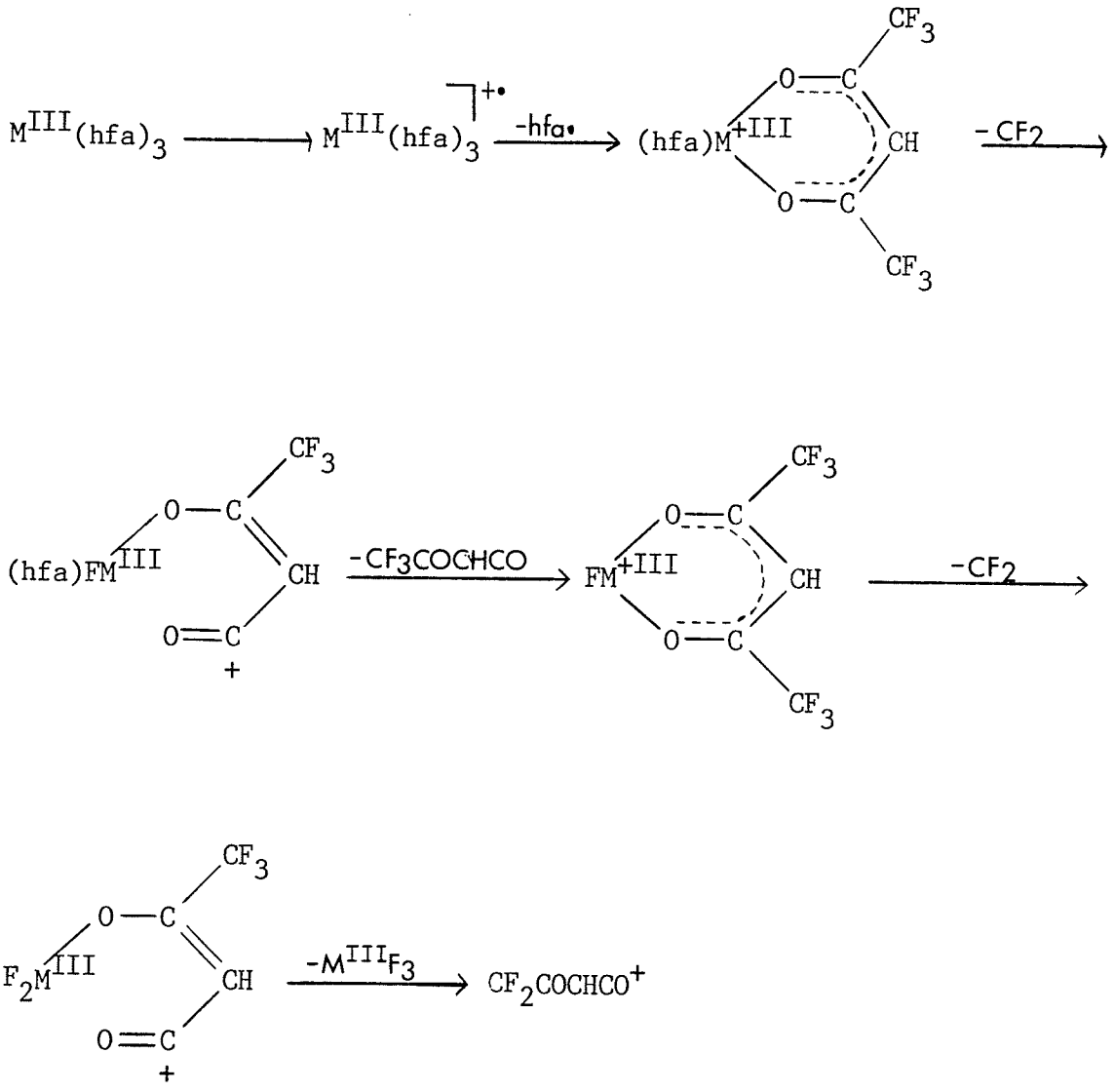

HSAB theory could not account for small differences in some of the rearrangement reactions indicated above. For example, elimination of neutral AlF_2L instead of AlF_3 as in the $Cr(hfa)_3$ and $Fe(hfa)_3$ chelates, or in the case of $Zn(hfa)_2$ where a neutral metal fluoride did not appear to be produced even though the mass spectra contained evidence that migration of fluorine to the metal occurred.

In the gas phase, since no solvent is present, the acidity of the metal is influenced only by its ligands. Among the fluorinated or partially-fluorinated beta-diketonates the hardest acid case would be the hfa chelates. If a CF_3 group was to be replaced with a more electron rich species such as a methyl, ethyl, isopropyl, phenyl or a thienyl group for example, resulting in the softening of the acidity of the metal, the expected consequence would be that fluorine rearrangement to the metal is less prevalent. Relevant data for complexes of $(CF_3COCHCOR)_3M$ are given in table 10 (24). As expected, it seems that fluorine rearrangement ions become less important (lower relative intensity) as the softness of the metal environment increases.

A number of the beta-diketonate chelates shown in table 10 give rise to a reaction in which HF is lost (figure 13). In all cases this loss was verified by a metastable peak (24). $Cr(hfa)_3$, however, is the only hfa chelate to demonstrate this loss, while if one of the CF_3

Figure 13

Generalized Scheme for Loss of HF

from a) $M^{III}L_3$ and b) $M^{II}L_2$

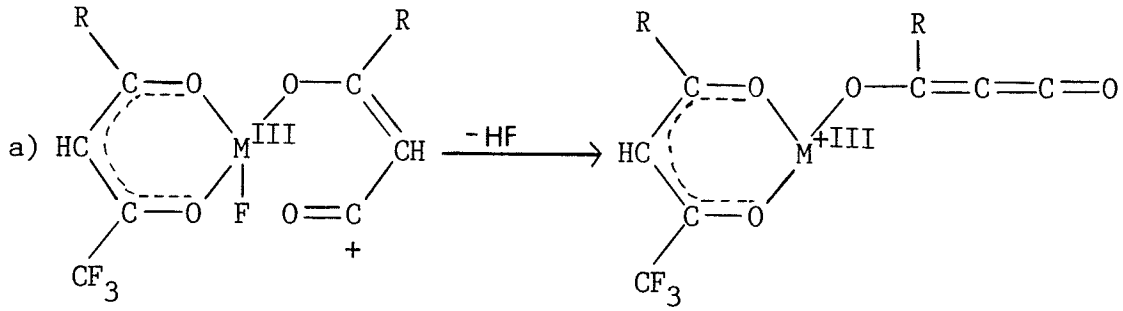
a)
HC
M III
F
CH
O=C
+
CF3
-HF
+III

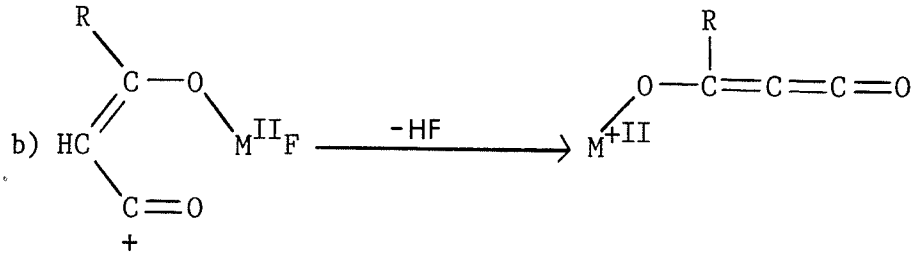
b)
HC
M II F
C=O
+
-HF
+II

substituents is replaced by methyl or phenyl, iron and aluminum chelates demonstrate HF loss as well. For ligands containing other halogens (in addition to fluorine), deuterium labeling showed that HF loss involved only the γ-hydrogen (or bridging hydrogen) of the ligand. It was therefore concluded that softening the metal environment weakened its ability to compete with the proton for the fluorine.

Table 10

Fluorine Rearrangement Ions for $(CF_3COCHOR)_3M$[a]

	CF_3	CH_3	C_2H_5	$i\text{-}C_3H_7$	$t\text{-}C_4H_9$	C_6H_5	C_4H_3S
$Fe^{III}F_2(L\text{-}CF_3)^+$	5	1.5	0.3	0	0	1.5	2
$Fe^{II}F(L\text{-}CF_3)^+$	80	46	33	30	29	27	25
$Cr^{III}F_2(L\text{-}CF_3)^+$	20	12	7	4	0	9	b
$Cr^{II}F(L\text{-}CF_3)^+$	21	20	16	17	14	13	0

[a] Intensity relative to $ML_2^+ = 100$. [b] Data not taken.

CHAPTER 2

EXPERIMENTAL

PART A: MEASUREMENT OF MASS SPECTRA

All the spectra were obtained using a Hitachi Perkin-Elmer RMU-6D single focusing mass spectrometer and recorded on a Honeywell model 1508 visicorder. The samples were introduced into the ion source with a solids inlet probe that was warmed from room temperature until reproducible mass scans, characteristic of the compound and the minimum backbround interference, were achieved. Spectra were recorded at this point.

The sample temperatures were different for each compound depending on its particular volatility. The ionization chamber temperature was approximately 100°C. All the spectra were recorded at an ionizing energy of 70 eV.

PART B: PREPARATION OF LIGANDS AND TRANSITION METAL COMPLEXES

i) Preparation of ligands

The simplest and most efficient method for the preparation of monothio-beta-diketonates is the reaction of the appropriate beta-diketonate with hydrogen sulfide (26). To get satisfactory yields of the desired products using this method, however, does require very strict control of the experimental conditions such as acidity of the medium and temperature.

A) Monothioacetylacetone (HSacac)

Monothioacetylacetone was prepared as described by Duus et al (27). A solution of acetylacetone (20.0g ; 0.2moles) in 300 ml of acetonitrile was cooled to -50°C and a stream of hydrogen sulfide gas was bubbled through it for 1.5 hours, during which time the temperature was allowed to rise to -40°C. A low temperature bath consisting of CO_2 and acetonitrile was used to attain these temperatures. While keeping the reaction temperature carefully at -40°C a stream of dry HCl was then bubbled through the solution for 1.5 hours. After a further supply of H_2S gas had been bubbled through the reaction solution for two hours at -40°C, the reaction mixture was poured into a mixture of 500 ml ice-water,

300 ml pentane and 100 ml of ether while stirring. The layers were separated and the aqueous layer extracted five times using 200 ml of a 3:1 mixture of pentane and ether. The combined organic extracts were washed twice with water and dried using $CaSO_4$. Solvents were removed at room temperature using a rotary evaporator, leaving a reddish-yellow oil as the crude product. Since monothio-acetylacetone is thermally unstable and distillation of the crude product at reduced pressures leads to partial decomposition, no purification of the crude product was attempted.

The proton nmr spectrum of the crude product (figure 14) shows four sharp signals at δ 2.10(3H), 2.34(3H), 6.14(1H) and 13.22(1H). These results would seem to indicate the existence of either of the tautomers B or C shown in figure 15. Some work done by Duus et al. (27), however, indicates that these two tautomers exist as an equilibrium mixture with the equilibrium percentage of C estimated to be some what higher than 25%.

Chelated enethiolic protons give rise to signals in the region δ 4.8-8.5, while enolic protons give rise to signals in the region δ 12-17 (28). It is seen, however, from the proton nmr of this ligand (figure 15) that the signal which represents the chelated proton occurs at δ 13.22. This is evidence supporting the existence of a mixture of tautomers B and C. In beta-thioxo ketones it

Figure 14

Proton NMR spectrum of monothioacetylacetone

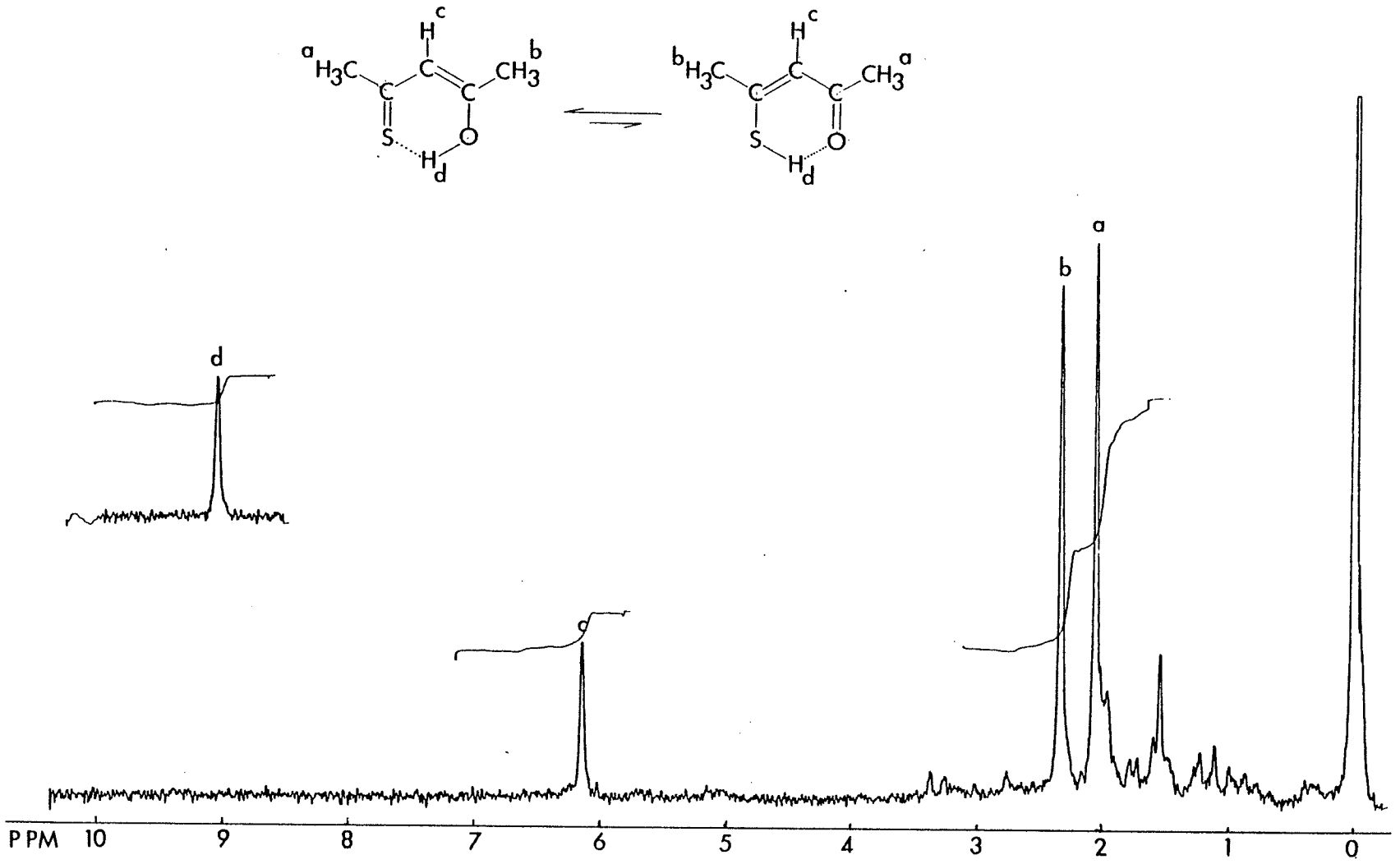
a
H3C
H
c
C
CH3
b
C
C
S
O
Hd
b
H3C
H
c
C
CH3
a
C
C
S
O
Hd
d
b
a
PPM
10
9
8
7
6
5
4
3
2
1
0

is thought that there is a very rapid interconversion between these equilibrated tautomers (27). If the interconversion B$\rightleftharpoons$C takes place at a rate much higher than the difference in resonance frequencies between the nmr signals from the two tautomers, a single spectrum will be observed, where the protons of the resonance signals are weighted averages of the chemical shifts of the seperate tautomers.

B) Trifluoromonothioacetylacetone (HStfacac)

Trifluoromonothioacetylacetone was prepared as described by Ho et al (29). A solution of trifluoro-acetylacetone (5.0g ; 32.5 mmol) in 200 ml ethanol was cooled to -70°C using a low temperature ($EtOH/CO_2$) bath. Streams of H_2S and dry HCl were then bubbled through the reaction mixture for 20 and 10 minutes, respectively. The reaction flask was then fitted with a calcium chloride tube to prevent access of moisture and allowed to warm to room temperature. After standing overnight, thus allowing the reaction to go to completion, the reaction mixture was extracted five times with light petroleum ether and dried over anhydrous sodium sulfate. The solvent was then removed at room temperature using a rotary evaporator, to leave a red liquid as the crude product. As with HSacac this ligand is thermally unstable and distillation of the crude product at reduced pressure

Figure 15

Potential tautomeric forms of ligands H(Sacac) and H(Stfacac)

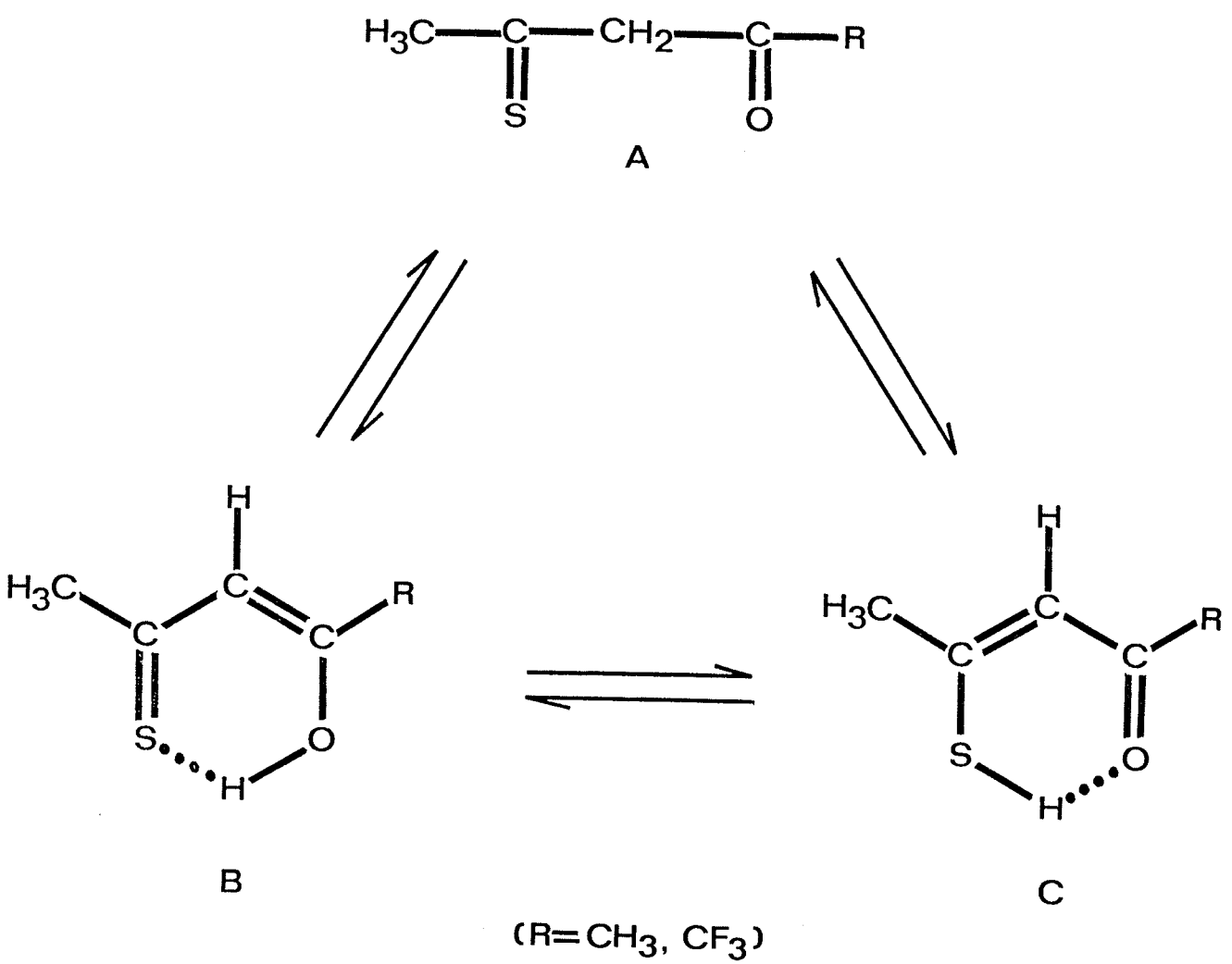
H3C
C
CH2
C
R
S
O
A
H
H3C
C
R
C
S
O
H
B
H
H3C
C
R
C
S
O
H
C
(R=CH3, CF3)

leads to partial decomposition, therefore no purification was attempted.

The proton nmr spectrum of the product shown in figure 16, shows three sharp signals at δ 2.26(3H), 6.74(1H) and 8.32(1H). Using the same argument to prove the existence of an equilibrium mixture of tautomers B and C in HSacac, (enethiolic proton occurs at δ 8.32) it seems clear that in HStfacac the equilibrium lies substantially in the direction of the enethiolic tautomer C.

The pure ligands were obtained from the companies listed below.

Ligand	Company
Hacac	Fisher Scientific Co.
Htfa	PCR Research Chemicals Inc.
Hhfa	PCR Research Chemicals Inc.

ii) Preparation of Transition Metal Complexes

$Rh(acac)_3$

$Rh(acac)_3$ was prepared as described by Dwyer et al. (30) with some minor differences. To a solution of $Rh(NO_3)_3$ (0.10g ; 0.31mmol) in 10 ml of 0.2M nitric acid was added a 10% solution of sodium bicarbonate until the pH reached 4.0. At this pH rhodium hydroxide just begins to form. Acetylacetone (5.0g ; 50mmol) was then added and

Figure 16

Proton NMR spectrum of

trifluoromonothioacetylacetone

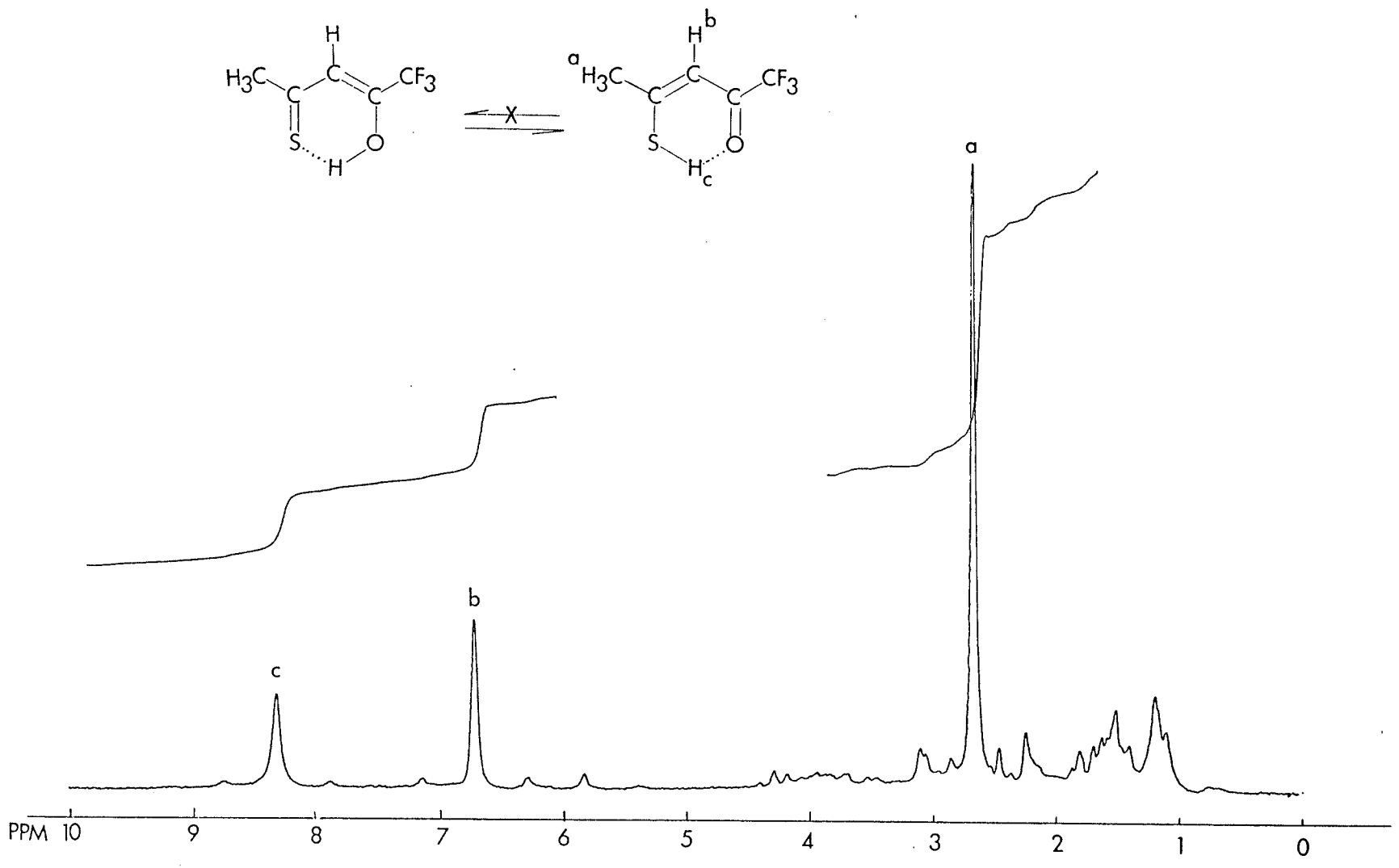
H
H3C
C
CF3
C
S
O
H
X
a
H3C
H
b
C
CF3
C
S
O
Hc
a
b
c
PPM 10
9
8
7
6
5
4
3
2
1
0

the reaction mixture was refluxed for 45 minutes (readjusting the pH after 30 minutes). The reaction mixture was then allowed to cool, after which it was extracted three times with chloroform. The solvent was removed at room temperature using a rotary evaporater, to leave a crude orange-yellow product behind. The crude product was then recrystallized from aqueous methanol.

$Rh(tfa)_3$

This complex was prepared using a method suggested by Fay et al. (31). $Rh(NO_3)_3$ (0.13g ; 0.40mmol) in water was treated with solid sodium bicarbonate. Once a pH of 4.0 was attained trifluoroacetylacetone (0.18g ; 1.17mmol) was added and the reaction mixture was refluxed for 30 minutes. Sodium bicarbonate was again added to the reaction mixture until the pH reached a value of 5.0. This was followed by refluxing for an additional 15 minutes. The reaction mixture was cooled, dried over sodium sulfate and the solvent was removed. The product was bright yellow in color and was purified by TLC using a 1:2 $CHCl_3$/hexanes solvent system.

$Rh(hfa)_3$

$Rh(hfa)_3$ was prepared in a similar manner to that suggested by Collman et al. (32). $Rh(NO_3)_3$ (0.13g ; 0.40mmol) in water was treated with a 10% aqueous sodium

bicarbonate solution until rhodium hydroxide just began to precipitate. To this solution hexafluoroacetylacetone (0.25g ; 0.40mmol) was added and the resulting reaction mixture was refluxed for 30 minutes. The solution was then cooled and more aqueous sodium bicarbonate added until once again rhodium hydroxide began to precipitate. The mixture was then refluxed for an additional 30 minutes. Using chloroform the product was extracted and dried over sodium sulfate. The solvent was removed at room temperature using a rotary evaporator, leaving behind a yellow-orange crystalline product.

$Rh(Sacac)_3$

$Rh(Sacac)_3$ was prepared as described by Kawanishi et al.(33). To a solution of monothioacetylacetone (100mg ; 0.86mmol) in 10 ml of ethanol, a solution of $RhCl_3 \cdot 3H_2O$ (86.2mg ; 0.33mmol) in 10 ml of hydrochloric acid (0.1M) was added. The pH of the resulting solution was then adjusted to 2.5 using sodium hydroxide (0.2M). After standing for five hours at room temperature the reaction mixture was extracted with chloroform, washed with water and dried over sodium sulfate. The solvent was then removed at room temperature leaving a product which contained a mixture of both the desired product and rhodium dithioacetylacetone. This mixture was then chromatographed on a column packed with dry silica gel.

The yellow band, containing the $Rh(Sacac)_3$ was isolated by extraction with dichloromethane. Removal of the solvent left behind a yellow-brown crystalline product.

$Rh(tfSacac)_3$

This complex was prepared using a modification to that used in the preparation of tris(1,1,1-trifluoro-4-mercapto-5-methyl-3-en-2-anato)rhodium(III) by Livingstone et al.(34). $Rh(Cl)_3 \cdot 3H_2O$ (0.5g ; 1.85mmol) in 15 ml ethanol was added to a solution of monothiotrifluoro-acetylacetone (1.0g ; 6.1mmol) in 15 ml ethanol. The reaction mixture was refluxed for 2 hours, cooled and then extracted with chloroform. The removal of the solvent at room temperature left a dark red-brown product.

$Pd(acac)_2$, $Pd(tfa)_2$ and $Pd(hfa)_2$ were all prepared as given by Okeya et al.(35) with some minor differences.

$Pd(acac)_2$

To a solution of $K_2[PdCl_4]$ (1.63g ; 5.0mmol) and acetylacetone (2.50g ; 25.0mmol) in 10 ml water, 4 ml sodium hydroxide (5M) was added with constant stirring to form a yellow precipitate. This precipitate was vacuum filtered and washed with water, methanol and diethyl ether. The product was then dissolved in dichloromethane and gravity filtered to remove any insoluble materials. The solvent was allowed to evaporate at room temperature

leaving behind gold colored crystals.

$Pd(tfa)_2$

To a soluton of $K_2[PdCl_4]$ (0.98g ; 3.0mmol) in 20 ml of methanol was added trifluoroacetylacetone (1.36g ; 9mmol) with stirring. Sodium carbonate (finely ground in a mortor and pestle) was added in small quantities to produce a yellow precipitate. The addition of sodium carbonate was stopped when no more precipitate was produced. This crude product was vacuum filtered, washed with water, methanol and ether and then dried under vacuum. Recrystallization from 1:1 mixture of dichloromethane and ethanol yielded yellow needles.

$Pd(hfa)_2$

Red mercury (11) oxide (3.25g ; 15.0mmol) was dissolved in 30 ml of (1M) perchloric acid. To the resulting solution of mercury (II) perchlorate was added with constant stirring an aqueous solution of (10 ml) $K_2[PdCl_4]$ (1.63g ; 5.0mmol) kept at 0 $^{\circ}$C. A greenish-yellow precipitate appeared immediately but stirring was continued for several more minutes. To the reaction mixture a solution of sodium hexafluoroacetylacetonate was added dropwise. The sodium hexafluoroacetylacetonate had been prepared by dissolving hexafluoroacetylacetone (4.0g ; 26.0mmol) in 10 ml of sodium hydroxide (2M). The

resulting precipitate was vacuum filtered, washed several times with water and dried under vacuum. The red-brown powder was then dissolved in hexane and gravity filtered to remove any insoluble materials. The solvent was removed at room temperature to leave fine yellow needles.

$Pd(tfSacac)_2$

This complex was prepared as given by Das et al.(36) with some minor changes. $K_2[PdCl_4]$ (0.80g ; 2.5mmol) in 25 ml water was added to a solution of trifluoromonothioacetylacetone (0.85g ; 5.0mmol) in acetone (25 ml). The reaction mixture was extracted with chloroform and dried with sodium sulfate. The solvent was removed at room temperature to yield red-orange crystals.

$Ni(acac)_2$

$Ni(acac)_2$ was prepared as described by Burg et al.(37). $Ni(NO_3)_2 \cdot 6H_2O$ (2.5g ; 8.6mmol) in 50 ml of water was buffered immediately before use by adding $CH_3COONa \cdot 3H_2O$ (2.5g ; 18.4mmol). The buffered metal ion solution was shaken with an alcoholic solution of acetylacetone (2.6g ; 26.0mmol) until precipitation appeared complete. The precipitate was then vacuum filtered and washed with ethanol and water to yield a green powder as the final product.

$Ni(tfa)_2$ and $Ni(hfa)_2$

Both these nickel chelates were prepared in the same manner. To an aqueous solution of $Ni(Ac)_2 \cdot 4H_2O$ the appropriate ligand was added with constant stirring, to produce an immediate precipitate. Both precipitates were vacuum filtered and washed with ethanol and water.

Metal Complex	Ligand	$Ni(Ac)_2 \cdot 4H_2O$	Product color
$Ni(tfa)_2$	0.154g ; 1.00mmol	0.083g ; 0.33mmol	blue-green
$Ni(hfa)_2$	0.208g ; 1.00mmol	0.083g ; 0.33mmol	green

$Zn(acac)_2$

$Zn(acac)_2$ was prepared as reported by Morgan et al. (38). An excess of acetylacetone (2.47g ; 24.7mmol) was added to zinc hydroxide (1.0g ; 0.75mmol) in 20 ml of water. This reaction mixture was then refluxed for 30 minutes. On cooling well-defined colorless needles were obtained. These crystals were then filtered under vacuum and dried.

$Zn(tfa)_2$

This complex was synthesized using the method of Kidd et al.(39). To trifluoroacetylacetone (1.25g ; 8.12mmol) in 20 ml water a concentrated solution of ammonium hydroxide (0.55 ml) was added. Immediately after the addition of an aqueous solution of $ZnCl_2$ (0.56g ;

4.08mmol) to this reaction mixture a white precipitate was formed. This precipitate was filtered under vacuum and recrystallized from hot toluene.

$Co(tfa)_3$

Trifluoroacetylacetone (1.16g ; 75.0mmol) was dissolved in 12.5 ml of aqueous alcohol (40% ethanol). $Na[Co(CO_3)_3]:3H_2O$ (0.91g ; 2.50mmol) and 5 ml of nitric acid were added and the mixture allowed to reflux for 30 minutes. The resulting green precipitate was collected, washed with water, air dried and purified by column chromatography. Alumina was used as the stationary phase and a 9:1 mixture of petroleum ether and ethyl acetate used as the solvent system.

The following complexes were obtained from Dr. M. Das (Department of Chemistry, University of New South Wales).

$Pd(Sacac)_2$	$Zn(hfa)_2$	$Co(acac)_3$
$Ni(Sacac)_2$	$Zn(Sacac)_2$	$Co(Sacac)_3$
$Ni(Stfacac)_2$	$Zn(Stfacac)_2$	$Co(Stfacac)_3$

CHAPTER 3

MASS SPECTROMETRIC STUDIES

PART A GENERAL PRINCIPLES OF MASS SPECTROMETRY

i) Introduction

The principles of the single-focussing magnetic sector mass spectrometer, which was used in this study basically involve accelerating the ions formed by electron impact bombardment of a sample by an electric field and the subsequent separation of the accelerated ions by a variable magnetic field into ion beams, each with a specific mass to charge ratio (m/e). The ion beams are focused and collected, and the electric current produced by the ion beam amplified and then recorded. The intensity of the ion current indicates the amount of the ion formed. A mass spectrum consists of the relative intensities of the ion currents at different mass-to-charge ratios.*

In the ionization chamber, a beam of energetic electrons is emitted from a heated filament. These electrons strike a stream of molecules which have been introduced from the sample system and ionize the molecules in the sample stream by removing electrons from them, thus creating positive ions. These positive ions are then directed toward a series of accelerating plates, by a repeller plate which carries a positive

*In reporting mass spectra the abscissa is reported as m/z (i.e., the mass to charge number ratio), IUPAC recommendation (40).

electrical potential. A large potential difference, applied across these accelerating plates produces a beam of rapidly travelling positive ions. These ions are directed into a narrow uniform beam by one or more focusing slits.

The energy required to remove an electron from an atom or molecule is its ionization energy. The beam of electrons striking the stream of molecules should have energy from 50 to 70 electron volts to create ions with high efficiency, and to give reproducible spectra.

From the ionization chamber, the beam of ions passes through a short (approx. 10 cm) field free region. From there the beam enters the mass analyzer region where the ions are separated according to their mass-to-charge ratio.

The positive ions produced in the ion source are accelerated (i.e., gain kinetic energy) by falling through a potential of V; therefore the work done on the positive ions is eV, which is equal to the kinetic energy aquired (equation 10)

$$zV = (1/2)mv^2 \qquad \underline{10}$$

where m is the mass of the ion, v is the velocity of the ion, z is the charge number of the ion and V is the potential of the ion accelerating plates. In the presence of a magnetic field perpendicular to the direction of

motion of the positive ion beam, each ion experiences a force at right angles to both its direction of motion and the direction of the magnetic field, thereby bending or deflecting the beam of ions. The equation which yields the radius of curvature of this path is given in equation 11

$$r = mv/zB \qquad 11$$

where r is the radius of curvature of the path and B is the magnetic induction. Combining equations 10 and 11, one obtains;

$$m/z = B^2r^2/2V \qquad 12$$

This equation shows the manner of the dependence of the mass-to-charge ratio of the ions apon the magnetic field and upon the accelerating potential. The analyzer tube of the instrument is constructed to have a fixed radius of curvature, so that to focus ions of given m/z values on the detector system, either B or V must be varied. It is seen from equation 12 that increasing the magnetic field will focus heavier and heavier ions on the detector and that increasing the acceleration potential will focus successively lighter ions on the detector.

The detector of most instruments consists of an electron multiplier which produces a current that is proportional to the number of ions which strike it.

Through the use of amplifier circuits this current can be read with great sensitivity. The signal from the detector is fed to a recorder, which produces the mass spectrum itself.

ii) Types of Ions in Mass Spectra

The ionization of the gaseous sample can be carried out in numerous ways, such as electron impact, photoionization, field ionization and thermal ionization, the most popular being electron impact.

When an electron of sufficient energy (ie., 10-100eV), strikes a molecule several reactions can take place.

A) Molecular Ions

When an atomic or a molecular species is bombarded by electrons of energy between 10 and 100eV, one of the reactions is the removal of an electron from the species forming a molecular or an atomic ion whose m/e ratio gives the molecular weight of the compound. The reaction may be denoted as follows;

$$M + e \longrightarrow M^+ + 2e \qquad 13$$

B) Fragment Ions

Fragment ions are produced when various bond cleavage processes occur in the molecular ion or other

fragment ions. Their formation is determined by several factors, such as the Frank-Condon principle, the relative bond dissociation energies, the stability of the neutral fragment after cleavage, the vibrational frequencies and the number of degrees of freedom of the parent ion. The processes can be denoted as;

$$M + e \longrightarrow F_1^+ + N_1 + 2e \qquad 14$$

$$F_1^+ \longrightarrow F_2^+ + N_2 \qquad 15$$

F_1^+, F_2^+ = fragment ions

N_1, N_2 = neutral fragments

C) Rearrangement Ions

Rearrangement of atoms or groups of atoms occurs at the moment of unimolecular dissociation of the parent ions. The ions produced in the mass spectrum cannot be accounted for by a simple mechanism involving cleavage of a single bond. The reaction may be denoted as;

$$ABC + e \longrightarrow AC^+ + B + 2e \qquad 16$$

It is a general rule that reactions involving rearrangements tend to lead to products of high stability (41). This is necessary to offset the low frequency factors of these reactions. In other words, for rearrangement reactions to occur at rates which result in observable amounts of product their high entropies of

activation must be compensated by particularly low activation energies. It has been observed that a number of fluorine containing compounds show rearrangement ions under electron impact, some of which are rather random rearrangements. Rearrangements involving hydrogen atoms are very common, particulary in unsaturated hydrocarbons and saturated branched-chain hydrocarbons. It should also be noted that such rearrangements are not restricted to adjacent atoms along the carbon chain.

D) Metastable Ions

In the ion source of the mass spectrometer molecules can receive sufficient energy from impacting electrons to fragment. If the rate of decomposition is sufficiently slow, some of the metastable ions will live long enough to be repelled from the ionization chamber and begin their trip toward the accelerating region. These ions at some point disintegrate into smaller neutral molecules and new positively charged ions. These decompositions may occur along the path of the ion, from the ionization region and into the analyzer tube. If the metastable transition occurs before the ion undergoes acceleration a normal ion is formed. However, if the decomposition, say, from the "parent" ion, M_p, to the "daughter" ion, M_d, occurs in the field-free region of the mass spectrometer between the ion acceleration region and the magnetic field, characteristic peaks are recorded on the mass scale, neither at a mass

corresponding to that of M_p nor to that of M_d, but rather at an effective mass, M^*. M^* can be calculated according to the following equation (equation 17), derived by Hipple, Fox and Condon (42).

$$M^* = M_d{}^2/M_p \qquad 17$$

This equation was developed for single-focussing magnetic sector-type mass spectrometers. Some characteristics of metastable peaks are as follows;

1) They are of low intensity, about 0.01% to 1% of the base peak.

2) They usually are observed at non-integral masses.

3) They are broad and may have widths extending several mass units.

Metastable peaks can be very useful in the determination of the fragmentation processes of molecules under electron impact.

E) Multiply Charged Ions

If the electron beam is of sufficiently high energy, two electrons can be removed from the molecule or atom.

$$M + e \longrightarrow M^{2+} + 3e \qquad 18$$

$$\text{or} \quad M^+ + e \longrightarrow M^{2+} + 2e \qquad 19$$

The probability of the secondary ionization process (equation 19) is less, due to the low concentration of M^+

ions in the ion source.

Identification of ions in a mass spectrum is determined from the m/e ratios and the relative intensities of the peaks produced by the ion currents. Some chemical elements have isotopes. In a mass spectrum, if a particular ion contains such elements, the ratio(s) of the intensities of the peaks due to that ion is given by the natural abundances of the isotopes of the elements. Since the natural isotopic abundance of the common elements are all well known, the correct ratio of the peak intensities in a given ion indicates the presence of a particular element in that ion.

iii) Theory of Electron Impact Ionization

During a collision between an electron and an atom or molecule, energy can be transfered from the electron to the atomic system. According to the amount of energy transfered from the electron to the molecule, the latter may be vibrational or electronic.

This interaction of electrons with matter and the consequent absorption of energy can be explained in terms of the Frank-Condon Principle. The fundamental assumption is that the time of interaction is so short (of the order of 10^{-15}sec or less), that nuclei may be considered as fixed at their equilibrium distances during the ionization

process. Thus the molecular ion immediately after electron impact has the same nuclear configuration that it has in the ground state (43).

In terms of an energy diagram the position of the molecular ion is vertically above the point in the neutral molecule from which the transition started. Two ionization potentials may therefore be different and the magnitude of this difference will be related to the shapes of the potential functions which are appropriate to the molecule and molecular ion.

The Morse electronic potential curves for a diatomic molecule in the ground state AB and its excited states are shown in figure 17.

From the classical picture of vibrational motion, which does not differ greatly from simple harmonic motion, a vibrationally excited molecule will spend the bulk of its time at one or other of the extremes of its vibrational motions. Therefore, the transition to the ion will most likely occur from one or other of these turning points. Quantum theory, does not however agree with the classically derived picture when the lowest vibrational level of each excited electronic state is concerned and in particular the ground state vibration. In these instances as seen in figure 17A, the most probable position of the electron is not at the extremes of the classical limits, but at the center of the potential energy curve.

Figure 17

Possible Frank-Condon transitions
for the diatomic molecule AB

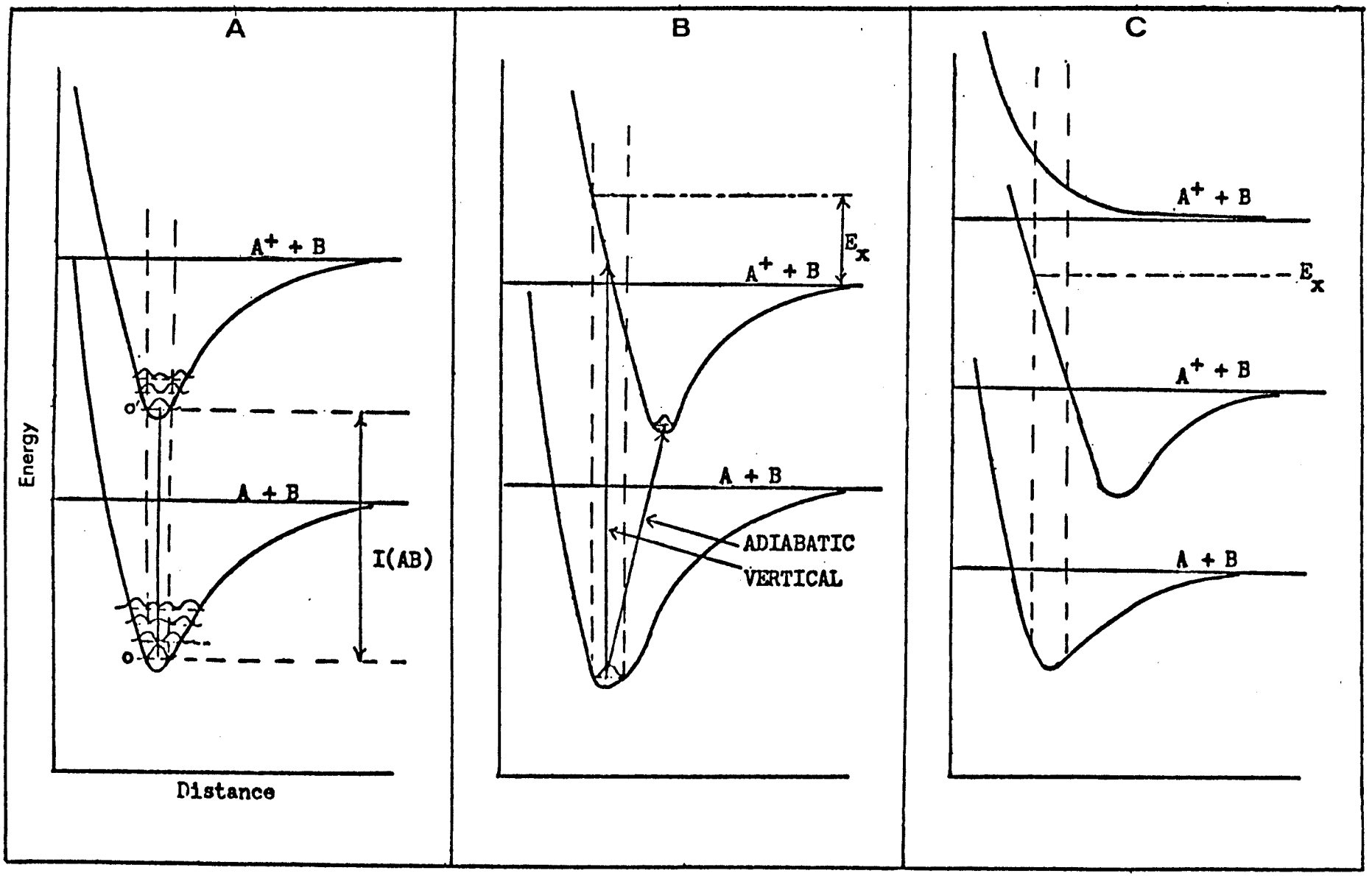
A
B
C
Energy
Distance
A+ + B
A + B
I(AB)
o'
o
Ex
ADIABATIC
VERTICAL

Therefore the vertical transitions will most probably occur from this point than from any other in this vibrational level. As already stated these transitions will be vertical ones and therefore the vibrational level at which the ion is formed will have the same internuclear distance as the neutral molecule. The vibrational level of the ion is determined both by the shape of the potential function of the ion and its possible displacement relative to that of the neutral molecule.

When equilibrium distances are very much the same for the neutral species and the ion, the vertical transition will occur with the highest probability to the lowest vibrational level of the ion (figure 17A). The resulting ionization potential will be very close to the "adiabatic" value (in other words, the energy required to remove an electron from a molecule from the lowest vibrational level of the ground electronic state to the lowest vibrational level in the first excited electronic state).

Generally the removal of an electron usually decreases the stability of the species, resulting in an increased equilibrium distance between the nuclei (figure 17B). Vertical ionization in this case leaves the ion in a vibrationally excited state of the first excited electronic state.

Finally, the internuclear distance may be so great

in the AB^+ molecule that all transitions lie in the continuum (figure 17C). Then, the dissociation of the molecule accompanies all transitions from the ground state AB to the upper electronic state.

PART B: RESULTS AND DISCUSSION

i) Mass spectra of some transition metal acetylacetonate complexes.

The dependence of fragmentation on various properties of acetylacetonates has been briefly discussed by Macdonald and Shannon (44). After the initial loss of an electron to yield the molecular ion $M^{+\cdot}$ subsequent dissociation reactions are dependent upon the odd or even electron character of the ion, the ability of the metal to change its oxidation state, the substituent groups on the ligand and as more recently proposed, dependent upon the hard and soft acid base character of both the metal and ligand (22,24,44).

Ionization of a molecule occurs through the loss of an electron and therefore the molecular ion is a radical species. Such a radical ion, either molecular or fragment, with an unpaired electron is called a odd-electron and is designated by the symbol "+·". Those ions in which the outer shell electrons are fully paired are called even-electron ions and are designated by the symbol "+". Simple homolytic cleavage of a bond in an odd-electron ion will usually yield an even-electron ion and an odd-electron neutral fragment. To produce an odd-electron ion (loss of an even-electron neutral fragment) it would be necessary for the molecular ion to undergo

multiple bond cleavage or rearrangement normally requiring a greater amount of energy than simple homolytic cleavage. The loss of even-electron fragments from odd-electron ions thus will not occur unless a driving force is present (ie., loss of extremely stable neutral even-electron fragments such as H_2O and CO).

Even-electron ions can conceivably fragment by either loss of an odd-electron neutral fragment or an even electron neutral fragment. Since loss of an odd-electron neutral fragment is accompanied by the formation of the usually less stable odd-electron ion this process is not very favorable. The loss of an even-electron neutral fragment, however, involves multiple bond cleavage or rearrangement requiring considerable energy. Therefore if sufficient excitation energy is present one may conclude that even-electron ions (with stability due to electron pairing) should give the predominant peaks in a spectrum with only minor fragmentation to odd-electron ions. Studies on organic compounds (45) show that losses of even-electron neutral fragments from even-electron ions are usually energetically more favorable than the loss of odd-electron neutral fragments and corresponding formation of odd-electron ions.

The mass spectra of $Co(acac)_3$ and $Rh(acac)_3$, obtained by direct insertion of the sample into the ion source and ionized at an electron energy of 70eV are

summarized in table 11. Also present in the mass spectra of all complexes contained in this thesis were ligand fragments, and only the most important of these are reported in the tables. They were of variable intensity and possibly could arise from ionization and fragmentation of the metal chelate or from thermal decomposition products. The mass spectrum for $Co(acac)_3$ is in good agreement with that reported by Reichert (46). Any differences may be attributed to differences in experimental conditions. The mass spectrum of $Rh(acac)_3$ did not, however, seem to be in good agreement with the earlier qualitative results reported by MacDonald and Shannon (44). Many ions with significant relative intensities in the present spectrum were not reported by them. The results do, however, agree with those reported in a more recent paper by Morris and Koob (47).

As can be seen from table 11 the base peak in the mass spectra of $Co(acac)_3$ and $Rh(acac)_3$ occurs by the loss of the odd-electron neutral species acac from the molecular ion. With this loss the resulting ion $MetL_2^+$ is an even-electron species and not likely to lose an odd-electron neutral fragment. This same result was found in a number of other transition metal acetylacetonate complexes studied by Reichert (46).

If the metal is also stable in another oxidation state it is possible for an electron to be transferred

Table 11

m/z (relative intensities) of metal-containing ions in the mass spectra of trivalent acetylacetonates, at an electron energy of 70eV. (L = acac)

Ion	Assignment	$Co(acac)_3$	$Rh(acac)_3$
M	$MetL_3^+$ (a)	356(40.0)	400(70.2)
M-18	$[MetL_3-H_2O]^+$	338(3.9)[a]	-
M-42	$[MetL_3-COCH_2]^+$	314(3.9)[a]	-
M-99	$MetL_2^+$ (b)	257(100)	301(100)[a]
M-114	$[MetL_2-CH_3]^+$ (c)	242(45.5)[b]	-
M-141	$[MetL_2-COCH_2]^+$	215(1.9)[b]	-
M-155	$LMetCOCH_3^+$	-	245(5.3)[b]
M-183	$LMetCH_3^+$ (d)	-	217(33.7)
M-197	$LMetH^+$	-	203(19.0)
M-198	$MetL^+$ (e)	158(46.7)[c]	-
M-199	$[MetL-H]^+$	-	201(19.4)[d**]
M-213	$[MetL-CH_3]^+$	143(5.5)[e]	187(6.2)
M-227	$[MetL-CHO]^+$	-	173(15.0)
M-228	$MetC_4H_5O^+$	-	172(6.4)
M-229	$MetC_4H_4O^+$	-	171(3.7)
M-241	$[MetL-CH_3CO]^+$,$Met(CO)_2^+$	115(2.4)	159(8.9)
M-243	$MetC_2H_2CO^+$	-	157(13.4)
M-254	$MetCH_3CO^+$	-	146(8.5)
M-255	$MetCOCH_2^+$	-	145(8.2)
M-256	$MetCHCO^+$	-	144(10.7)
M-257	$MetC_3H_4^+$	-	143(8.1)
M-269	$MetC_2H_4^+$,$MetCO^+$	87(7.7)	131(13.7)

Table 11 continued

Ion	Assigmnent	$Co(acac)_3$	$Rh(acac)_3$
M-270	$MetC_2H_3^+$	-	130(6.2)
M-271	$MetC_2H_2^+$	-	129(8.4)
M-282	$MetCH_3^+$	74(4.4)	-
M-297	Met^+	59(3.2)	103(8.4)
100	LH^+	m	m
85	$[HL-CH_3]^+$	m	m
71	$[L-CO]^+$	-	w
69	$COCHCO^+$	-	w
57	$CH_3COCH_2^+$	w	w
55		w	w
43	CH_3CO^+	s	s

*Identified metastable transitions are indicated by subscripts which relate the daughter ion to its precursor in column 2. (The relative intensities of the ions in the lower part of the table, which do not contain a metal atom, are indicated qualitatively by s=strong, m=medium and w=weak.)

**Metastable transition observed by morris and Koob (47)

from the ligand to the metal or vica versa thereby changing the oxidation state of the metal by one unit. A change in oxidation state will also result in changing the odd-electron ion to an even-electron ion or vica versa. Some dissociation pathways of $Co(acac)_3$ are shown in scheme 1. $Co(acac)_3$ after the loss of the odd-electron neutral species acac to form an even-electron ion CoL_2^+, may undergo a formal change in oxidation state from Co(III) to Co(II) by an electron transfer from a ligand orbital to a metal orbital (denoted by a cross-hatched arrow). This Co(II) odd-electron ion then in turn loses the neutral odd-electron radical $CH_3\cdot$ to yield $[Co^{II}L_2-CH_3]^+$ (m/z 242). That cobalt is being reduced is evident by the fact that a neutral odd-electron species such as the methyl radical is lost, for as earlier stated, the loss of an odd-electron species from an even-electron ion is energetically an unfavorable process. After the subsequent loss of the remainder of the ligand to yield $[Co^{II}L]^+$, cobalt once again undergoes reduction to cobalt in the +I oxidation state. This is evident by the presence of peaks corresponding to the ions $[Co^{I}L-CH_3]^+$ (m/z 143) and Co^{+I} (m/z 59). The relative intensities of these ions are, however, considerably less than that of the $[Co^{II}L_2-CH_3]^+$ and $Co^{II}L^+$ ions. This is presumably due to the greater stability of the cobalt in the +II oxidation state. The mass spectrum of $Co(acac)_3$ also

SCHEME 1

Suggested decomposition pathways for the formation of ions in the mass spectrum of $Co(acac)_3$. (L = acac)

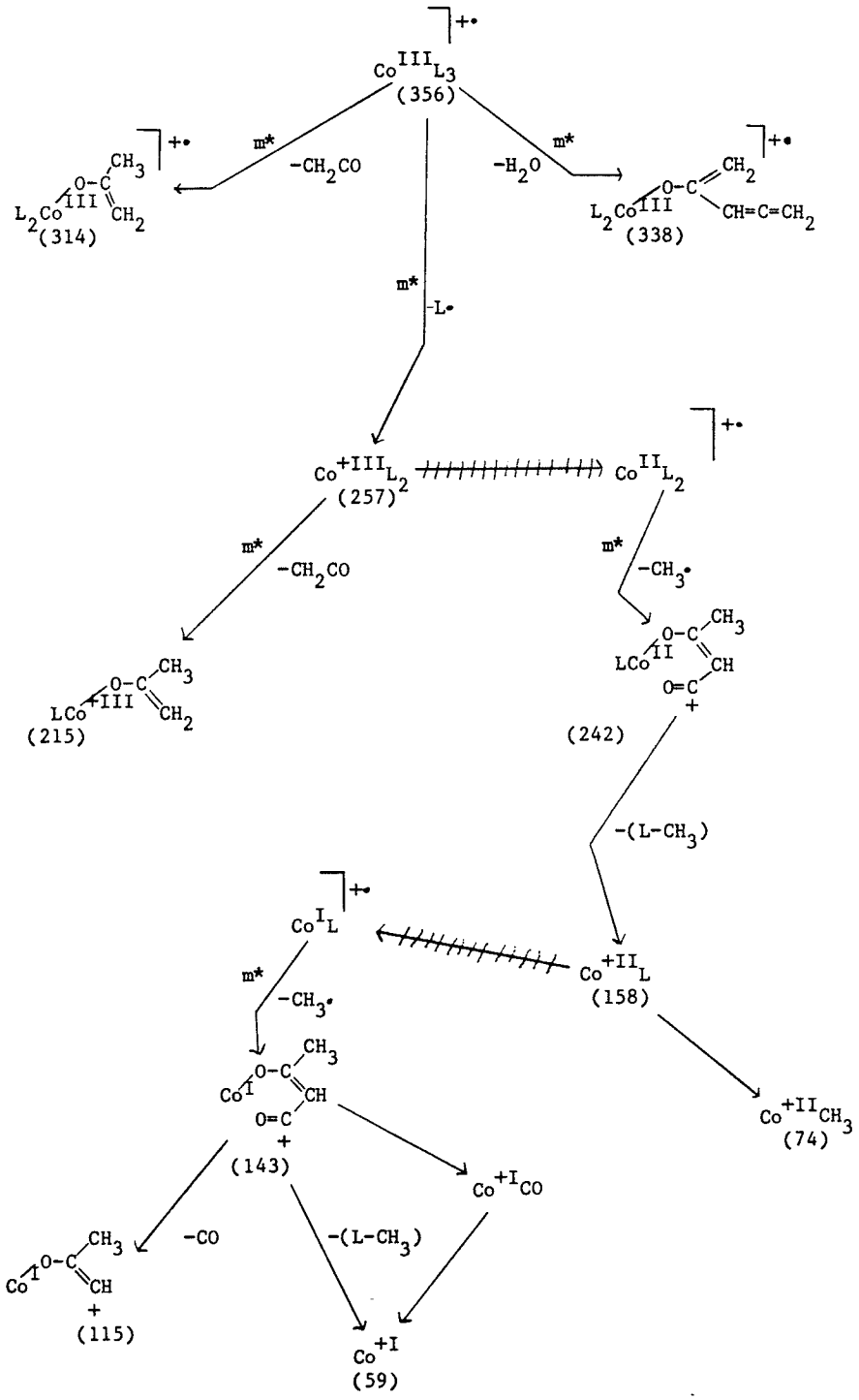

contains peaks due to the loss of even-electron neutral fragments H_2O and CH_2CO from the molecular ion. Since loss of an even-electron neutral fragment from an odd-electron ion is an energetically unfavorable process it is understandable why the ions corresponding to the loss of these neutral fragments have very low relative abundances. Both these rearrangement process are supported by the presence of a metastable transition (see table 11). The ability of cobalt in the +I oxidation state to form complexes with pi-acid ligands such as a carbonyl or alkene is indicated by the $[M-241]^+$ and $[M-269]^+$ ions.

Unlike the mass spectrum of $Co(acac)_3$ the mass spectrum of $Rh(acac)_3$ does not show evidence of metal reduction except in the most minor of dissociation reactions. Some of the most intense peaks in the mass spectrum of $Rh(acac)_3$ are due to ions corresponding to $LRhH^+$, $LRhCOCH_3^+$, $[RhL-H]^+$, $[RhL-CH_3]^+$, $\{Rh(CO)_2^+$, $RhC_2H_4CO^+\}$, $\{RhCO^+$, $RhC_2H_4^+\}$ and Rh^+. Morris and Koob (45) examined the contributions of both $RhCO^+$ and $RhC_2H_4^+$ to m/z=131 and of $Rh(CO)_2^+$ and $RhC_2H_4CO^+$ to m/z=159 via deuteration of $Rh(acac)_3$. They concluded that in both cases both the alkene and carbonyl complexes made a contribution to their respective peaks, to what extent was not indicated. The pathways leading to some fragments are indicated in scheme 2, some of which are verified by metastable peaks. Based on the formation of the peak

SCHEME 2

Suggested decomposition pathways for the formation of ions in the mass spectrum of $Rh(acac)_3$ (L = acac)

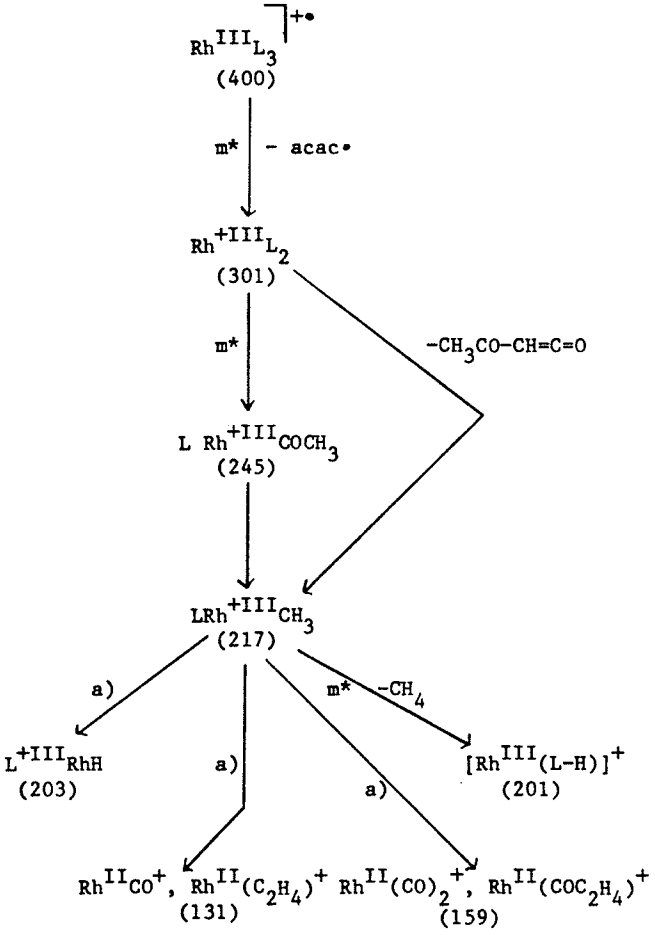

a) Similar decomposition in $Rh(tfa)_3$, verified by observation of metastable transition.

$[RhL-H]^+$ from the precursor ion $LRhCH_3^+$ through loss of methane, verified by a metastable transition, Morris and Koob had suggested that a comparable reaction might account for the peak corresponding to $[RhL-CH_3]^+$ (daughter ion to $[LRhH]^+$) since the more usual explanation for the appearance of such a peak, loss of a methyl radical from $MetL^+$, is weakend by the absence of the RhL^+ ion. Alkene and alkyne complexes account for peaks found at m/z 129, 130 and 143, while combinations of acetylene with CO and $COCH_3$ may be used to rationalize peaks m/z 157 and 172 respectively. The ease with which rhodium forms complexes with carbonyls and alkenes is not unexpected, since rhodium in the +I oxidation state is well known for its ability to form complexes with pi-acid ligands (48).

Fragmentation for divalent acetylacetonate complexes proceeds in much the same way as for the trivalent complexes. The mass spectra obtained for $Ni(acac)_2$, $Zn(acac)_2$ and $Pd(acac)_2$, by direct insertion of the sample into the ion source, at an electron energy of 70eV are shown in table 12. The base peaks in the mass spectra of $Ni(acac)_2$ and $Pd(acac)_2$ occur as the molecular ion, while the peak corresponding to the loss of a methyl radical from the molecular ion is the base peak for $Zn(acac)_2$. All three complexes show evidence of fragment ions for which the metal is in the +I oxidation state, produced by the loss of two odd-electron neutral fragments from $M^{+\bullet}$.

Table 12

m/z (relative intensities) of metal-containing ions in the mass spectra of divalent acetylacetonates, at an electron energy of 70eV. (L = acac)

Ion	Assignment	$Ni(acac)_2$	$Zn(acac)_2$	$Pd(acac)_2$
M	$MetL_2^+$ (a)	256(100)	262(87.2)	304(100)
M-15	$[MetL_2-CH_3]^+$ (b)	241(85.7)[a]	247(100)[a]	289(30.5)[a]
M-42	$[MetL_2-COCH_2]^+$	-	220(11.3)	262(7.0)
M-57	$[LMetCOCH_2]^+$ (c)	199(3.4)	205(33.3)[b]	247(5.3)
M-71	$LMetCO^+$	-	-	233(4.5)
M-84	$LMetCH_3^+$	-	-	220(4.3)
M-98	$LMetH^+$	158(36.5)	-	-
M-99	$MetL^+$ (d)	157(64.6)[b]	163(59.1)[c]	205(54.6)
M-114	$[MetL-CH_3]^+$	142(19.7)[d]	148(6.3)	190(9.6)
M-115	$[MetL_2-CH_3-HL]^+$	141(16.0)	-	189(13.0)
M-117	$[MetL-H_2O]^+$	-	145(4.8)	-
M-127	$[MetL-CO]^+$	-	-	177(16.8)
M-141	$[MetL-COCH_2]^+$	-	-	163(6.2)
M-155	$MetCH_3CO^+$	-	-	149(24.4)
M-157	$MetCHCO^+$	-	-	147(11.2)
M-170	$MetCO^+$, $MetC_2H_2^+$	86(18.5)	-	134(13.4)
M-171	$MetC_2H_3^+$	-	-	133(17.9)
M-183	$MetCH_3^+$	-	-	121(14.3)
M-198	Met^+	58(16.0)	64(6.2)	106(13.7)
100	LH^+	s	s	s
99	L^+	-	-	w
85	$[HL-CH_3]^+$	m	s	m

Table 12 continued

Ion	Assignment	$Ni(acac)_2$	$Zn(acac)_2$	$Pd(acac)_2$
71	$[L-CO]^+$	-	-	w
69	$COCHCO^+$	w	w	w
57	$CH_3COCH_2^+$	w	w	w
55		w	w	w
43	CH_3CO^+	s	s	s

*Values of m/z are based on ^{58}Ni, ^{64}Zn, and ^{106}Pd. Identified metastable transitions are indicated by subscripts which relate the daughter ion to its precursor in column 2. (The relative intensities of the ions in the lower part of the table, which do not contain a metal atom, are indicated qualitatively by s=strong, m=medium and w=weak.)

By observing the peak intensities of the $[MetL-CH_3]^+$ and Met^+ ions for each metal it is evident that Ni, having the greatest abundances of these ions, is the most stable in the +I oxidation state followed by Pd then Zn.

The pi-bonding ability of Pd is manifested by the numerous Pd-carbonyl ions present (m/z 233, 149 and 134). Here the filled Pd d orbitals overlap with the empty p-pi antibonding molecular orbitals of the carbonyl. Ni also demonstrates the same ability although to a lesser extent (m/z 86). Some suggested decomposition pathways for the formation of ions in the mass spectra of these three divalent acetylacetonates are shown in schemes 3-5.

SCHEME 3

Suggested decomposition pathways for the formation of ions in the mass spectrum of $Ni(acac)_2$ (L = acac)

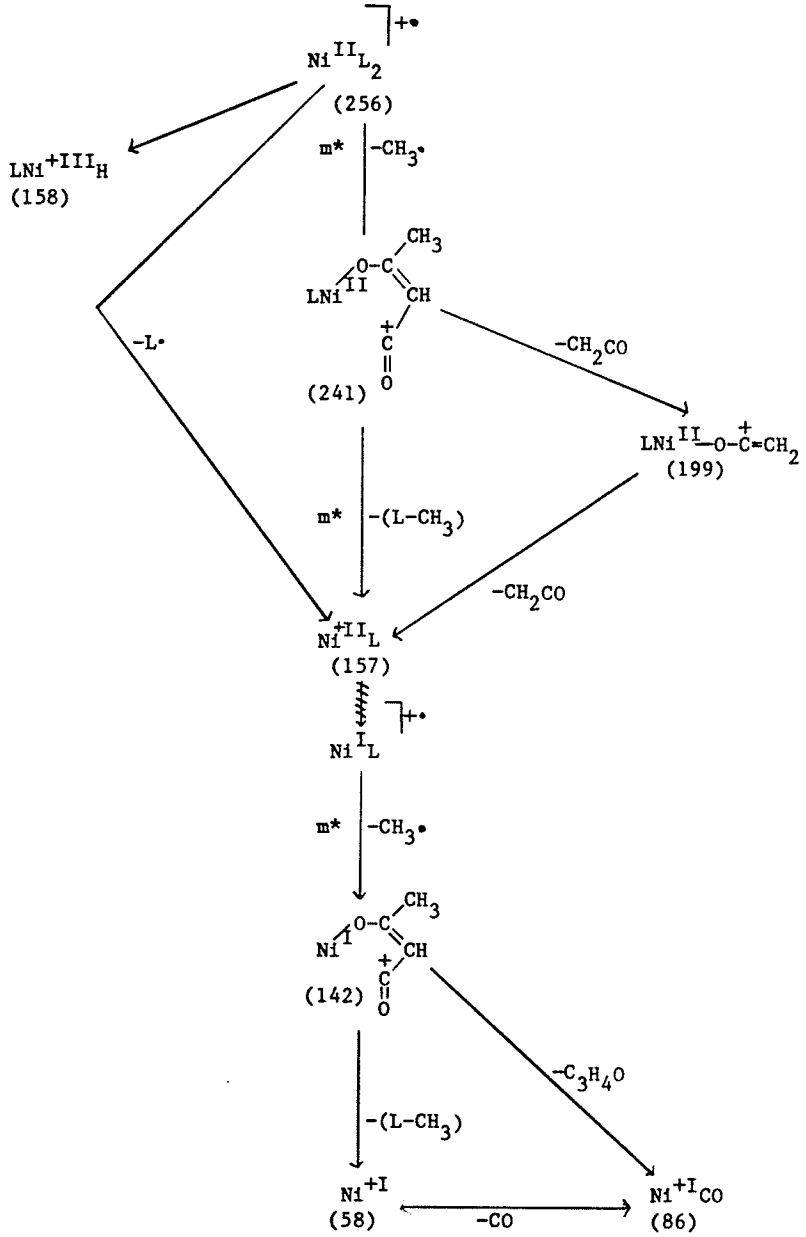

SCHEME 4

Suggested decomposition pathways for the formation of ions in the mass spectrum of $Zn(acac)_2$ (L = acac)

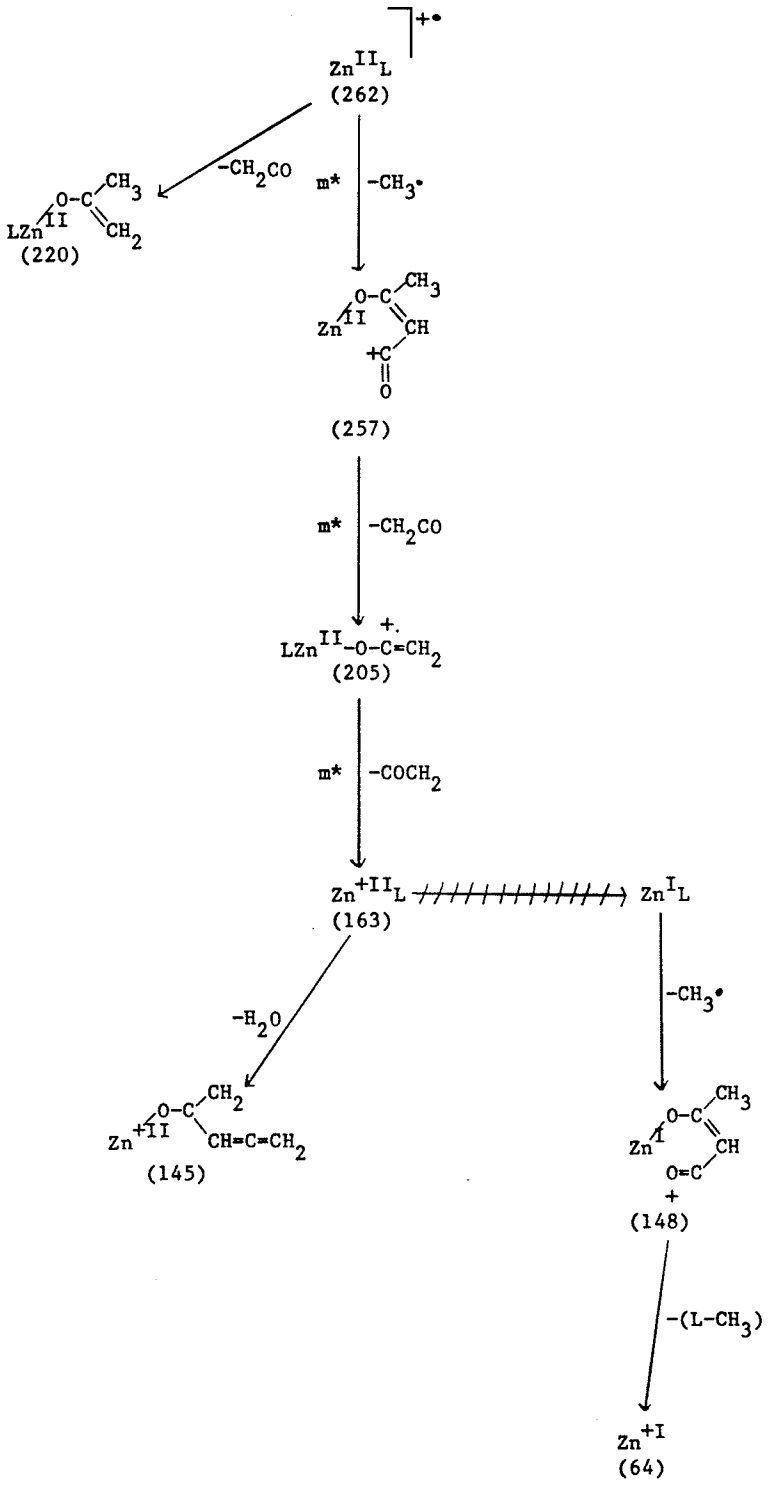

SCHEME 5

Suggested decomposition pathways for the formation of ions in the mass spectrum of $Pd(acac)_2$ (L = acac)

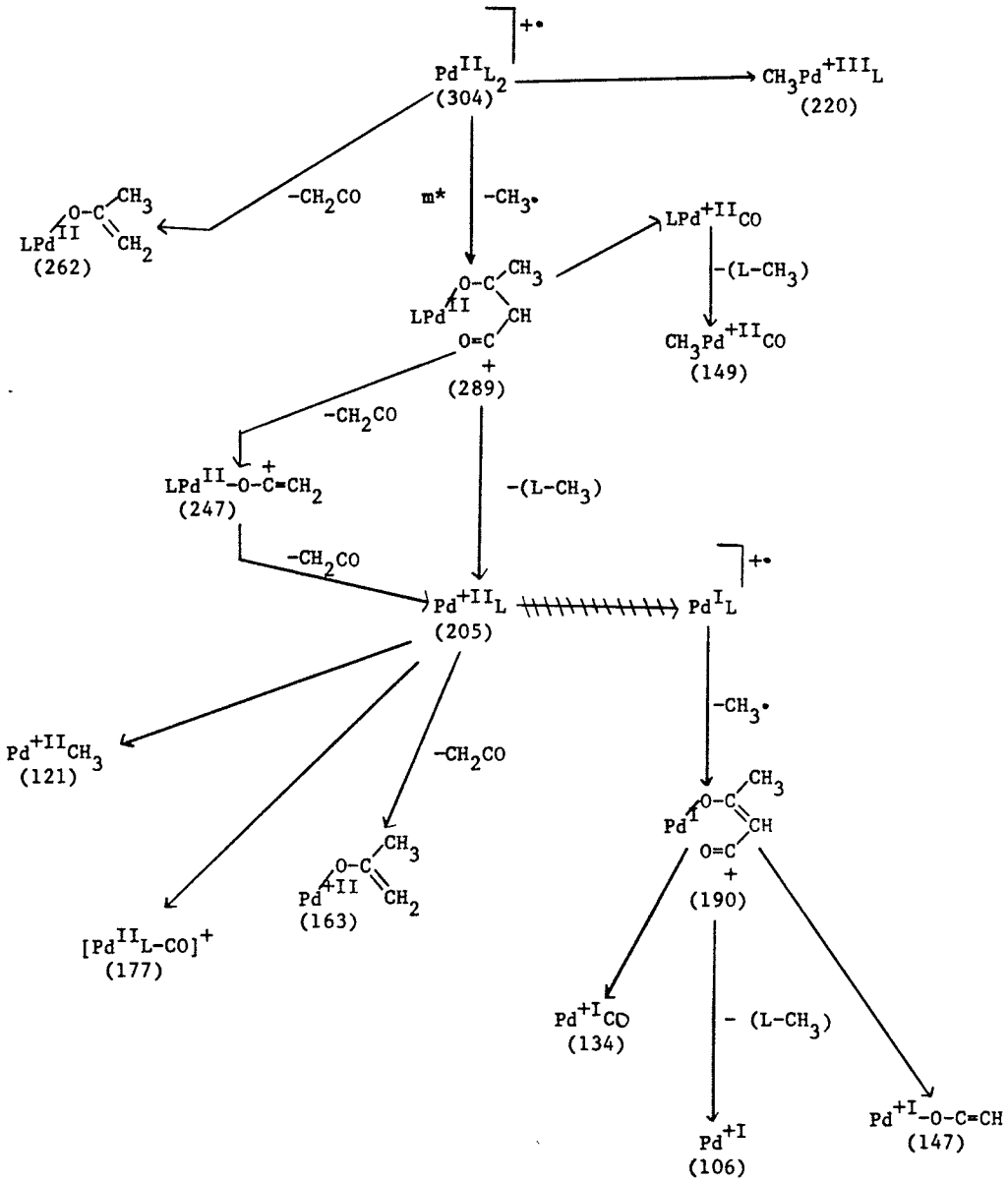

ii) Mass spectra of some fluorinated transition metal acetylacetonates

The relative intensities of all metal-containing ions in the mass spectra of trifluoro- and hexafluoro-acetylacetonates of divalent Ni, Zn and Pd and trivalent Co and Rh are given in tables 13-16, respectively.

The results are consistent with the facile loss of one odd-electron neutral fragment (•F, $•CF_3$, $•CH_3$, •acac, •tfa and •hfa) as discussed for the acetylacetonates, after which further odd-electron neutral fragments are not readily lost unless the metal can undergo reduction.

Compared with the spectra of the acetylacetonates, it is apparent that under electron impact, substitution of CF_3 for CH_3 leads to a more extensive fragmentation of the molecule. There is a decrease in relative intensity of the molecular ion, and consequent increase in the number and intensity of the fragment ion peaks in the spectra of the fluorinated species. The greater fragmentation of these fluorinated chelates can be attributed to;

1) The relative instability of the molecular ion due to, for example, weak $C-CF_3$ bonds (46,49).

2) The relative stability of some of the products due to high Met-F bond energies (46,49)

3) The destabilization of a $C-CH_3$ or $C-CF_3$ bond owing to the increase of positive charge on the carbon atom via the electron withdrawing ability of the CF_3

Table 13

m/z (relative intensities) of metal-containing ions in the mass spectra of divalent trifluoroacetylacetone, at an electron energy of 70eV. (L = tfa)

Ion	assignment	$Ni(tfa)_2$	$Zn(tfa)_2$	$Pd(tfa)_2$
M	$MetL_2^+$ (a)	364(53.7)	370(100)	412(100)
	$MetL_2^{2+}$	-	-	205.5(28.5)
M-15	$[MetL_2-CH_3]^+$ (b)	349(15.4)[a]	355(33.8)	397(3.6)
M-19	$[MetL_2-F]^+$	345(5.3)[a]	-	393(5.0)
M-43	$[MetL_2-CH_3CO]^+$	-	-	369(17.3)
M-69	$[MetL_2-CF_3]^+$ (c)	295(100)	301(95.5)	343(40.9)
M-111	$LMetCOCH_2^+$ (d)	253(12.8)[c]	259(28.6)[c]	-
M-138	$LMetCH_3^+$	-	-	274(1.8)
M-153	$LMet^+$ (e)	211(67.8)[d]	217(36.5)[b,d]	259(45.1)
M-168	$[MetL-CH_3]^+$	196(4.4)	-	244(2.4)
M-181	$[MetL-CO]^+$	-	189(3.3)	231(3.7)
M-195	$[MetL-CH_2CO]^+$	-	-	217(3.4)
M-203	$[MetL-CF_2]^+$	161(61.2)[e]	167(28.0)[e]	-
M-207	$[L-CF_3)MetCH_3^+$	-	-	205(23.7)
M-222	$[MetL-CF_3]^+$	142(9.3)	-	190(10.0)
M-223	$[MetL-CF_2-HF]^+$	141(8.0)	-	-
M-265	$MetCHCO^+$	-	-	147(19.5)
M-278	$MetCO^+$	86(23.8)	-	134(12.4)
M-291	$MetCH_3^+$	-	-	121(70.9)
M-306	Met^+	56(41.4)	64(7.4)	106(34.0)
154	LH^+	w	m	-

Table 13 continued

Ion	Assignment	$Ni(tfa)_2$	$Zn(tfa)_2$	$Pd(tfa)_2$
85	$[HL-CF_3]^+$	s	s	w
69	CF_3^+, $COCHCO^+$	s	s	w
67		w	w	-
57	$CH_3COCH_2^+$	m	-	w
55		s	w	w
43	CH_3CO^+	s	s	s

*Values of m/z are based on ^{58}Ni, ^{64}Zn, and ^{106}Pd. Identified matastable transitions are indicated by subscrips which relate the daughter ion to its precursor in column 2. (The relative intensities of the ions in the lower part of the table, which do not contain a metal atom, are indicated qualitatively by s=strong, m=medium and w=weak.)

Table 14

m/z (relative intensities) of metal-containing ions in the mass spectra of trivalent trifluoroacetylacetonates, at an electron voltage of 70eV. (L = tfa)

Ion	Assignment	$Co(tfa)_3$	$Rh(tfa)_3$
M	$MetL_3^+$ (a)	518(34.0)	562(46.8)
M-19	$[MetL_3-F]^+$	499(3.5)	543(2.4)
M-42	$[MetL_3-CH_2CO]^+$	476(16.2)[a]	-
M-43	$[MetL_3-CH_3CO]^+$	-	519(<1)[a]
M-153	$MetL_2^+$ (b)	365(100)	409(100)[a]
	$MetL_2^{2+}$	182.5(1.7)	-
M-168	$[MetL_2-CH_3]^+$	350(18.1)[b]	-
M-196	$[MetL_2-CH_3CO]^+$	-	366(3.7)[b]
M-222	$[MetL_2-CF_3]^+$ (c)	296((75.8)[b]	-
M-264	$LMetCOCH_2^+$ (d)	254(5.0)[c]	-
M-237	$LMetCF_3^+$	-	325(2.7)
M-291	$LMetCH_3^+$ (e)	227(2.3)	271(20.5)[b]
M-305	$LMetH^+$	-	257(8.5)[e**]
M-306	$LMet^+$	212(39.7)[c,d]	256(4.9)
M-307	$[LMet-H]^+$	-	255(3.6)
M-321	$[MetL-CH_3]^+$	-	241(5.1)
M-335	$[CH_3Met[L-CO_2)]^+$	-	227(5.3)[e**]
M-347	$[MetL-CHCO]^+$	-	215(1.8)
M-349	$[MetL-COCH_3]^+$	-	213(2.6)
M-356	$[MetL-CF_2]^+$	162(41.0)	-
M-362	$MetCF_3CO^+$	-	200(2.6)

Table 14 continued

Ion	Assignment	$Co(tfa)_3$	$Rh(tfa)_3$
M-371	$[MetL-CF_2-CH_3]^+$	147(10.0)	-
M-375	$[MetL-CF_3]^+$	-	187(4.2)
M-377	$MetC_2F_3H^+$	-	185(1.9)
M-403	$Met(CO)_2^+$,$[MetL-CF_3CO]^+$	-	159(5.2)e**
M-416	$MetCH_3CO^+$	-	146(3.5)
M-417	$MetCH_2CO^+$	-	145(3.2)
M-431	$MetCO^+$	-	131(13.0)e**
M-444	$MetCH_3^+$	-	118(2.9)
M-459	Met^+	-	103(12.5)
	$Met[L-CF_3]_2^{+2}$	113.5(1.8)	-
154	LH^+	w	w
85	$[HL-CF_3]^+$	m	w
69	CF_3^+,$COCHCO^+$	m	w
67		w	w
57	$CH_3COCH_2^+$	w	w
55		w	w
43	CH_3CO^+	s	s

*Identified metastable transitions are indicated by subscripts which relate the daughter ion to its its precursor in column 2. (The relative intensities of the ions in the lower part of the table, which do not contain a metal atom, are indicated qualitatively by s=strong, m=medium and w=weak.)

**Metastable transition observed by Morris and Koob (47)

Table 15

m/z (relative intensities) of metal-containing ions in the mass spectrum of divalent hexafluoroacetylacetonates, at an electron energy of 70eV. (L = hfa)

Ion	Assignment	$Ni(hfa)_2$	$Zn(hfa)_2$	$Pd(hfa)_2$
M	$MetL_2^+$ (a)	472(43.2)	478(27.3)	520(75.2)
M-19	$[MetL_2-F]^+$	453(10.0)	459(3.0)	501(14.8)
M-50	$[MetL_2-CF_2]^+$	422(48.6)	-	-
M-69	$[MetL_2-CF_3]^+$ (b)	403(100)	409(92.5)[a]	451(44.8)[a]
M-138	$[MetL_2-2CF_3]^+$,$LMetCF_3^+$	-	340(2.6)	-
	$[MetL_2-2CF_3]^{2+}$	-	170(15.6)	-
M-207	$MetL^+$ (c)	265(64.0)	271(14.2)[b]	313(78.8)[b]
M-226	$[MetL-F]^+$	-	252(3.9)	-
M-235	$[MetL-CO]^+$	-	243(6.8)	-
M-257	$[MetL-CF_2]^+$	215(90.1)[c]	221(100)[c]	259(4.4)
M-276	$[MetL-CF_3]^+$	196(19.5)	202(5.5)	244(97.6)[c]
M-304	$[MetL-CF_3CO]^+$	-	-	216(1.6)
M-345	$[MetL-2CF_3]^+$,$MetCF_3^+$	-	133(2.6)	175(6.6)
M-373	$MetCHCO^+$	-	105(7.1)	147(7.4)
M-386	$MetCO^+$	-	-	134(5.6)
M-414	Met^+	58(98.4)	64(11.2)	106(100)
208	LH^+	-	-	w
169	$[HL-HF_2]^+$	-	-	w
139	$[HL-CF_3]^+$	w	w	m
119	$CF_2COCHCO^+$	w	s	w
91		w	w	m

Table 15 continued

Ion	Assignment	$Ni(hfa)_2$	$Zn(hfa)_2$	$Pd(hfa)_2$
85		s	-	w
75		w	w	w
69	CF_3^+, $COCHCO^+$	s	s	m
64		-	w	w
57		m	-	w
55		s	-	w
53		-	w	w
43	CH_3CO^+	s	w	w

*Values of m/z are based on ^{58}Ni, ^{64}Zn and ^{106}Pd. Identified metastable transitions are indicated by subscripts which relate the daughter ion to its precursor in column 2. (The relative intensities of the ions in the lower part of the table, which do not contain a metal atom, are indicated qualitatively by s=stromg, m=medium and w=weak.)

Table 16

m/z (relative intensities) of metal-containing ions in the mass spectra of trivalent hexafluoroacetylacetonate, at an electron energy of 70eV. (L = hfa)

Ion	Assignment	$Co(hfa)_3$ **	$Rh(hfa)_3$
M	$MetL_3^+$ (a)	680(21.0)	724(33.1)
M-19	$[MetL_3-F]^+$	-	705(8.1)
M-69	$[MetL_3-CF_3]^+$ (b)	611(1.0)	655(1.9)[a]
M-207	$MetL_2^+$ (c)	473(35.0)	517(100)[a,b]
M-276	$[MetL_2-CF_3]^+$ (d)	404(100)	448(2.0)[c]
M-304	$[MetL_2-CF_3CO]^+$ (e)	-	420(7.4)[c,d]
M-326	$[MetL_2-CF_3-CF_2]^+$	354(1.0)[d]	-
M-332	$[MetL_2-CF_3CO-CO]^+$	-	392(1.9)[e]
M-345	$[MetL_2-2CF_3]^+$, $LMetCF_3^+$	-	379(7.4)c
	$[MetL_2-2CF_3]^{2+}$	-	189.5(2.4)
M-373	$[MetL_2-CF_3CO-CF_3]^+$	-	351(1.7)
M-386	$[MetL_2-CF_3-CF_3CHCO]^+$	-	338(3.6)
M-401	$[MetL_2-2CF_3CO]^+$	-	323(2.2)
M-414	$MetL^+$ (g)	266(24.0)	310(29.1)[c]
M-442	$[MetL-CO]^+$	-	282(2.9)[g]
M-455	$[MetL-CHCO]^+$	-	269(1.6)
M-464	$[MetL-CF_2]^+$	216(58.0)[d,f]	-
M-483	$[MetL-CF_3]^+$ (h)	-	241(13.3)[g]
M-484	$[MetL-CF_2-HF]^+$	196(2.0)	-
M-511	$[MetL-COCF_3]^+$ (i)	-	213(15.9)[h]
M-524	$MetCF_3CO^+$	-	200(6.6)

Table 16 continued

Ion	Assignment	$Co(hfa)_3$**	$Rh(hfa)_3$
M-539	$MetC_2F_3H$	-	185(7.7)[i]
M-552	$MetCF_3^+$,$MetCOCHCO^+$	-	172(3.7)
M-593	$MetCO^+$	-	131(18.0)
M-621	Met^+	-	103(25.9)
208	LH^+		s
139	$[HL-CF_3]^+$		w
119	$CF_2COCHCO^+$		w
91			s
85			s
75			w
71			w
69	CF_3^+,$COCHCO^+$		s
67			w
57			w
55			w
53			w

*Identified metastable transitions are indicated by subscripts which relate the daughter ion to its precursor in column 2. (The relative intensities of the ions in the lower part of the table, which do not contain a metal atom, are indicated qualitatively by s=strong, m=medium and w=weak.)

**Data obtained from reference (52,53).

substituent (50); and

4) The destabilization of metal-ligand bonds owing to the electron withdrawing ability of the CF_3 substituent (51).

Evidence in support of (1) may be found by examining the mass spectra of trifluoroacetylacetonate complexes. In all those studied in this thesis and in those studied by Reichert et al (49) it was found that the peaks corresponding to the loss of the CF_3 odd-electron radical are always considerably more intense than the corresponding peaks due to the loss of the CH_3 odd-electron radical. The weakness of this bond is presumably due to the electron withdrawing ability of fluorine.

A number of rearrangement peaks involving the loss of a CF_2 group with the assumed formation of a metal-fluorine bond are present in the spectra for some of the metals studied. The migration of the fluorine proceeds by a concerted process involving the breaking of one of the metal-oxygen bonds followed by rotation about the 2,3 carbon-carbon bond bringing one of the fluorines of the CF_3 group close to the metal:

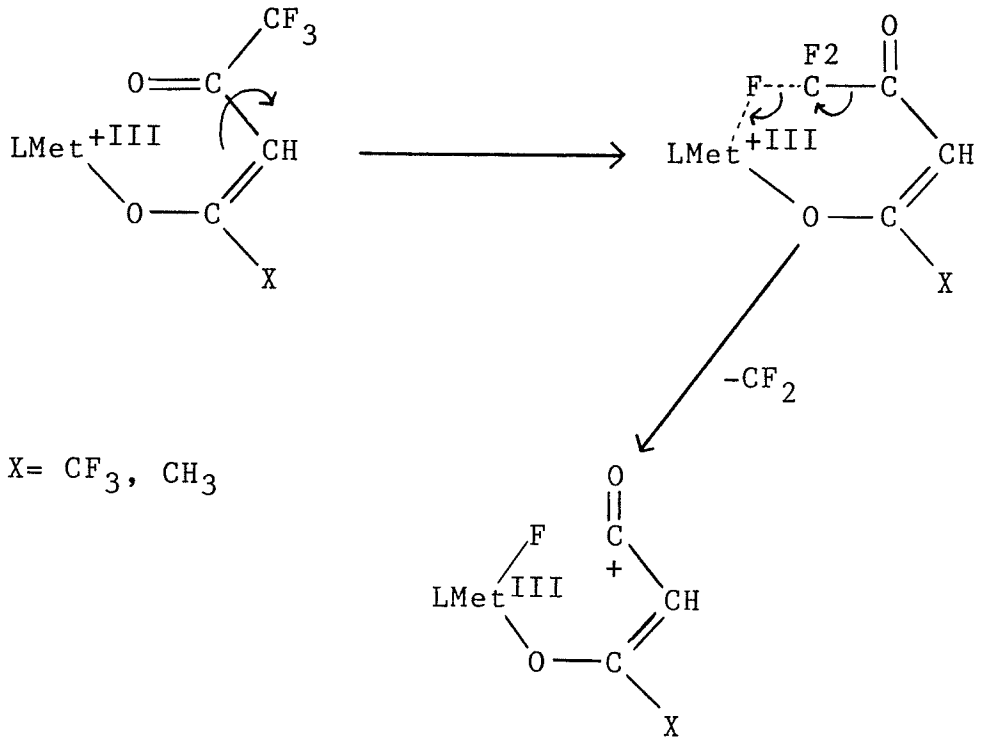

That metal-fluorine bonds are indeed formed is confirmed by the observations of Morris and Koob (24) who observed metastable peaks for the elimination of neutral metal fluorides from fragment ions in the mass spectra of $Mn(hfa)_2$, $Cr(hfa)_3$, $Fe(hfa)_3$, $Fe(hfa)_2$, $Co(hfa)_2$ and $Ni(hfa)_2$. In $Al(hfa)_3$, AlF_2L is eliminated as a neutral fragment. Since CF_2 is an even-electron species, it would preferentially be eliminated from even-electron ions rather than from odd-electron ions. Elimination of CF_2 from the molecular ion has not been observed for any of the trivalent fluorinated complexes studied in this thesis or in those reported by Reichert et al (46,49). This might be due to the fact that the $MetL_3^+$ ions are odd-

electron species or because the concerted mechanism proposed for the transfer of a fluorine to the metal may be sterically hindered. The $[MetL_2-CF_2]^+$ ion was, however, observed for $Ni(hfa)_2$. In this case the the $MetL_2^+$ ion is an odd-electron species unless oxidation of the metal occurs. A similar situation is found to occur in both $Fe(tfa)_2$ and $Fe(hfa)_2$ complexes (46,49).

The effect of the hardness (or softness) of the metal on the extent of fluorine migration to the metal can be seen in the relative intensities of the $[MetL-CF_2]^+$ ions (table 17).

Table 17

	Ion	Clasification of metal	Relative intensity of $[MetL-CF_2]^+$
hardest	$[Zn^{II}(hfa)]^+$	B	100
↓	$[Zn^{II}(tfa)]^+$	B	28.0
	$[Ni^{II}(hfa)]^+$	B	90.1
	$[Ni^{II}(tfa)]^+$	B	61.2
	$[Co^{II}(hfa)]^+$	B	58.0
	$[Co^{II}(tfa)]^+$	B	41.0
	$[Pd^{II}(hfa)]^+$	S	4.4
	$[Pd^{II}(tfa)]^+$	S	-
softest	$[Rh^{II}(hfa)]^+$	S	-

B= borderline acid S= Soft acid

For both the hexafluoro and trifluoro complexes the relative intensity of the of the $[MetL-CF_2]^+$ ion increases with the hardness of the metal, with the exception of $Zn^{II}(tfa)^+$. It is also evident from this table that for each metal, the peak due to the $[MetL-CF_2]^+$ ion in the hexafluoro complex is more intense than for the trifluoro complex. This may be explained in two ways;

1) Greater statistical probability of the process due to the additional CF_3 substituent. (46)

2) The ability of the additional CF_3 group to increase the hardness of the metal.

In its tendency to undergo metal reduction $Rh(hfa)_3$ is very similar to $Co(hfa)_3$. The rhodium complex, however, exhibits moderately important peaks corresponding to its futher reduction to Rh(I) whereas the cobalt complex does not. This difference could possibly be attributed to competition between reduction of the metal and fluorine migration from the ligand to the metal. Rh(II) is considered to be a soft acid (see table 5) and therefore would not preferentially bind to fluorine, a very hard base. Co(II),on the other hand, is a borderline acid and thus would have a greater tendency to bind with fluorine. As well, Co is much more stable in the +II oxidation state than Rh and therefore would be less prone to reduction. Proof that this competition does indeed exist in $Co(hfa)_3$ and in $Co(tfa)_3$ as well is found by

examining the mass spectra of $Co(acac)_3$. Here, unlike the fluorinated complexes of Co, peaks corresponding to Co in the +I oxidation state do exist. They are, however, of relatively low intensity. This is not unexpected since, as just mentioned, Co is extremely stable in the +II oxidation state. The lack of fluorine migration to the metal for Rh(II) is also paralleled in the spectra of $Pd(hfa)_2$ and $Pd(tfa)_2$. This is not suprising since Pd(II) like Rh(II) is a soft acid.

In the mass spectrum of the $Pd(tfa)_2$ complex there exist two possible pathways leading to the fragment ion $[(L\text{-}CF_3)Pd^{II}CH_3]^+$. One pathway involves the loss of a ligand except CH_3 from the molecular ion yielding the odd-electron fragment ion $LPd^{II}CH_3^{+\bullet}$, followed by the loss of the odd-electron neutral fragment $CF_3^\bullet$ from the remaining ligand. The alternative pathway involves the initial loss of first the CF_3 radical then the loss of the remaining ligand except CH_3. The latter pathway is energetically more favorable since the first pathway involves the initial loss of an even-electron neutral fragment from the odd-electron molecular ion. The low probability of the first pathway is consistent with the low relative intensity of the $[LPd^{II}CH_3]^{+\bullet}$ ion.

In the mass spectra of $Rh(hfa)_3$ the four most intense peaks correspond to the molecular ion and the successive loss of the three ligands. The resulting ions

are $Rh^{III}(hfa)_3^+$, $Rh^{III}(hfa)_2^+$, $Rh^{II}(hfa)^+$ and Rh^{+I}. The four peaks account for approximately 62% of the total metal-containing ion intensity. The loss of the second ligand is an indicator that Rh(III) has undergone reduction to Rh(II), while the loss of the odd-electron neutral fragment CF_3 from $Rh^{II}(hfa)^+$ indicates reduction of Rh(II) to Rh(I). In contrast to $Rh(hfa)_3$, the spectra of $Rh(tfa)_3$ and $Rh(acac)_3$ do not show much evidence for rhodium reduction except in the most minor of dissociation steps. Thus, it seems that reduction of Rh in $Rh(hfa)_3$ is considerably more important than in the other two complexes. The only similarity between the mass spectra of these three complexes is the loss of one ligand from their molecular ions, all of which are base peaks. $Rh(hfa)_3$ and $Rh(tfa)_3$ are also similar in that fluorine migration to the metal does not occur. That the dissociative behavior of $Rh(tfa)_3$ much more strongly follows that shown by $Rh(acac)_3$ might suggest that the presence of the CH_3 substituent(s) on the ligand provides an alternative pathway to decomposition which is kinetically favored over the reduction of the metal.

In all the fluorinated complexes studied in this thesis thus far, with the exception of $Rh(tfa)_3$, decomposition seems to follow either the route of fluorine migration to the metal and/or the reduction of the metal through transfer of an electron from the ligand to the

metal. The extent of either pathway is dependent upon the metal's ability to undergo reduction as well as its hard or soft acid character. Some suggested decomposition pathways for the formation of ions in the mass spectra of these fluorinated acetylacetonates are seen in schemes 6-15.

SCHEME 6

Suggested decomposition pathways for the formation of ions in the mass spectrum of $Ni(tfa)_2$ (L = tfa)

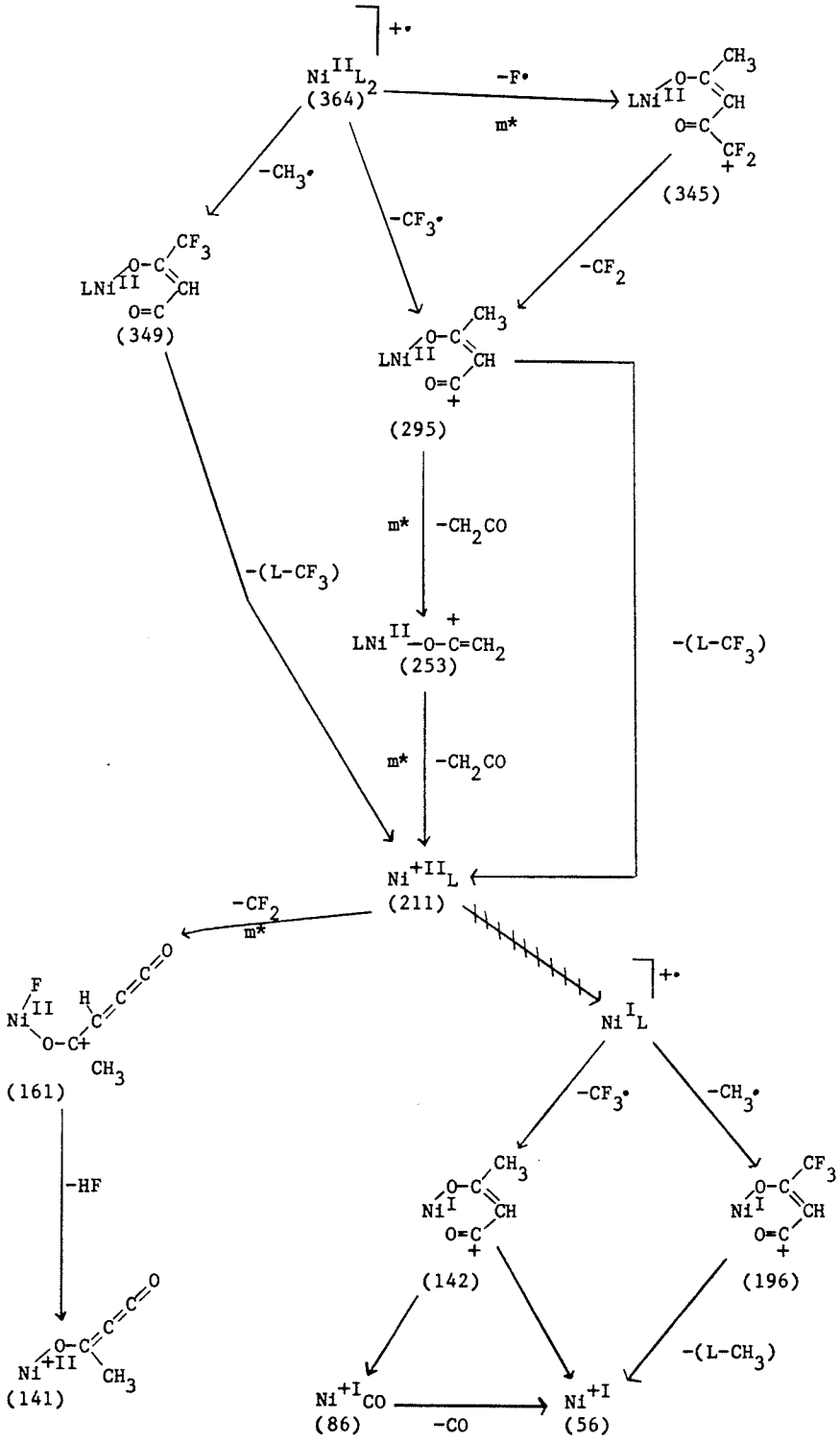

SCHEME 7

Suggested decomposition pathways for the formation of ions in the mass spectrum of $Ni(hfa)_2$ (L=hfa)

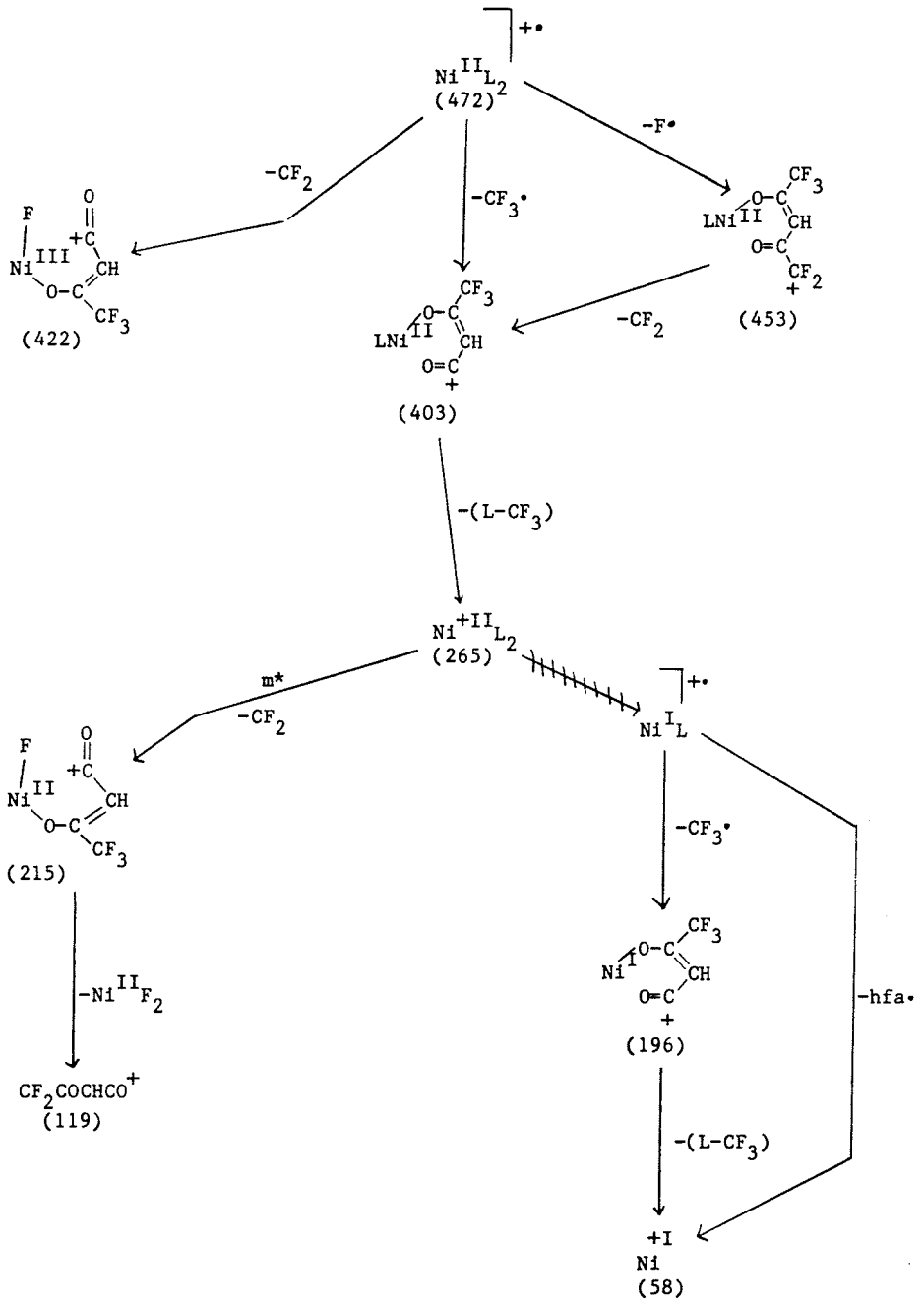

SCHEME 8

Suggested decomposition pathways for the formation of ions in the mass spectrum of $Zn(tfa)_2$ (L = tfa)

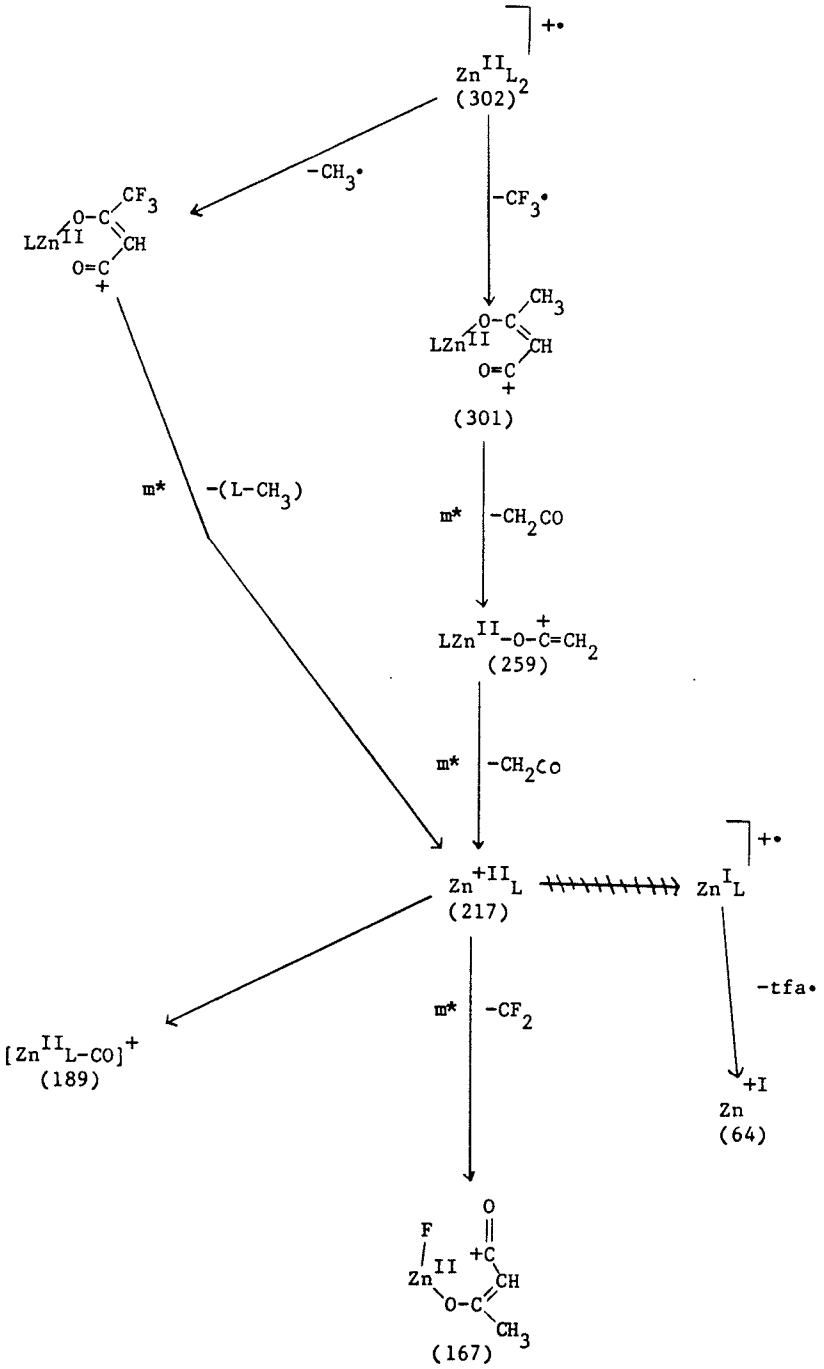

SCHEME 9

Suggested decomposition pathways for the formation of ions in the mass spectrum of $Zn(hfa)_2$ (L=hfa)

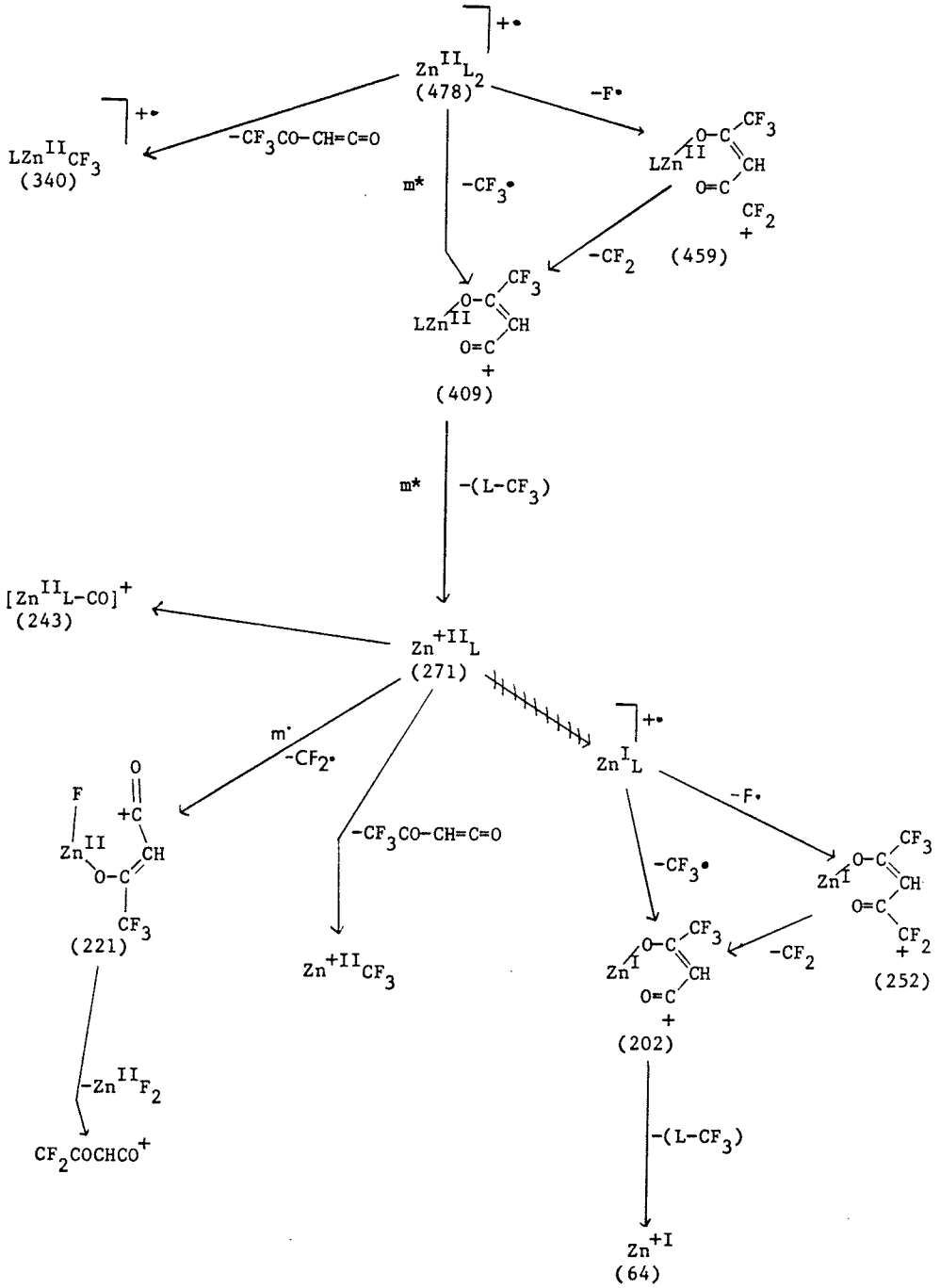

SCHEME 10

Suggested decomposition pathways for the formation of ions in the mass spectrum of $Pd(tfa)_2$ (L = tfa)

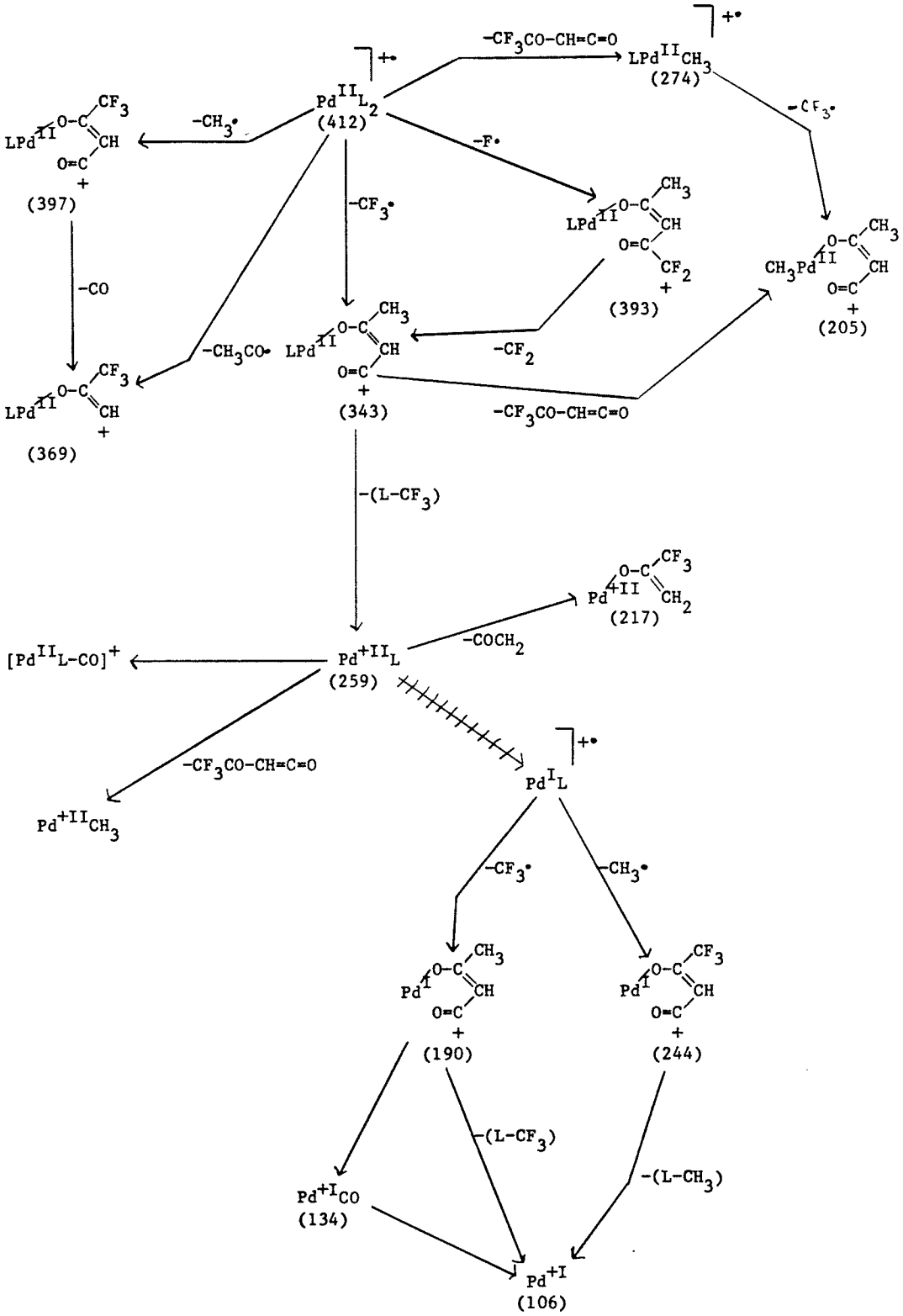

SCHEME 11

Suggested decomposition pathways for the formation of ions in the mass spectrum of $Pd(hfa)_2$ (L=hfa)

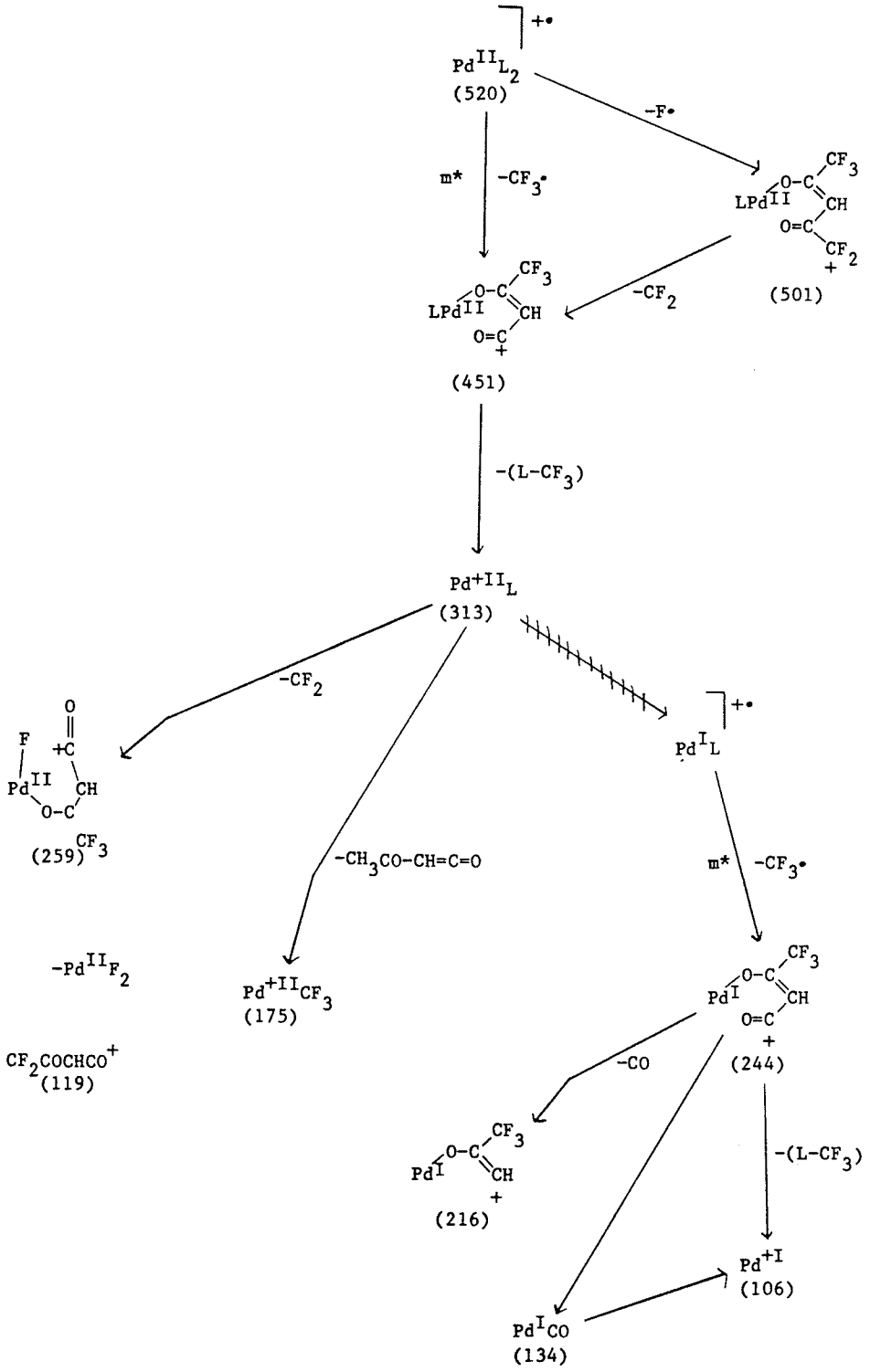

SCHEME 12

Suggested decomposition pathways for the formation of ions in the mass spectrum of $Co(tfa)_3$ (L=tfa)

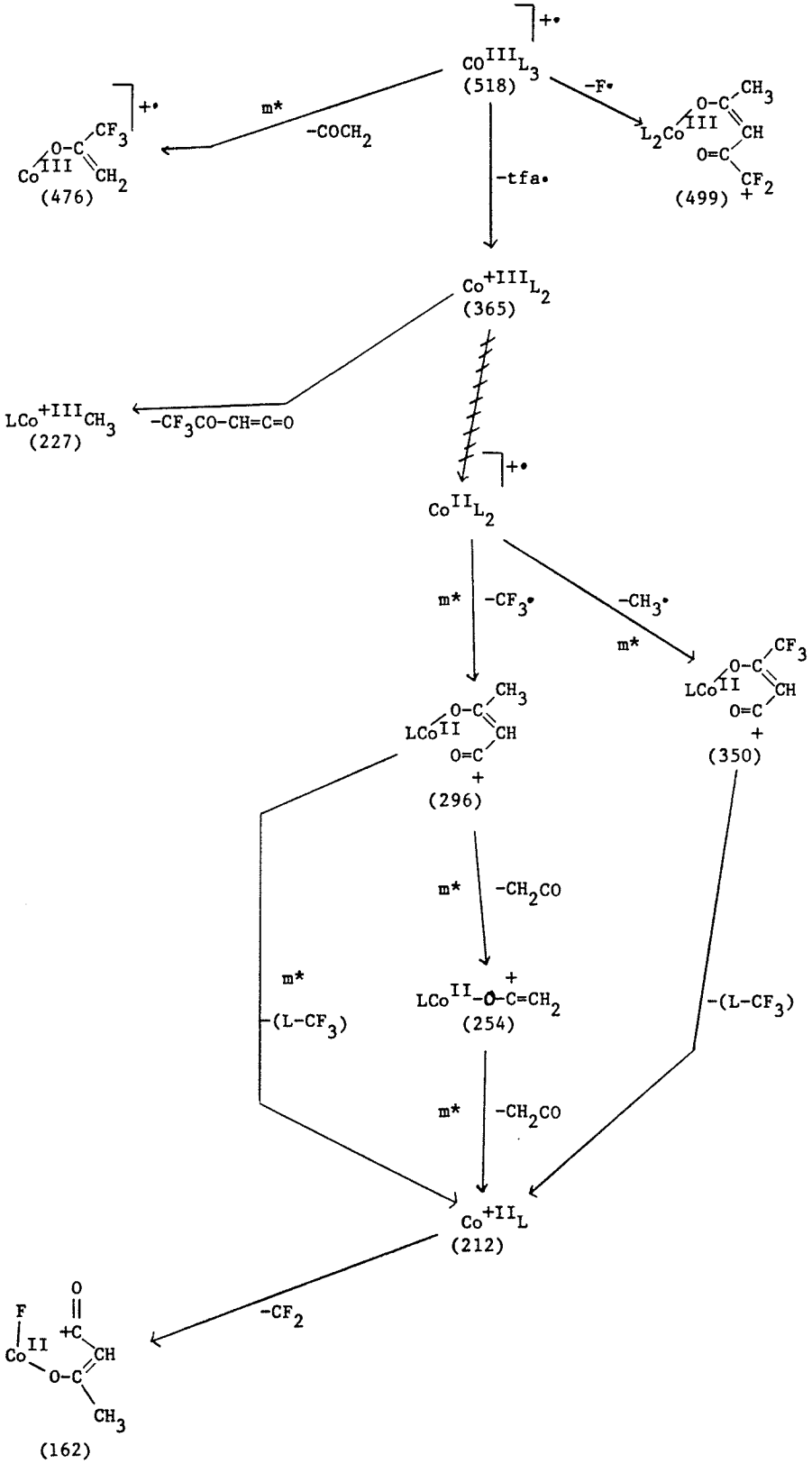

SCHEME 13

Suggested decompostion pathways for the formation of ions in the mass spectrum of $Co(hfa)_3$ (L = hfa)

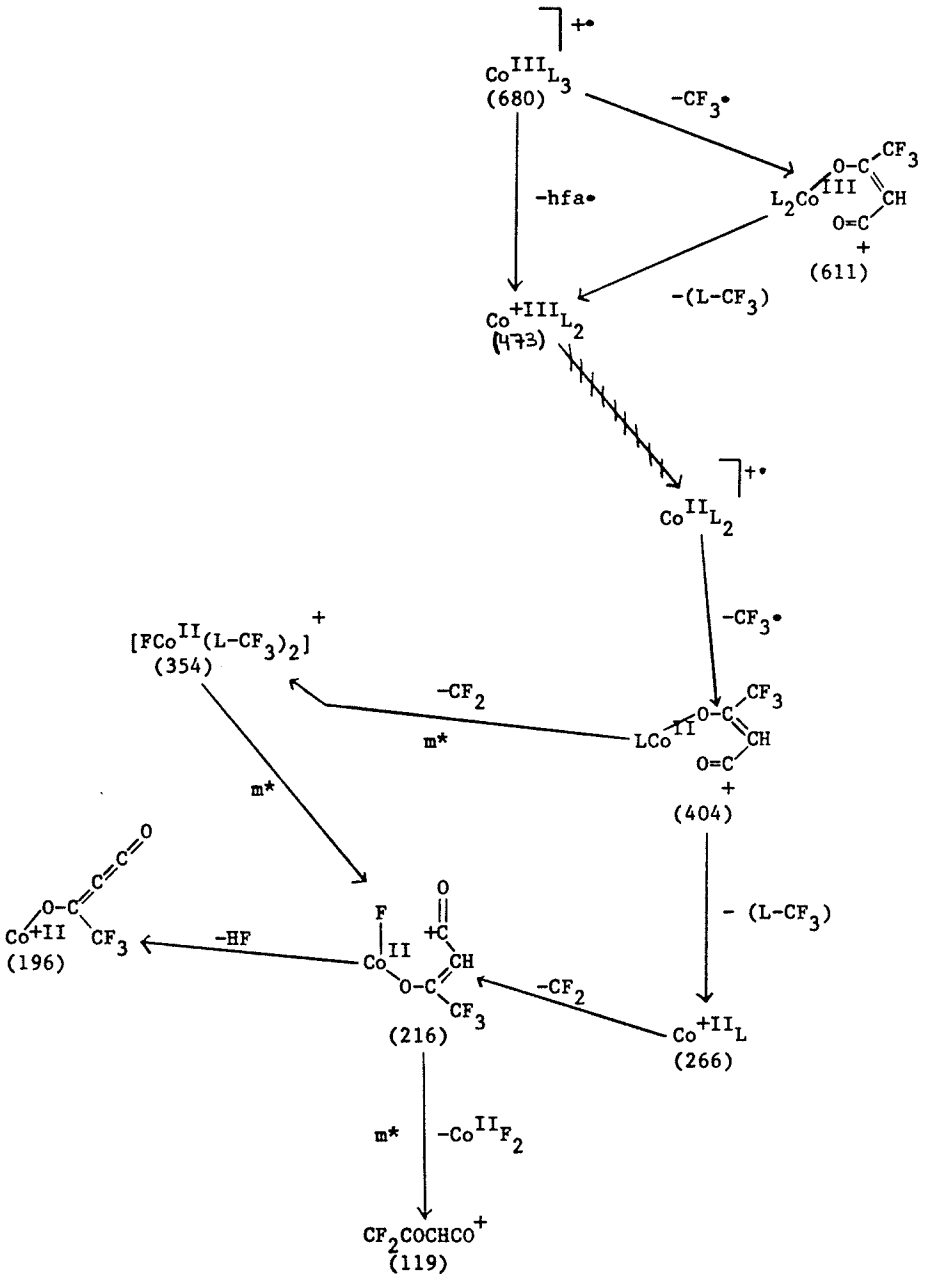

SCHEME 14

Suggested decomposition pathways for the formation of ions in the mass spectrum of $Rh(tfa)_3$ (L=tfa)

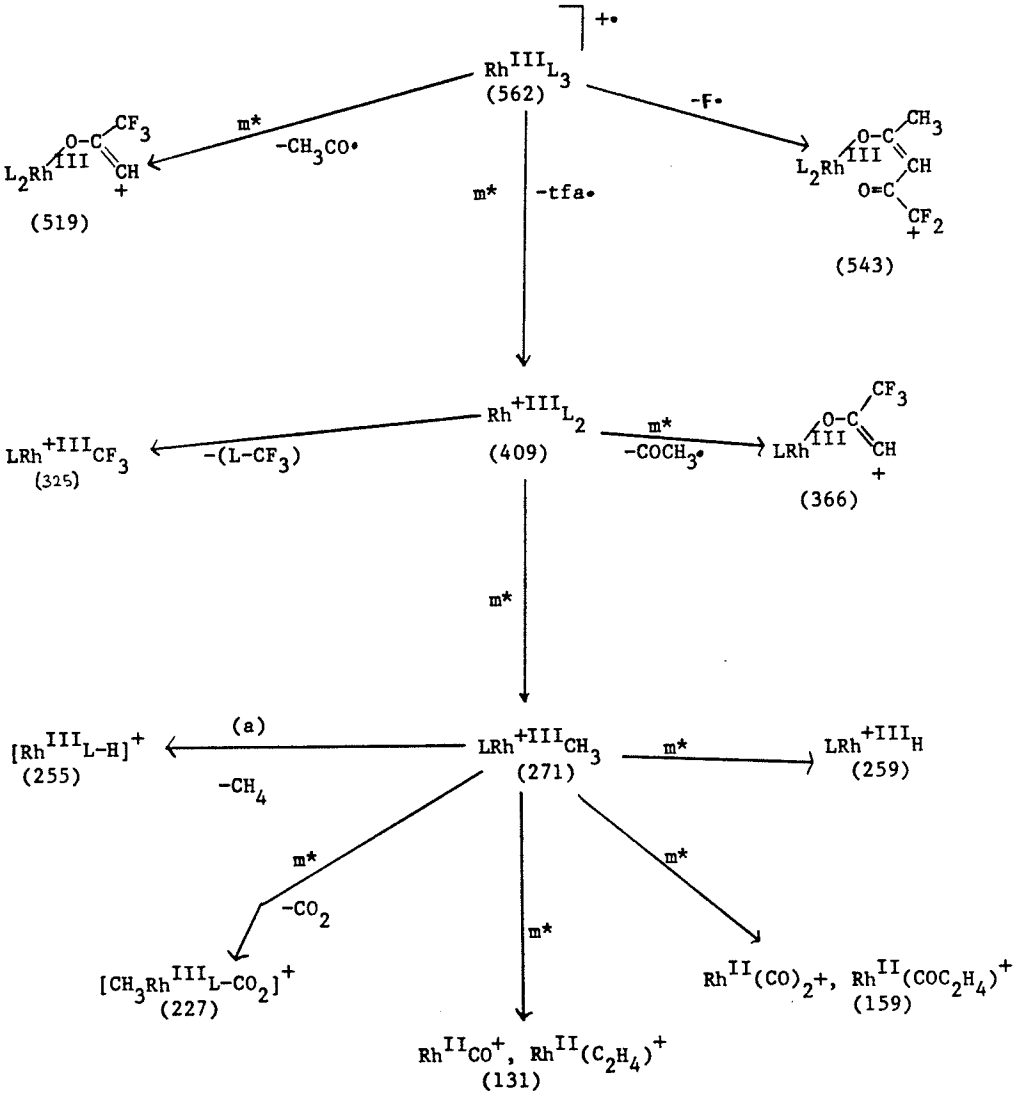

SCHEME 14 (continued)

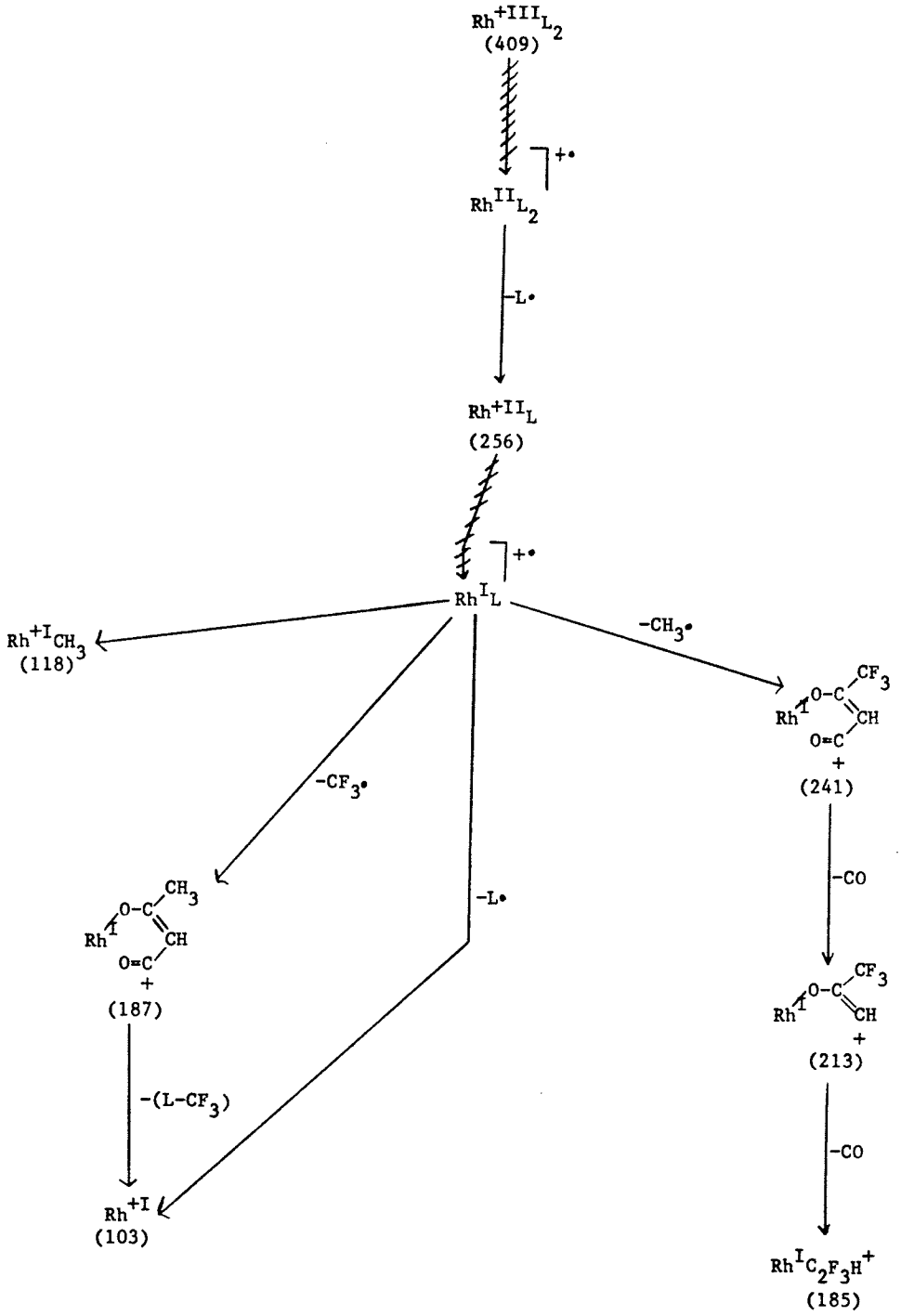

(a) similar decomposition in $Rh(acac)_3$, verified by observation of metastable transition.

SCHEME 15

Suggested decomposition pathways for the formation of ions in the mass spectrum of $Rh(hfa)_3$ (L=hfa)

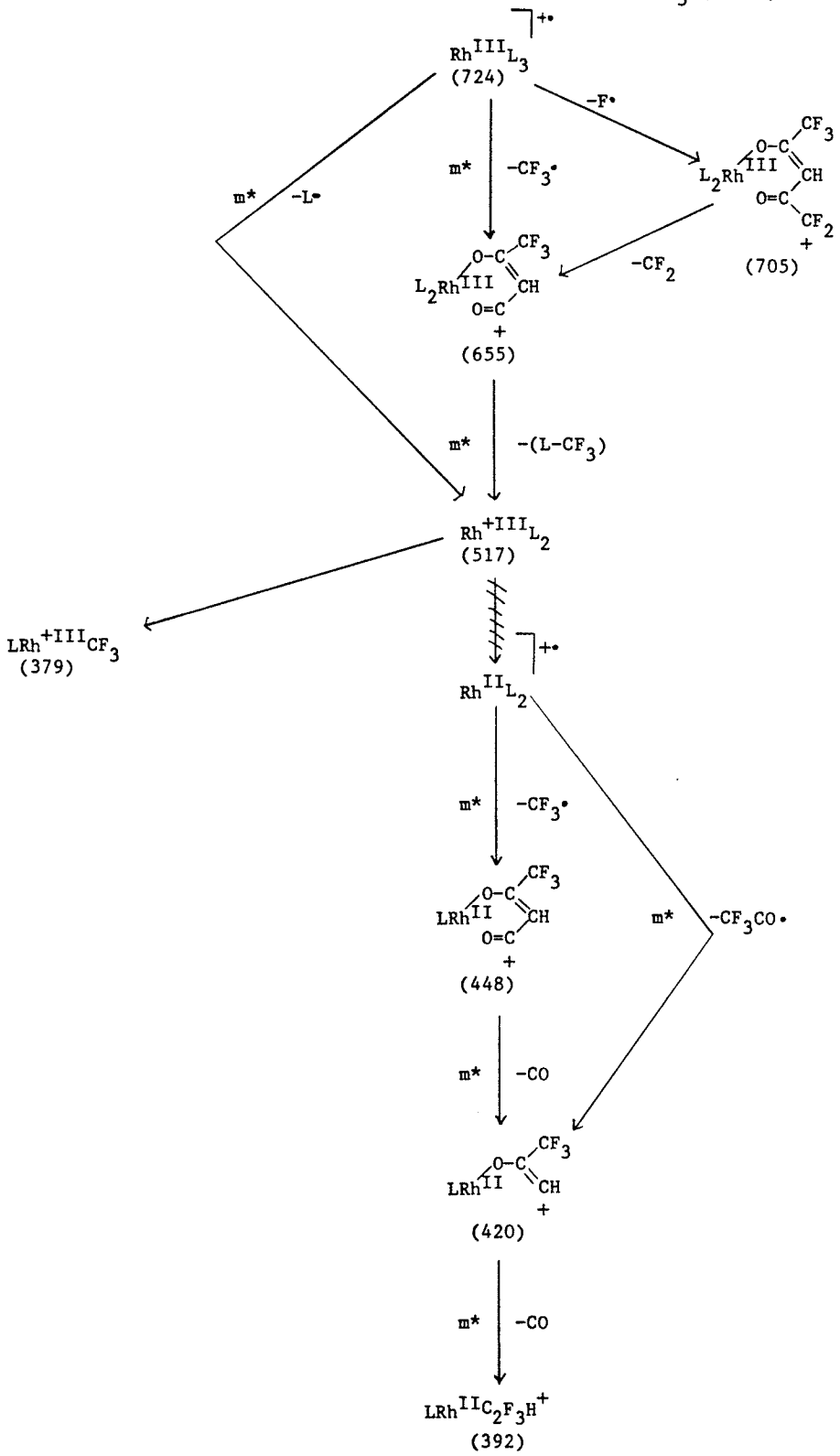

SCHEME 15 (continued)

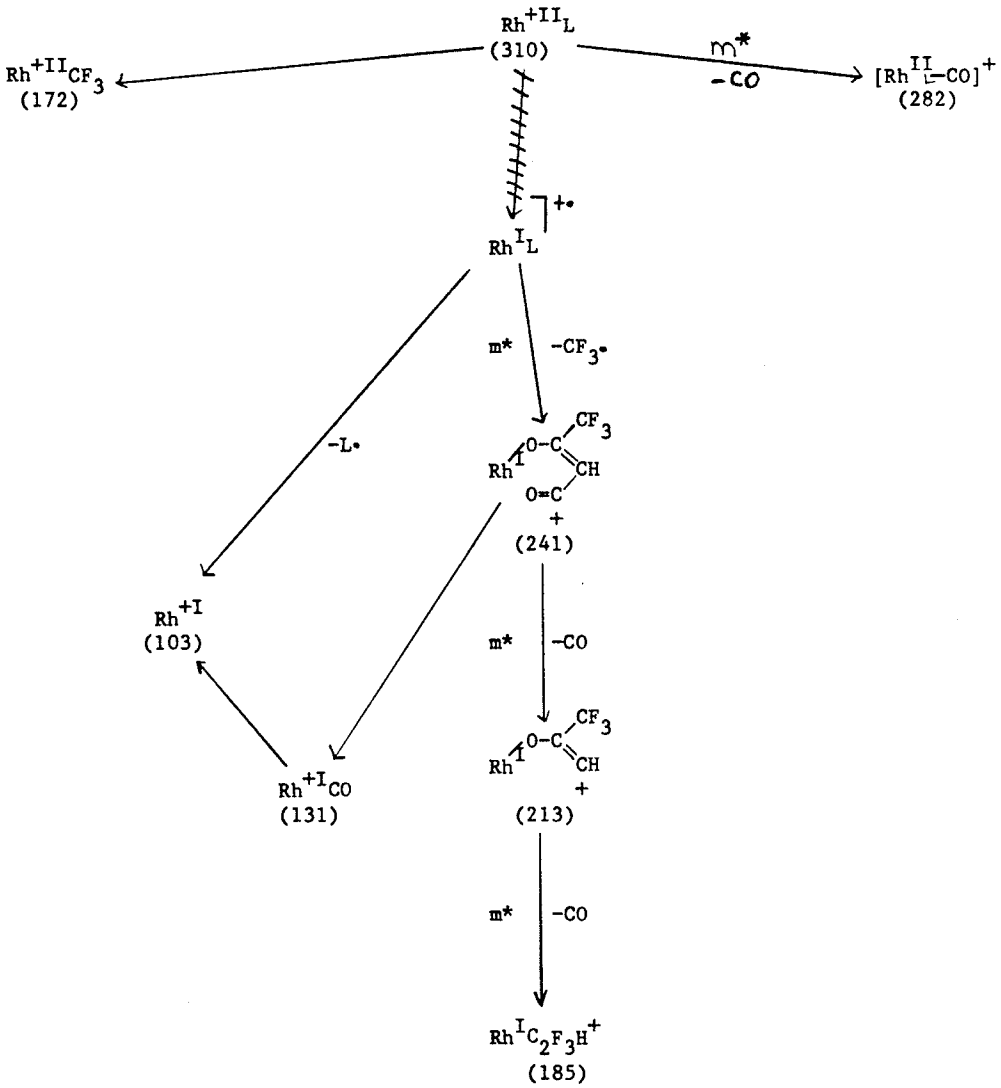

iii) Mass spectra of some transition metal monothio- and trifluoromonothioacetylacetonates.

The mass spectra obtained for the monothio- and trifluoromonothioacetylacetonates of Zn(II), Ni(II), Pd(II), Co(III) and Rh(III), by direct insertion of the sample into the ion source at an electron energy of 70eV are summarized in tables 18-21. Unlike their oxygen analogs the mass spectra of these complexes showed very little indication of metastable transitions. This made it difficult in assigning the correct decomposition pathway of ions which had more than one possible parent ion. In cases such as this, the choice of pathway was made by reference to similar fragmentations which occurred in the mass spectra of the acetylacetonate and fluorinated acetylacetonate metal complexes and by choosing the pathway which led to the most stable ion.

The unwillingness of Zn to undergo reduction, seen in the mass spectra of $Zn(acac)_2$ and $Zn(tfa)_2$, is also evident in the mass spectra of their thio analogs. No peaks are observed below the mass corresponding to $Zn^{II}L^+$ in the mass spectrum of $Zn(Sacac)_2$ and only peaks due to the $[MetL-CF_2]^+$ and $[MetL-CF_2-HF]^+$ ions below this mass in that of $Zn(Stfacac)_2$. $Rh(Sacac)_3$, as did $Rh(acac)_3$, showed very little evidence for reduction, except in the most minor of dissociation steps. The molecular ion, and loss of one ligand from the molecular ion, together make

Table 18

m/z (relative intensities) of metal containing ions in the mass spectra of divalent monothioacetylacetonates, at an electron energy of 70eV. (L = Sacac)

Ion	Assignment	$Ni(Sacac)_2$	$Zn(Sacac)_2$	$Pd(Sacac)_2$
M	$MetL_2^+$ (a)	288(100)	294(95.4)	336(100)
M-15	$[MetL_2-CH_3]^+$	-	279(22.4)	-
M-32	$[MetL_2-S]^+$	256(6.3)	262(28.6)[a]	-
M-33	$[MetL_2-SH]^+$	-	-	303(8.3)
M-42	$[MetL_2-COCH_2]^+$	-	-	294(10.1)
M-82	$LMetSH^+$	206(9.0)	-	254(8.4)
M-83	$LMetS^+$	205(4.9)	211(7.6)	-
M-114	$LMetH^+$	174(17.1)	-	-
M-115	$LMet^+$	173(18.6)	179(100)	221(15.4)
M-116	$[MetL-H]^+$	-	-	220(21.9)
M-126	$[SMetL-CH_3CO]^+$	-	-	210(10.1)
M-143	$[MetL-CO]^+$	145(6.3)	-	-
M-148	$[MetL-SH]^+$	140(24.8)	-	188(16.9)
M-157	$[MetL-COCH_2]^+$	131(7.6)	-	-
M-158	$[MetL-CH_3CO]^+$	130(8.1)	-	178(15.6)
M-159	$[MetL-CS]^+$	129(4.8)	-	177(23.0)
M-184	$MetCS^+$	-	-	150(22.6)
M-189	$MetCHCO^+$	-	-	147(30.3)
M-215	$MetCH_3^+$	-	-	121(11.5)
M-230	Met^+	58(8.3)	-	106(19.2)
115	L^+	s	s	s
101		w	m	w

Table 18 continued

Ion	Assignment	$Ni(Sacac)_2$	$Zn(Sacac)_2$	$Pd(Sacac)_2$
100	$[L-CH_3]^+$	-	m	m
85	$[L-2CH_3]^+$	w	m	s
83	$[L-S]^+$	w	-	w
71		w	w	w
69		w	w	m
59	CH_3CS^+	w	w	w
58	CH_2CS^+	-	-	m
57	$[L-CH_2CS]^+$	w	w	w
55	$[L-COS]^+$	w	w	w
43	CH_3CO^+	s	s	s

*Values of m/z are based on ^{58}Ni, ^{64}Zn and ^{106}Pd. Identified metastable transitions are indicated by subscripts which relate the daughter ion to its precursor in column 2. (The relative intensities of the ions in the lower part of the table, which do not contain a metal atom, are indicated qualitatively by s=strong, m=medium and w=weak.)

Table 19

m/z (relative intensities) of metal containing ions in the mass spectra of trivalent monothioacetylacetonates, at an electron energy of 70eV. (L = Sacac)

Ion	Assignment	$Co(Sacac)_3$	$Rh(Sacac)_3$
M	$MetL_3^+$	404(20.4)	448(100)
M-43	$[MetL_3-CH_3CO]^+$	-	405(1.5)
M-83	$SMetL_2^+$	-	365(1.5)
M-115	$MetL_2^+$	289(100)	333(55.5)
M-147	$[MetL_2-S]^+$	-	301(4.6)
M-148	$[MetL_2-SH]^+$	256(10.6)	-
M-158	$[MetL_2-CH_3CO]^+$	246(3.4)	290(3.5)
M-160	$[MetL_2-CHCO]^+$	-	288(2.3)
M-171	$LMetCH_3CS^+$	233(2.6)	-
M-173	$[MetL_2-CH_2CS]^+$	-	275(5.0)
M-183	$LMetCH_3S^+$	221(3.7)	265(2.7)
M-185	$LMetCSH^+$	-	263(3.2)
M-187	$LMetCH_3CO^+$	-	261(4.6)
M-197	$LMetSH^+$	207(14.7)	251(3.0)
M-198	$LMetS^+$	-	250(1.9)
M-199	$LMetCH_3O^+$	205(8.5)	249(2.1)
M-204	$LMetC_2H_4^+$	-	244(1.9)
M-215	$LMetCH_3^+$	-	233(3.1)
M-229	$LMetH^+$	-	219(1.8)
M-230	$LMet^+$	174(81.7)	-
M-231	$[MetL-H]^+$	-	217(2.1)
M-258	$[MetL-CO]^+$	146(5.2)	-

Table 19 continued

Ion	Assignment	$Co(Sacac)_3$	$Rh(Sacac)_3$
M-259	$[MetL-CHO]^+$	145(8.2)	189(3.1)
M-261	$[MetL-CH_3O]^+$	-	187(3.1)
M-262	$[MetL-S]^+$	142(3.3)	186(3.1)
M-263	$[MetL-SH]^+$	141(56.4)	-
M-272	$[MetL-CH_2CO]^+$	132(3.9)	-
M-273	$[MetL-CH_3CO]^+$	131(7.9)	-
M-274	$[MetL-CS]^+$	130(5.9)	-
M-275	$[MetL-CSH]^+$	-	173(4.2)
M-299	$MetCH_2S^+$	-	149(4.2)
M-301	$MetCS^+$	103(5.6)	147(1.8)
M-303	$MetCOCH_2^+$	101(12.1)	-
M-312	$MetSH^+$	92(13.1)	-
M-317	$MetCO^+$	-	131(5.8)
M-345	Met^+	59(12.0)	103(1.4)
116	LH^+	m	m
115	L^+	s	s
101		w	m
100	$[L-CH_3]^+$	w	w
99		w	w
85	$[L-2CH_3]^+$	w	m
83	$[L-S]^+$	-	w
73	$[L-CH_2CO]^+$	-	m
72	$[L-CH_3CO]^+$	w	w

Table 19 continued

Ion	Assignment	$Co(Sacac)_3$	$Rh(Sacac)_3$
71		w	w
69		w	m
67		w	w
59	CH_3CS^+	w	m
58	CH_2CS^+	-	w
57	$[L-CH_2CS]^+$	-	w
55	$[L-COS]^+$	w	w
43	CH_3CO^+	m	m

*Identified metastable transitions are indicated by subscripts which relate the daughter ion to its precursor in column 2. (The relative intensities of the ions in the lower part of the table, which do not contain a metal atom, are indicated qualitatively by s=strong, m=medium and w=weak.)

Table 20

m/z (relative intensities) of metal containing ions in the mass spectra of divalent monothiotrifluoroacetylacetonates, at an electron energy of 70eV. (L = Stfacac)

Ion	Assignment	$Ni(Stfacac)_2$	$Zn(Stfacac)_2$	$Pd(Stfacac)_2$
M	$MetL_2^+$	396(100)	402(100)	444(100)
M-19	$[MetL_2-F]^+$	377(7.0)	-	425(1.3)
M-32	$[MetL_2-S]^+$	-	-	412(2.6)
M-50	$[MetL_2-CF_2]^+$	346(3.5)	-	-
M-69	$[MetL_2-CF_3]^+$	347(3.9)	333(19.8)	375(3.8)
M-70	$[MetL_2-CF_2-HF]^+$	-	332(12.3)	-
M-97	$[MetL_2-COCF_3]^+$	299(6.3)	-	347(1.8)
M-136	$LMetSH^+$	260(3.3)	-	-
M-137	$LMetS^+$	259(4.7)	-	307(4.3)
M-169	$MetL^+$	227(28.2)	233(65.4)	275(9.9)
M-219	$[MetL-CF_2]^+$	-	183(33.5)	-
M-238	$[MetL-CF_3]^+$	177(15.6)	-	-
M-239	$[MetL-CF_2-HF]^+$	157(15.8)	163(18.5)	205(7.8)
M-266	$[MetL-COCF_3]^+$	-	-	178(4.0)
M-305	$MetSH^+$	-	-	139(7.9)
M-338	Met^+	58(8.8)	-	-
170	LH^+	w	w	w
169	L^+	s	s	s
150	$[L-F]^+$	w	s	w
149	$[L-HF]^+$	w	w	w
131		w	w	-
130		-	w	-

Table 20 continued

Ion	Assignment	$Ni(Stfacac)_2$	$Zn(Stfacac)_2$	$Pd(Stfacac)_2$
100	$[L-CF_3]^+$	w	s	w
85	$[L-CF_3-CH_3]^+$	w	s	m
72	$[L-COCF_3]^+$	w	w	w
71		w	w	w
69	CF_3^+	w	m	m
67		w	s	-
59	CH_3CS^+	w	m	w
55		w	w	w
45		w	w	w
43	CH_3CO^+	w	s	m

*Values of m/z are based on ^{58}Ni, ^{64}Zn and ^{106}Pd. Identified metastable transitions are indicated by subscripts which relate the daughter ion to its precursor in column 2. (The relative intensities of the ions in the lower part of the table, which do not contain a metal atom, are indicated qualitatively by s=strong, m=medium and w=weak.)

Table 21

m/z (relative intensities) of metal containing ions in the mass spectra of trivalent monothiotrifluoroacetylacetonate, at an electron energy of 70eV. (L = Stfacac)

Ion	Assignment	$Co(Stfacac)_3$	$Rh(Stfacac)_3$
M	$MetL_3^+$	566(5.2)	610(57.9)
M-19	$[MetL_3-F]^+$	547(1.2)	591(10.5)
M-169	$MetL_2^+$	397(100)	441(52.6)
M-238	$[MetL_2-CF_3]^+$ (a)	328(2.1)	-
M-266	$[MetL_2-CF_3CO]^+$	300(2.2)[a]	-
M-294	$[MetL_2-CF_3CO-CO]^+$	272(1.1)	-
M-305	$LMetSH^+$	261(6.5)	305(30.2)
M-306	$LMetS^+$	-	304(45.2)
M-337	$LMetH^+$	-	273(14.7)
M-338	$MetL^+$ (b)	228(21.7)	-
M-339	$[MetL-H]^+$	-	271(21.6)
M-375	$[SMetL-CF_3]^+$	-	235(100)
M-388	$[MetL-CF_2]^+$	178(11.7)[b]	-
M-402	$[HSMetL-COCF_3]^+$	-	208(32.0)
M-403	$[SMetL-COCF_3]^+$	-	207(35.8)
M-408	$[MetL-CF_2-HF]^+$	158(9.2)	-
M-416	$[MetL-CF_2CO]^+$	150(14.7)	-
M-435	$[MetL-COCF_3]^+$	131(6.7)	-
M-436	$[MetL-COCF_2-HF]^+$	130(2.7)	-
M-463	$MetCS^+$	103(2.0)	147(11.6)
M-479	$MetCO^+$	-	131(21.1)
M-507	Met^+	59(5.0)	103(13.2)

Table 21 continued

Ion	Assignment	$Co(Stfacac)_3$	$Rh(Stfacac)_3$
170	LH^+	w	w
169	L^+	s	s
150	$[L-F]^+$	s	-
149	$[L-HF]^+$	w	w
131		m	-
130		w	-
100	$[L-CF_3]^+$	m	w
85	$[L-CF_3-CH_3]^+$	w	m
72	$[L-COCF_3]^+$	w	w
71		w	w
69	CF_3^+	m	m
67		m	w
59	CH_3CS^+	m	m
55		w	w
45		w	m
43	CH_3CO^+	m	s

*Identified metastable transitions are indicated by subscripts which relate the daughter ion to its precursor in column 2. (The relative intensities of the ions in the lower part of the table, which do not contain a metal atom, are indicated qualitatively by s=strong, m=medium and w=weak.)

up approximately 68% and 55% of the total metal-containing ion intensities for the two rhodium compounds, respectively. $Rh(Stfacac)_3$, however, unlike its oxygen analog shows considerable tendency toward reduction of the metal as indicated by the presence of ions such as $[HSRh-COCF_3]^+$, $RhCO^+$ and Rh^+ which have quite high relative intensities. Peak assignments, particularly below that of the mass corresponding to the ligand, in the mass spectrum of $Rh(Stfacac)_3$ were very difficult to make due to their great number and because differentiation between metal-containing peaks and peaks due to ligand fragments could not be made (with our instramentation) since Rh has only one isotope.

When comparing fluorine migration to the metal in the monothiotrifluoroacetylacetonate complexes to that of the trifluoroacetylacetonate complexes it is evident that fluorine migration occurs to a lesser extent in the latter (table 22). This may be explained in terms of sulfur having the effect of softening the metal as an acid and thus weakening a metal-fluorine bond. One effect would be to labilize the bond by lowering its formation rate and increasing its rate of fission. For example, the $[Met-CF_2-HF]^+$ ion is observed only in the spectra of $Ni(Stfacac)_2$ and $Pd(Stfacac)_2$. That the $[MetL-CF_2]^+$ ion is not observed might suggest a labile metal fluorine-bond which can assist in the loss of fluorine as HF and yet

prevent the formation of high steady state concentrations of $[MetL-CF_2]^+$. Zinc being the hardest of the metals studied here is understandably the least effected by the presence of sulfur in the ligand. Although the relative intensity of the $[MetL-CF_2]^+$ ion is slightly higher for the $Zn(Stfacac)_2$ complex than the $Zn(tfa)_2$ complex, the presence of the $[MetL-CF_2-HF]^+$ ion in the mass spectrum of the latter suggests weakening of the metal-fluorine bond. The mechanism proposed for the loss of HF from $[MetL-CF_2]^+$ is shown on the following page (53);

Table 22

Effect of softening the metal as an acid, on the relative intensities of ions involving fluorine transfer to the metal.

Parent ion	$[MetL-CF_2]^+$	$[MetL-CF_2-HF]^+$
$[Ni^{II}(tfa)]^+$	61.2	8.0
$[Ni^{II}(Stfacac)]^+$	-	15.8
$[Zn^{II}(tfa)]^+$	28.0	-
$[Zn^{II}(Stfacac)]^+$	33.5	18.5
$[Pd^{II}(tfa)]^+$	-	-
$[Pd^{II}(Stfacac)]^+$	-	7.8
$[Co^{II}(tfa)]^+$	41.0	-
$[Co^{II}(Stfacac)]^+$	11.7	9.2

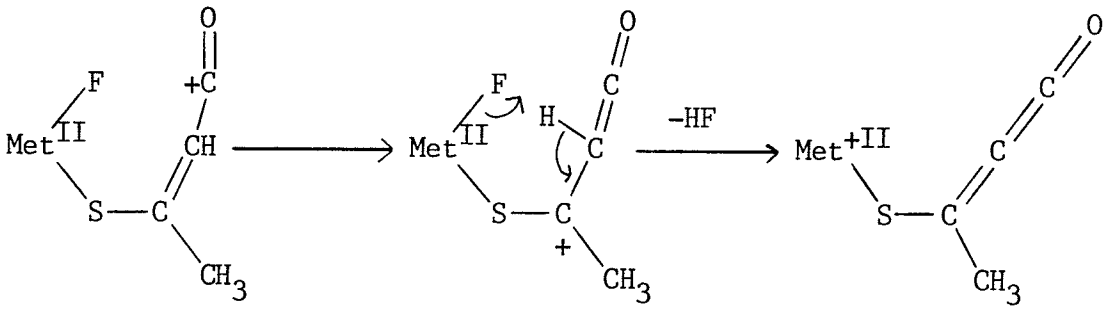

The reduction of Co(II) to Co(I) seen in the mass spectrum of $Co(acac)_3$ is also evident in the mass spectrum of $Co(Sacac)_3$. However, unlike $Co(tfa)_3$, $Co(Stfacac)_3$ also shows peaks corresponding to ions with Co in the +I oxidation state. Since the importance of the dissociation pathway leading to fluorine transfer from the ligand to the metal is reduced through softening of the metal by sulfur, the competing pathway leading to the reduction of the metal becomes more prominent.

A number of decomposition reactions involving sulfur are proposed for the monothio- and trifluoromonothio-acetylacetonate complexes. These mechanisms for some of the most common reactions are shown below; (R = CF_3, CH_3)

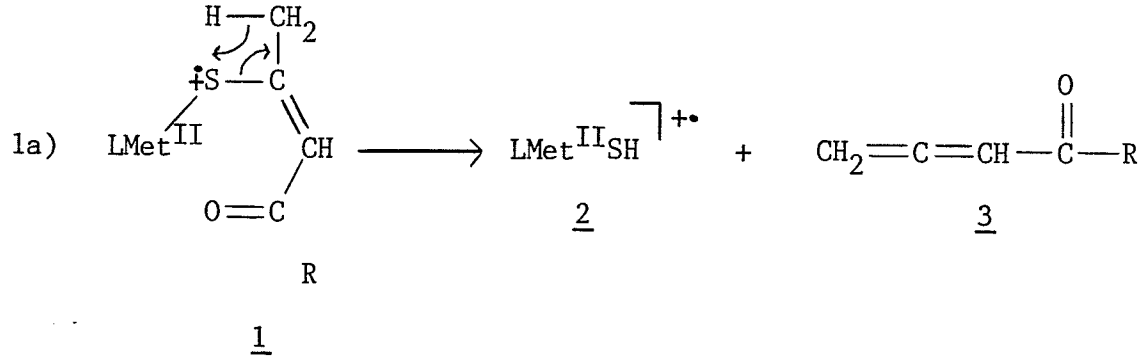

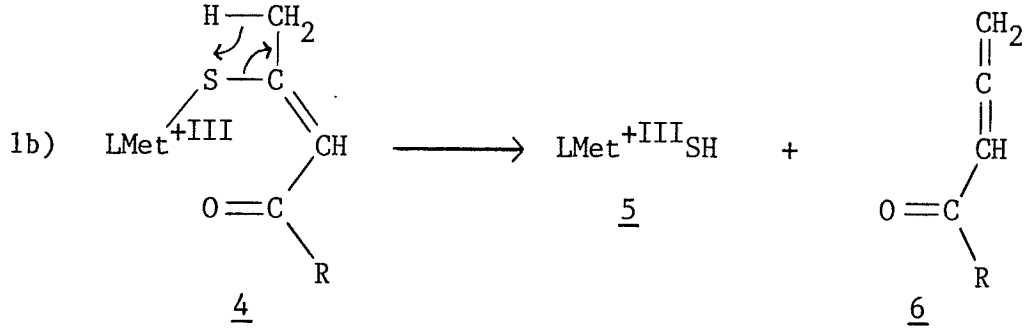

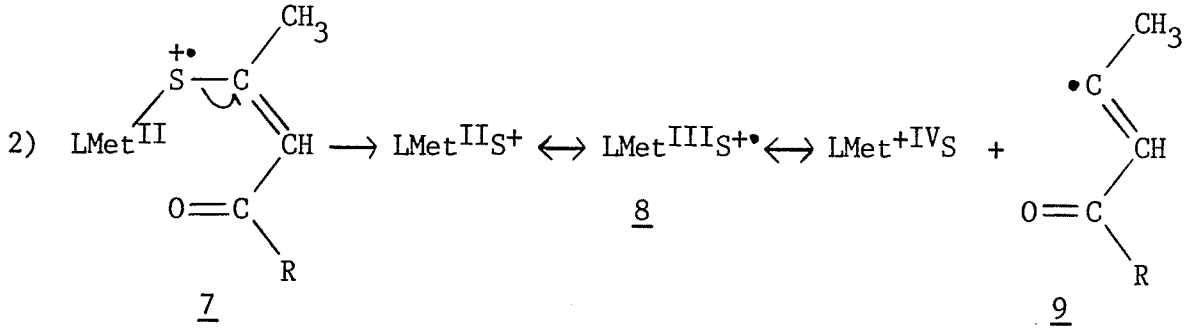

3)

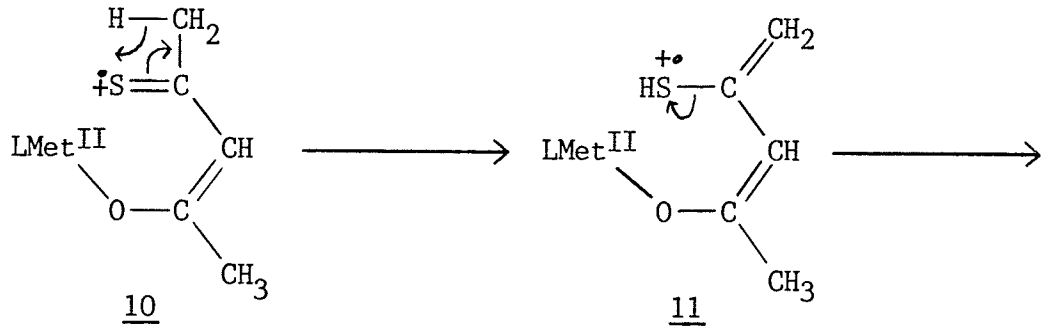

10 11

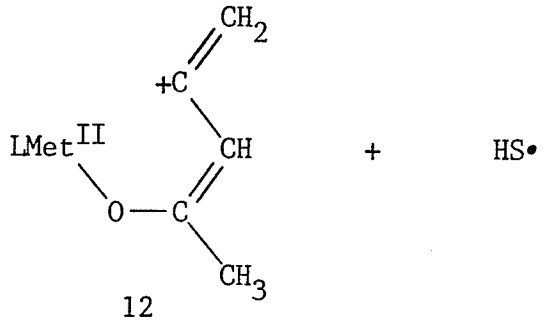

12

4a)

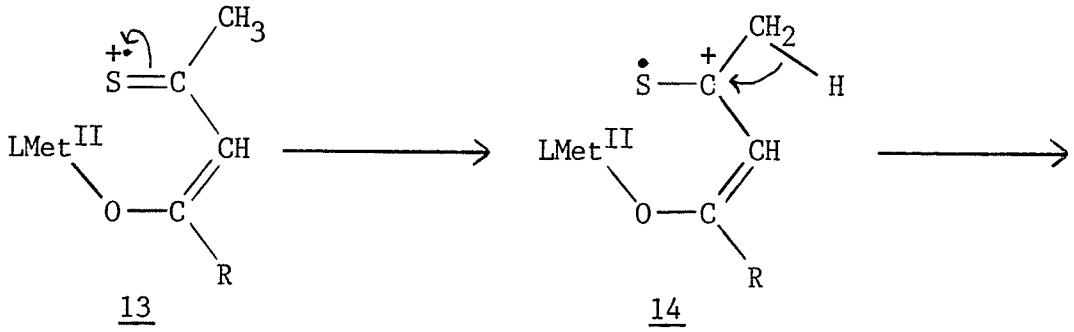

13 14

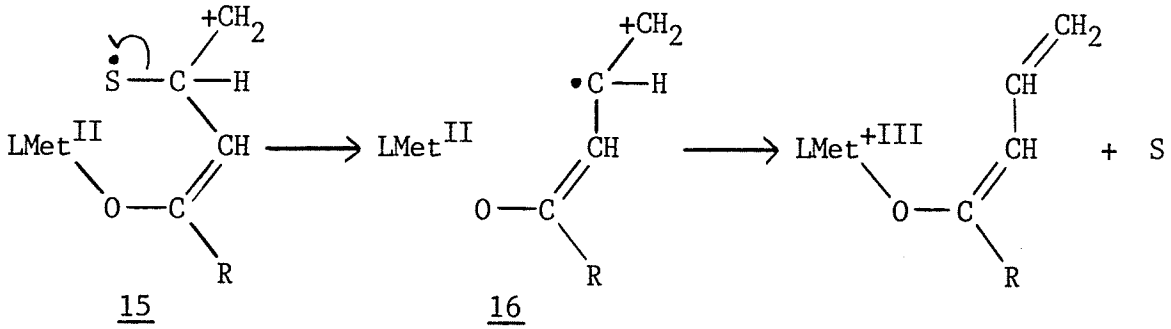

15 16

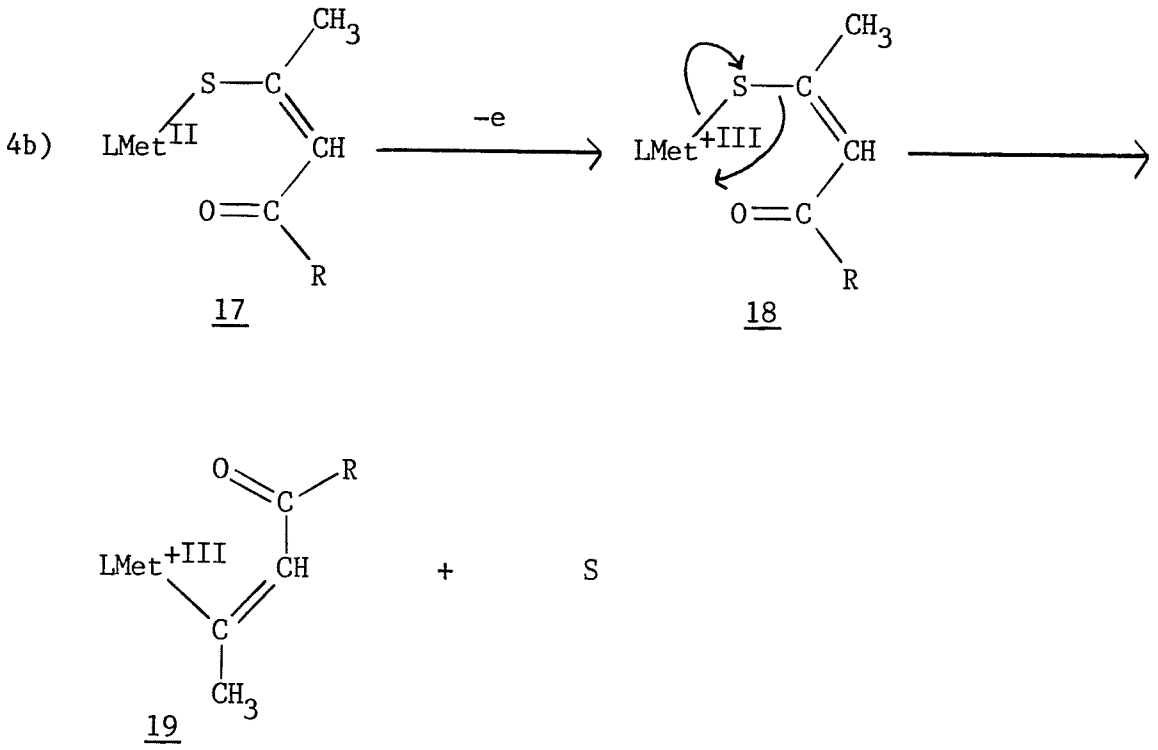

Mechanism 1a involves loss of a lone pair electron from sulfur to form the molecular ion. This is followed by hydrogen migration from the C1 carbon to the sulfur and simultaneous loss of the remainder of the ligand yielding the odd-electron fragment 2 and the even-electron neutral fragment 3. Mechanism 1b differs from 1a in that the loss of the initial electron to form the molecular ion occurs from the metal instead of the ligand. In other words the metal undergoes oxidation. The resulting daughter ion in this case is an even-electron fragment in the +III oxidation state. Which mechanism predominates is dependent upon the metal's ability to undergo oxidation since loss of an even-electron fragment from an odd-

electron ion is not an energetically favorable process. For example, the formation of the $[LZn^{II}SH]^+$ ion from $Zn(Stfacac)_2$ would be expected to follow mechanism 1a, since zinc in the +III oxidation state is known not to be stable. On the other hand, the formation of this ion from the complexes of $Ni(Sacac)_2$, $Ni(Stfacac)_2$ and $Pd(Stfacac)_2$ would be expected to follow the more energetically favored mechanism 1b, since both these metals can exist in the +III oxidation state. In the case of $Co(Sacac)_3$, $Co(Stfacac)_3$ and $Rh(Sacac)_3$ mechanism 1b involves hydrogen migration and breaking of the sulfur-carbon bond, after the loss of a ligand from the molecular ion. The $LMetS^+$ ion seen for $Ni(Sacac)_2$, $Ni(Stfacac)_2$, $Zn(Sacac)_2$, $Pd(Stfacac)_2$ and $Rh(Stfacac)_3$ could be generated as indicated by mechanism 2. This mechanism involves cleavage of the sulfur-carbon bond yielding the even-electron fragment 8 and the neutral radical 9. The formation of the $[MetL-SH]^+$ ion, observed in the $Ni(Sacac)_2$, $Pd(Sacac)_2$ and $Co(Sacac)_3$ complexes proceeds via mechanism 3 which involves hydrogen transfer from the C5 carbon to sulfur (structure 10), followed by the breaking of the remaining carbon-sulfur bond and thus eliminating the neutral radical •SH to form the even-electron ion 12. A metastable transition occurring at m/z = 233.5 in the spectrum of $Zn(Sacac)_2$ indicates that the $[MetL_2-S]^+$ ion is formed directly from the molecular ion.

Mechanism 4a involves loss of an electron from the sulfur and the breaking of one of the sulfur-carbon bonds to form the radical species 14. This is followed by hydrogen transfer from the C5 carbon and the loss of neutral sulfur by cleavage of the remaining carbon-sulfur bond to give 15, which, in turn, yields the ion 16. Mechanism 4b involves the simultaneous loss of sulfur (breaking the sulfur-carbon and metal-sulfur bonds) and the formation of a metal-carbon bond (18-19). As with mechanism 1b the molecular ion is formed by the loss of an electron from the metal (oxidation). The formation of the $[MetL_2-S]^+$ ion from $Zn(Sacac)_2$ would therefore follow mechanism 4a while the formation of this ion from $Ni(Sacac)_2$ and $Pd(Stfacac)_2$ would follow 4b.

A peak corresponding to the ion $LMetH^+$ occurs with quite high relative intensities in both the mass spectra of $Ni(acac)_2$ and $Ni(Sacac)_2$. One possible precursor to this ion is the molecular ion (no metastable transition occurred in the mass spectrum of either complex to verify the precursor to this ion). If this ion were to originate from the molecular ion two possible pathways might occur, depending on whether or not the molecular ion was formed through loss of an electron from the ligand or from the metal. If the molecular ion originated from the former, the pathway leading to the formation of $LMetH^+$ would involve the energetically unfavorable process of the loss

of an even-electron neutral fragment from an odd-electron ion. On the other hand, if the metal were to undergo oxidation (and Ni is known to be stable in the +III oxidation state), the formation of the $LMetH^+$ ion would involve the much more favorable process of loss of an even-electron neutral ion from an even-electron ion. A mechanism postulated for this pathway is shown below;

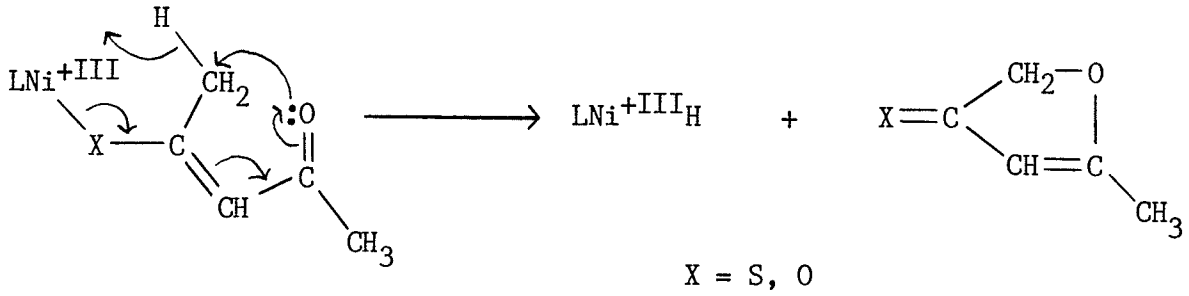

X = S, O

The decomposition schemes for the monothio- and trifluoromonothioacetylacetonate complexes of Zn(II), Ni(II), Pd(II), Co(III) and Rh(III) are shown in schemes 16-25.

SCHEME 16

Some suggested decomposition pathways for the formation of ions in the mass spectrum of $Zn(Sacac)_2$ (L=Sacac).

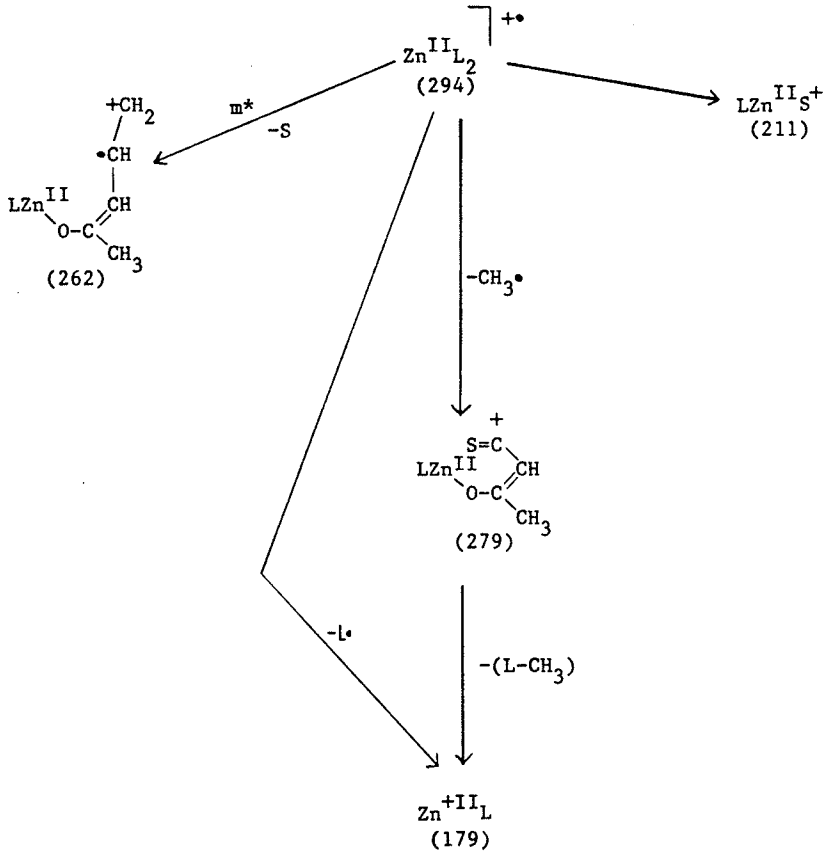

SCHEME 17

Some suggested decomposition pathways for the formation of ions in the mass spectrum of $Zn(Stfacac)_2$ (L=Stfacac)

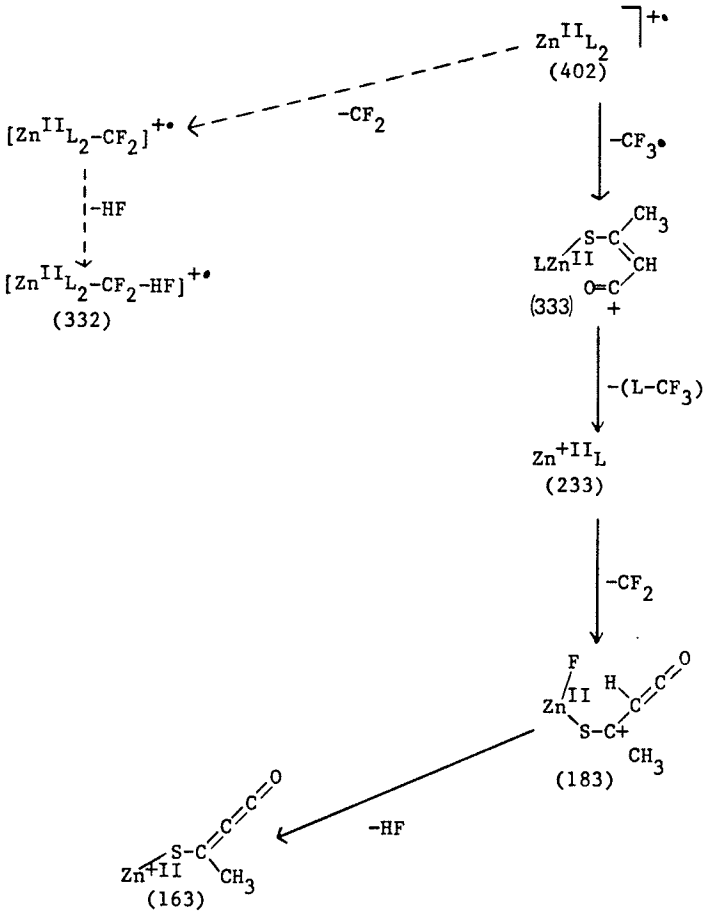

SCHEME 18

Some suggested decomposition pathways for the formation of ions in the mass spectrum of $Ni(Sacac)_2$ (L=Sacac)

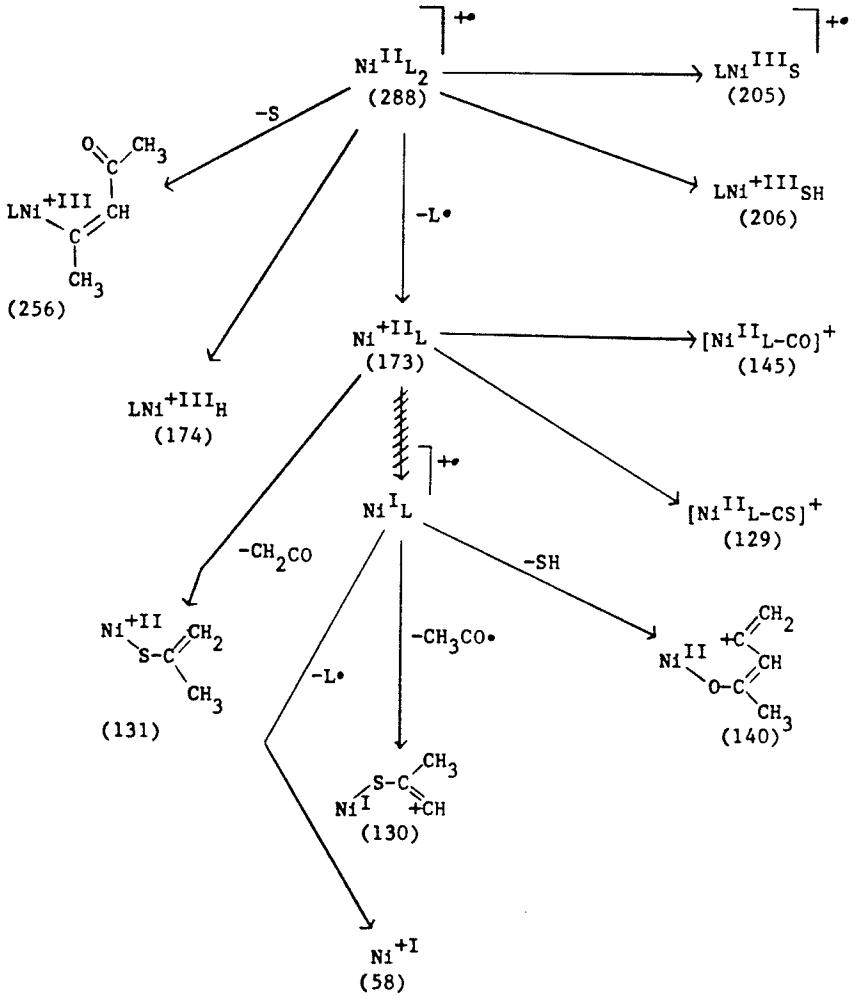

SCHEME 19

Some suggested decomposition pathways for the formation of ions in the mass spectrum of $Ni(Stfacac)_2$ (L=Stfacac)

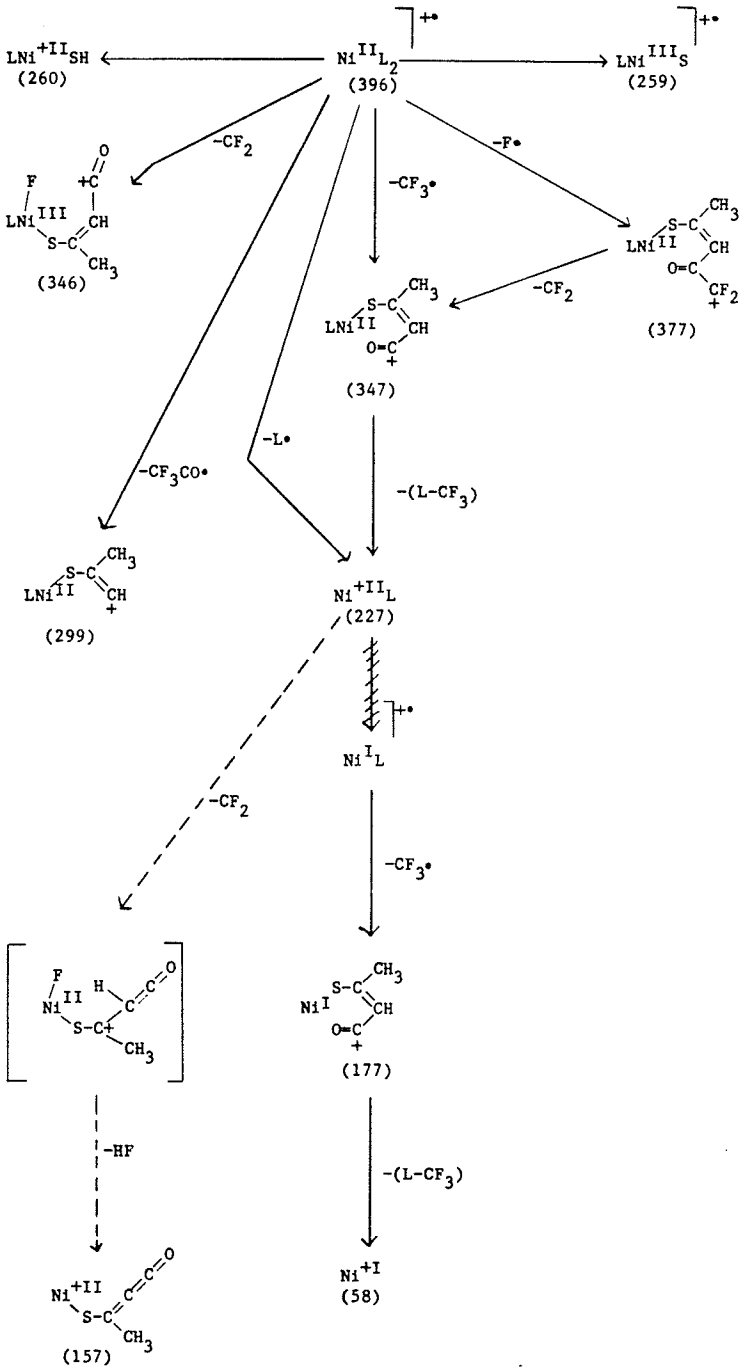

SCHEME 20

Some suggested decomposition pathways for the formation of ions in the mass spectrum of $Pd(Sacac)_2$ (L=Sacac)

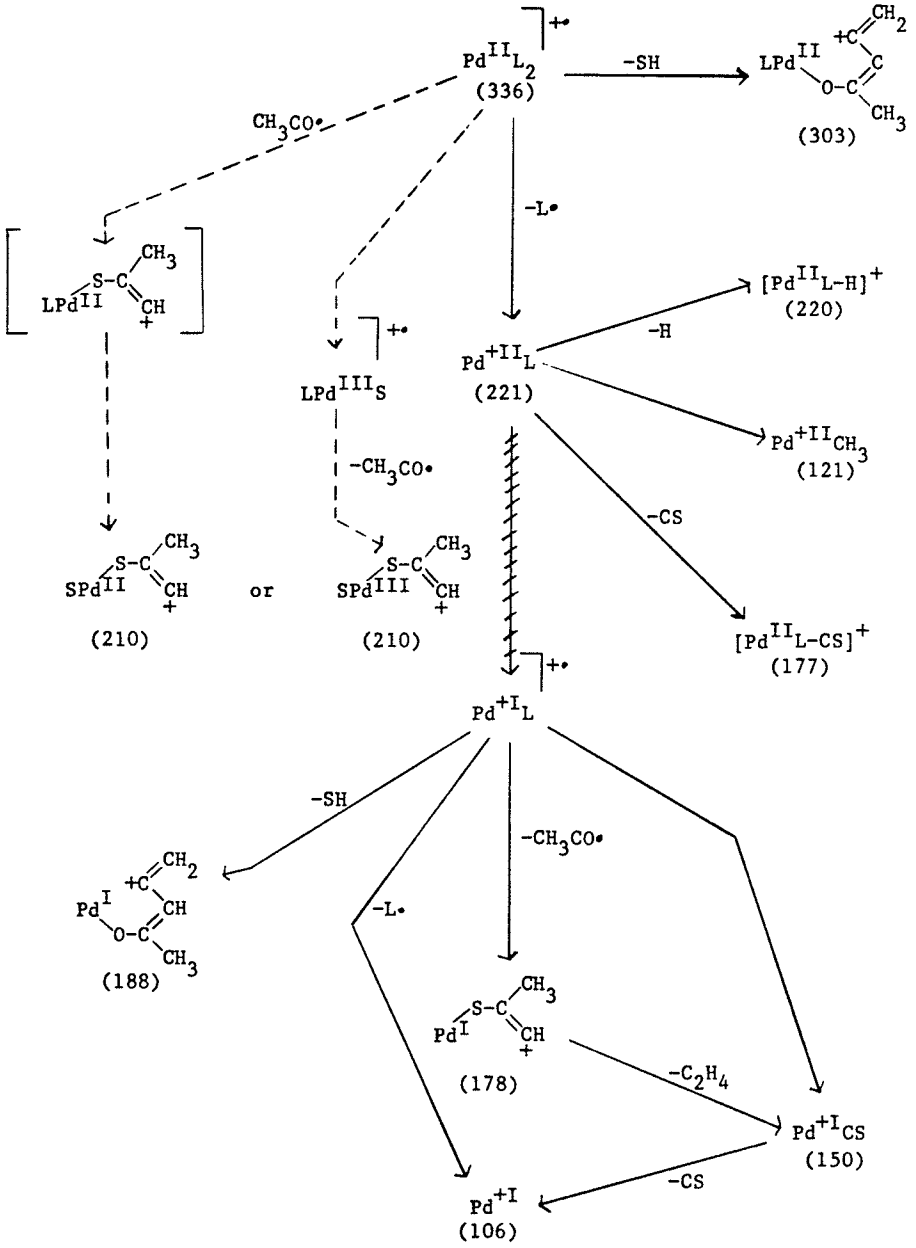

SCHEME 21

Some suggested decomposition pathways for the formation of ions in the mass spectrum of $Pd(Stfacac)_2$ (L=Stfacac)

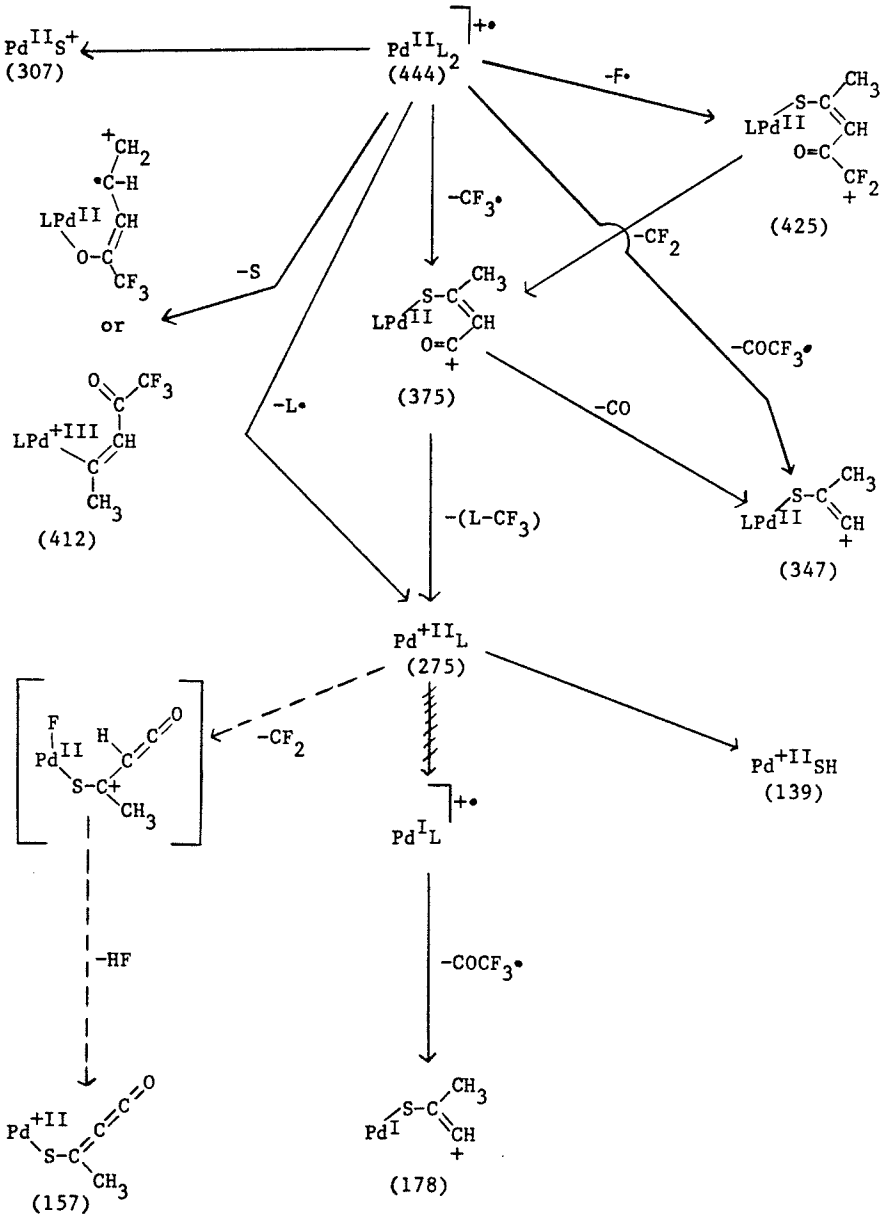

SCHEME 22

Some suggested decomposition pathways for the formation of ions in the mass spectrum of $Co(Sacac)_3$ (L=Sacac).

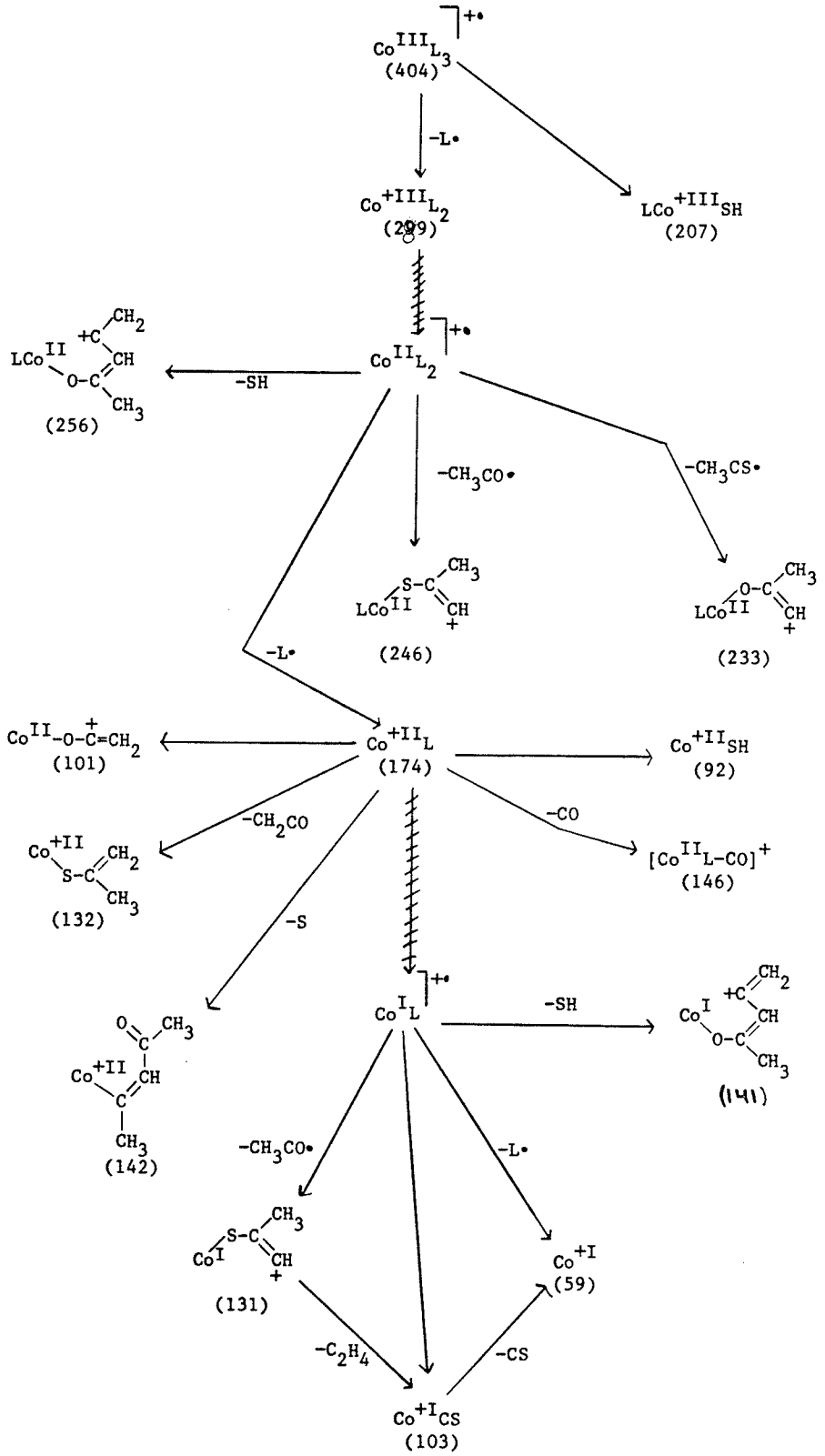

SCHEME 23

Some suggested decomposition pathways for the formation of ions in the mass spectrum of $Co(Stfacac)_3$ (L=Stfacac)

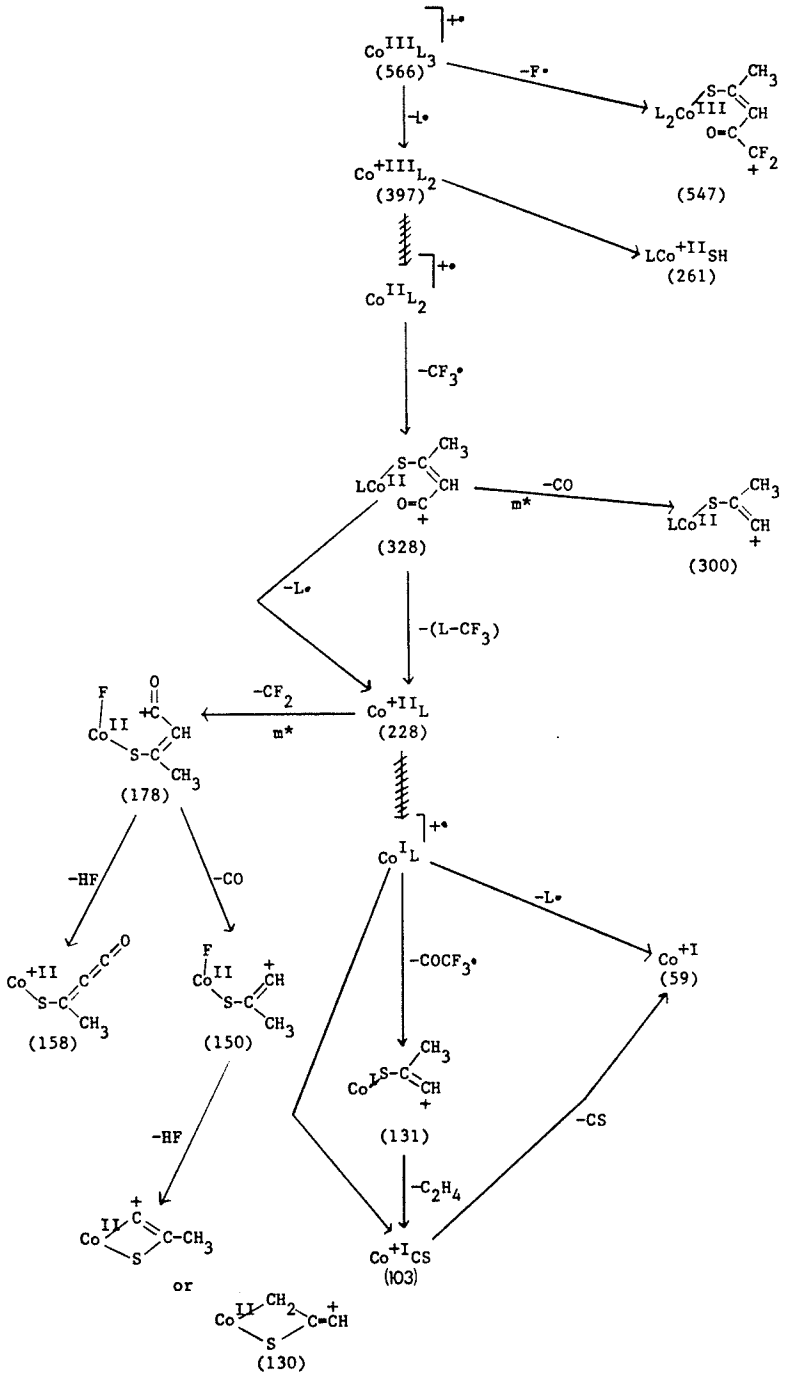

SCHEME 24

Some suggested decomposition pathways for the formation of ions in the mass spectrum of $Rh(Sacac)_3$ (L=Sacac)

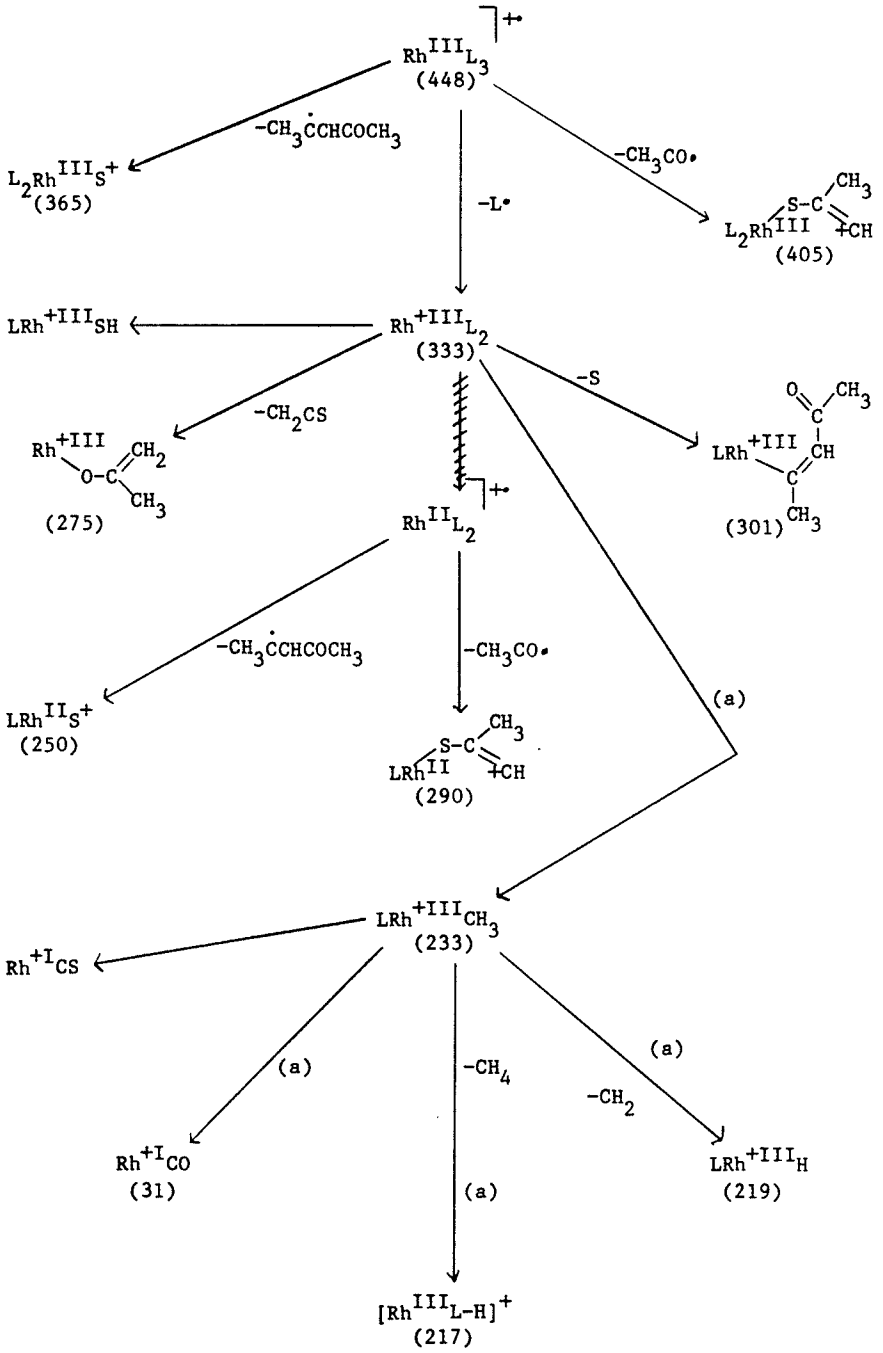

(a) Similar decomposition in $Rh(tfa)_3$ and/or $Rh(acac)_3$ verified by metastable transition.

SCHEME 25

Some suggested decomposition pathways for the formation of ions in the mass spectrum of $Rh(stfacac)_3$ (L=Stfacac)

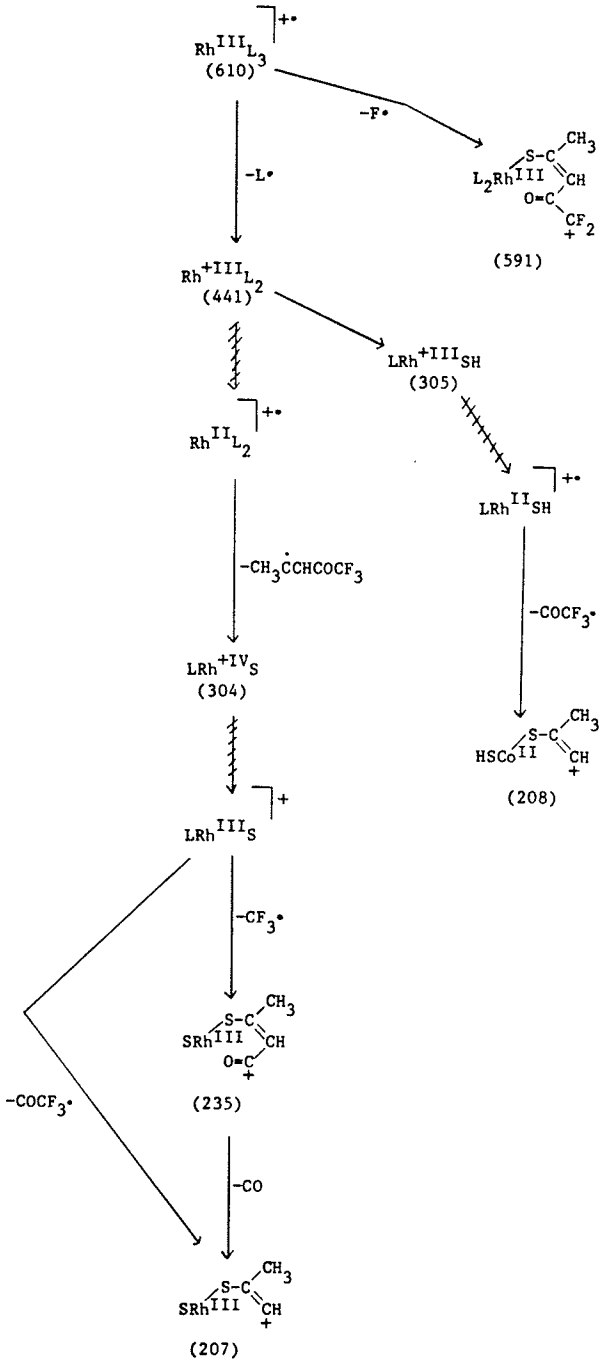

iv) Volatilities

Some trends in the volatilities of these complexes were recognized by observing the sample probe temperature required for vaporization of the sample (temperature at which a reasonable ion intensity was observed in the mass spectrometer). The appropriate probe temperatures were measured with a thermocouple when slowly increasing the voltage on a resistance heater. However, due to fluctuations in temperature (thermocouple would tend to drift) and the qualitative method of choosing the appropriate ion intensity at which to take the reading, an error of ± 0.25 mV ($6.25^{\circ}C$) was assigned to each value.

The following volatility differences were observed for chelates of the same ligand coordinated to different metals (see figure 18).

$Rh(hfa)_3 > Rh(tfa)_3 > Rh(Stfacac)_3 > Rh(Sacac)_3 > Rh(acac)_3$

$Co(hfa)_3 > Co(tfa)_3 > Co(Stfacac)_3 > Co(acac)_3 > Co(Sacac)_3$

$Pd(hfa)_2 > Pd(Stfacac)_2 > Pd(tfa)_2 > Pd(acac)_2 > Pd(Sacac)_2$

$Zn(hfa)_2 \approx Zn(acac)_2 > Zn(Stfacac)_2 \approx Zn(tfa)_2 > Zn(Sacac)_2$

$Ni(hfa)_2 \approx Ni(Stfacac)_2 > Ni(Sacac)_2 > Ni(tfa)_2 \approx Ni(acac)_2$

The first observation one makes is that under these conditions, for all five metals the hfa complexes are the most volatile. In the cases of Zn and Ni, $Zn(acac)_2$ and $Ni(Stfacac)_2$ are about equally as volatile as their

Figure 18

Volatility differences for chelates of the same ligand coordinated to different metals.

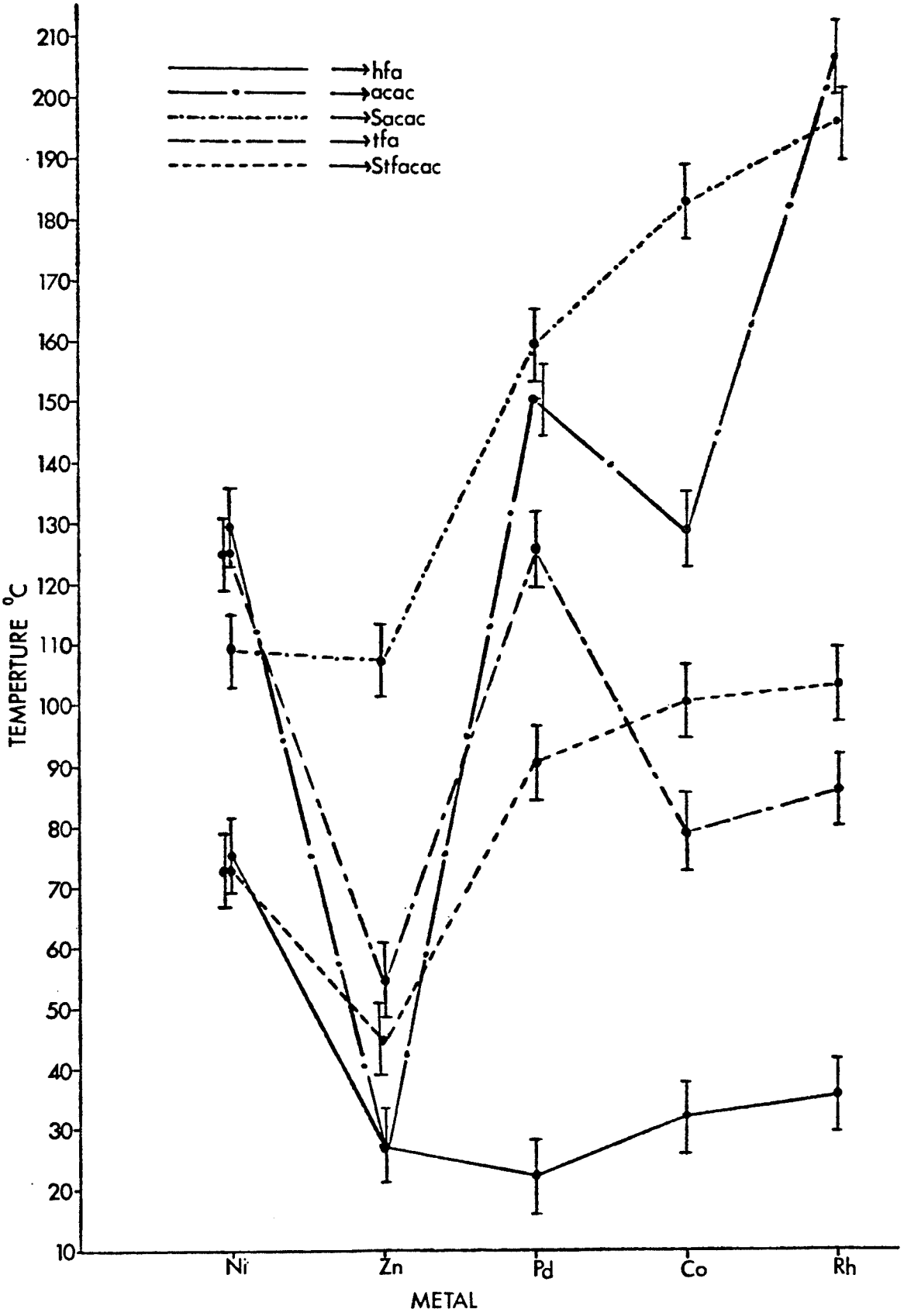
→hfa
→acac
→Sacac
→tfa
→Stfacac
TEMPERTURE °C
210
200
190
180
170
160
150
140
130
120
110
100
90
80
70
60
50
40
30
20
10
Ni
Zn
Pd
Co
Rh
METAL

respective hfa complexes. The relative volatilities of the zinc complexes show the greatest deviations from the general trends. In particular, $Zn(acac)_2$ appears remarkably volatile.

In summary, a general trend of increased volatility with increased fluorine substitution in the chelate ligand is observed.

SUMMARY AND CONCLUSIONS

The mass spectra of some transition metal acetylacetonates and monothioacetylacetonates show that odd-electron ions tend to fragment by the elimination of odd-electron neutral radicals with the formation of even-electron fragment ions. Even-electron ions tend to fragment less easily but when they do they tend to lose even-electron neutral fragments. In fluorinated metal beta-diketonates and monothio-beta-diketonates a competition exists between pathways involving fluorine transfer to the metal and reduction of the metal. Which pathway predominates is dependent upon the metal's ability to undergo reduction and the hardness of the metal as an acid. The presence of a CF_3 group in the ligand shell tends to harden the metal environment while the replacement of an oxygen atom by sulfur in the ligand tends to soften the metal environment, thus increasing and decreasing the extent of fluorine transfer from the ligand to the metal respectively.

It is generally noted that substitution of fluorine atoms for hydrogen atoms in the ligand shell greatly increases the volatility of both the beta-diketonate and monothio-beta-diketonate metal complexes.

References

1) K. J. Eisentraut and R. E. Sievers, J. Inorg. Nucl. Chem. 29, 1931 (1967).

2) W.R. Wolf, R.E. Sievers and G.H. Brown, Inorg. Chem. 11, 1995 (1972).

3) J.E. Sicre, J.T. Dubois, K.J. Eisentraut and R.E. Sievers, J. Am. Chem. Soc. 91, 3476 (1969).

4) R.E. Sievers, B.W. Ponder, M.L. Morris and R.W. Moshier, Inorg. Chem. 2, 693 (1963).

5) E.W. Berg and J.T. Truemper, Anal. Chim. Acta. 32, 245 (1965).

6) C S. Springer Jr., D W. Meek and R.E. Sievers, Inorg. Chem. 6, 1105 (1967).

7) W.B. Brown, J.F. Steinback and W.F. Wagner, J. Inorg. Nucl. Chem. 13, 119 (1960).

8) R.E. Sievers and J.E. Sadlowski, Science 201, 217 (1978).

9) M.F. Richardson and R.E. Sievers, Inorg. Chem.10, 498 (1971).

10) H.A. Swain Jr. and D.G. Karraker, Inorg. Chem. 9, 1766 (1970).

11) E.W. Berg and J.C. Acosta, Anal. Chim. Acta. 40, 101 (1968).

12) J.E. Schwarberg, R.E. Sievers and R.W. Moshier, Anal. Chem. 42, 1828 (1970).

13) K.J. Eisentraut, R.E. Sievers, J. Am. Chem. Soc. 87, 5254 (1965).

14) R. Belcher, W.I. Stephen, I.J. Thomson and P.C. Uden, J. Inorg. Nucl. Chem. 33, 1851 (1971).

15) R. Belcher, W.I. Stephen, I.J. Thomson and P.C. Uden, J. Inorg. Nucl. Chem. 34, 1017 (1972).

16) J.E. Huheey, Inorganic Chemistry Principles of Structure and Reactivity, 2nd Ed. Harper and Publishers N.Y.

17) R.G. Pearson, J. Am. Chem. Soc. 85, 3533 (1963).

18) R.G. Pearson, Chem. Commun. 65 (1968).

19) J.E. Huheey and R.S. Evans, Chem. Commun. 968 (1969).

20) J.E. Huheey and R.S. Evans, J. Inorg. Nucl. Chem. 32, 373 (1970).

21) J. Chatt, J. Inorg. Nucl. Chem. 8, 515 (1958).

22) J.M. Miller and R.B. Jones, Inorg. Chim. Acta. L75-L76 (1979).

23) R.G. Pearson, J. Chem. Ed. 45, 581 (1968).

24) M.L. Morris and R.D. Koob, Inorg. Chem. 20, 2737 (1981).

25) M. Yaqub, Synthesis and Spectrometric Study of Beta-Diketone complexes, Thesis, University of Michigan, Ann Arbor, 1970 (obtained from reference 23).

26) R.C. Mehrotra, R. Bohra and D.P. Gaur, Metal Beta-diketonates and Allied Derivatives, Academic Press (1978).

27) F. Duus and J.W. Anthonsen, Acta. Chimica. Scand. B31 40 (1977).

28) D.L. Pavia, G.M. Lampman and G.S. Kriz Jr., Introduction to Spectroscopy, Saunders College Publishing (1979).

29) R.K.Y. Ho, S.E. Livingstone and T.N. Lockyer, Aust. J. Chem. 19, 1179 (1966).

30) F.P. Dwyer and A.M. Sargeson, J. Am. Chem. Soc. 75, 984 (1953).

31) R.C. Fay and T.S. Piper, J. Am. Chem. Soc. 85, 500 (1965).

32) J.P. Collman, R.L. Marshall, W.L. Young and S.D. Goldby, Inorg. Chem. 1, 704 (1962).

33) S. Kawanishi, A. Yokoyama and H. Tanaka, Chem. Pharm. Bull. 21 (12), 2653 (1973).

34) S.E. Livingstone and N. Saha, Aust. J. Chem. 28, 1249 (1975)

35) S. Okeya, S. Ooi, K. Matsumoto, Y. Nakamura and S. Kawaguchi, Bull. Chem. Soc. Jpn. 54, 1085 (1981).

36) M. Das and S.E. Livingstone, Aust. J. Chem. 27, 749 (1974).

37) E.W. Berg, J.T. Truemper, J. Phys. Chem. 64, 467 (1960).

38) G.T. Morgan and H.W. Moss, J. Chem. Soc. 105, 189 (1913).

39) M.R. Kidd, R.S. Sager and W.H. Watson, Inorg. Chem. 6, 946 (1967).

40) IUPAC Recommendation, Pure Applied Chem. 50, 65 (1978).

41) R.G. Cooks, J.H. Beynon, R.M. Caproli and G.R. Lester, Metastable Ions, Elsevier Scientific Publishing Co. (1973).

42) J.A. Hipple, R.E. Fox and E.U. Condon, Phys. Rev. 69, 347 (1946).

43) R.I. Reed, Ion Production by Electron Impact, Academic Press (1962).

44) C.G. Macdonald and J.S. Shannon, Aust. J. Chem. 19, 1545 (1966).

45) F.W. McLafferty, Mass Spectrometry of Organic Ions, ed. F.W. Mclafferty, Academic press.

46) C. Reichert, Thesis, A Mass Spectrometric Study of Some Transition Metal Acetylacetonates., University of Manitoba (1969).

47) M.L. Morris and R.D. Koob, Inorg. Chem. 22, 3502 (1983).

48) F.A. Cotton and G. Wilkinson, Advanced Inorganic Chemistry, 4th Ed. John Wiley and sons N.Y. (1980).

49) C. Reichert, G.M. Bancroft and J.B. Westmore, Can. J. Chem. 48, 1362 (1970).

50) G.M. Bancroft, C.Reichert, J.B. Westmore, and H.D. Gesser, Inorg. Chem. 8, 474 (1969).

51) C. Reichert and J.B. Westmore, Can. J. Chem. 48, 3213 (1970).

52) R.D. Koob, M.L. Morris and A.L. Clobes, Chem Commun. 1177 (1969).

53) A.L. Clobes, M.L. Morris and R.D. Koob, Org. Mass. Spec. 5, 633 (1971).